Flexural nanopositioning stages design for synchrotron radiation applications at the Advanced Photon Source

Deming Shu

With my colleagues at ANL/APS, ANL/CNM, BNL/NSLS-II, SLAC/LCLS, and EXFEL

Advanced Photon Source
Argonne National Laboratory
Argonne, IL 60439, U.S.A.

ASD Seminar, Advanced Photon Source, Argonne National Laboratory

August 8, 2014

Acknowledgments

Thanks to my colleagues at ANL/APS, ANL/CNM, SLAC/LCLS, and EXFEL

for the development of stages for high precision x-ray monochromators and analyzers etc:

T. S. Toellner, E. E. Alp, Y. Shvyd'ko, S Stoupin, K-J. Kim, J. Ilavsky, S. D. Shastri, P. L. Lee, G. G. Long, W-K. Lee, L. Assoufid, D. Nocher, R. Ranay.

for the development of stages for x-ray nanoprobe instruments and MLL instruments:

J. Maser, W. Liu, M. Holt, R. Winarski, V. Rose, G. B. Stephenson, B. Lai, S. Vogt, I. McNulty, C. Preissner, S. Kearney, J. Anton, A. Macrander, Y. S. Chu, H. Yan, and MLL team.

for the development of UHV-compatible stages for double crystal monochromators and self-seeding monochromator:

- *APS 8-ID: S. Narayanan, A. Sandy, and et al*
- *APS 16-BM: W. Yang, E. Rod, G. Shen, and et al*
- *SLAC LCLS beamline monochromator: A. Robert, D. Fritz, V. Srinivasan, and et al*
- *SLAC LCLS self-seeding monochromator: J. Amann, P. Emma, and et al*
- *EXFEL: X. Dong, G. Galasso, H. Sinn, and et al*

Thanks to the APS management support: *J. Quintana, G. Pile, W. Ruzicka, L. Young, A. Zholents, …*

Commercial available *at A.J.R. Industrials, Inc., IL USA: Gregg Wojtowicz*

This work was supported by the U.S. Department of Energy, Office of Science, under Contract No. DE-AC02-06CH11357.

Outline

- *Introduction*
- *Stages design for APS high-energy-resolution monochromators and analysers*
- *Stages design for hard x-ray nanoprobes at the APS*
- *UHV monochromator stages design for APS, SLAC/LCLS beamlines and self-seeding project, as well as Argonne WFO project for European-XFEL*
- *Summary*

Introduction

- With brighter upgraded APS x-ray sources and more advanced x-ray optics, scientists at the APS will need more customized novel instruments. Nanopositioning techniques present a significant opportunity to support the state-of-the-art synchrotron radiation instrumentation research at the APS upgrade project.

- Precision ball-bearing- or roller-bearing-based positioning stage systems provide large travel range. However, it is not possible to meet requirements in sub-nanometer positioning resolution, high tilting stiffness, and sub-microradian straightness of trajectory repeatability with a single guiding system.

- Customized flexure mechanisms are needed for novel high precision synchrotron radiation instruments.

Introduction

Weak-link-based Artificial Channel-Cut Crystal Mechanism

Supported by Argonne LDRD, There are four major techniques developed for this challenging task at the APS since 1999:

- **A novel laser Doppler encoder system with multiple-reflection optics for sub-100-pm and 10-nrad-level linear and angular displacement measurement.**
- **A rotary, high-stiffness, weak-link mechanism with stacked thin metal sheets having 10-nrad driving sensitivity with excellent stability.**
- **A linear, high-stiffness, weak-link mechanism with stacked thin metal sheets having sub-100-pm driving sensitivity with excellent stability.**
- **A digital-signal-processor (DSP)-based, real-time, closed-loop feedback system for active relative vibration control on the nanometer scale.**

Laser Doppler encoder with multiple-reflection optics

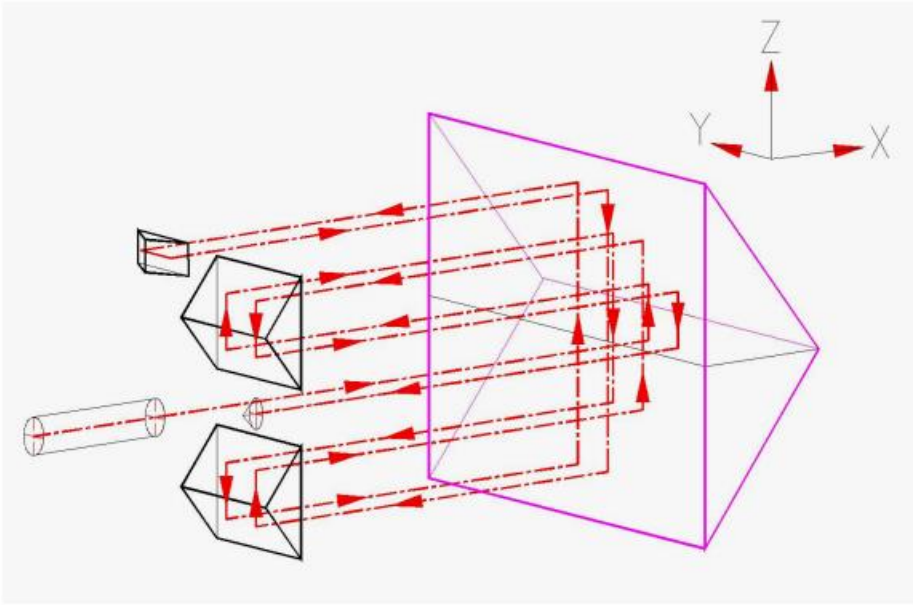

In the self-aligning multiple-reflection optical design for the LDDM system, the heterodyning detector is housed coaxially inside the frequency-stabilized laser source. Instead of a typical single reflection on the moving target, the laser beam is reflected back and forth twelve times between the fixed base and the moving target. The laser beam, which is reflected back to the heterodyning detector, is frequency-shifted by the movement of the moving target relative to the fixed base. With same LDDM laser source and detector electronics, this optical path provides twelve times greater resolution for the linear displacement measurement and encoding. A 0.03 nm resolution was reached by the prototype LDDM system.

D. Shu, Y. Han, T. S. Toellner, and E. E. Alp, Proc. SPIE, Vol. 4771 (2002) 78-90

Weak-link-based Artificial Channel-Cut Crystal Mechanism

In 1999, to overcome the obstacles in developing a 4-crystal in-line high-resolution hard x-ray monochromator using a nested channel-cut crystal geometry with meV bandpass, the first high-stiffness weak-link mechanism with stacked thin-metal sheets was developed for the APS high-energy-resolution beamline 3-ID. The precision and stability of this mechanism allowed us to align or adjust an assembly of crystals to achieve the same performance as a single channel-cut crystal, so we called it an "artificial channel-cut crystal."

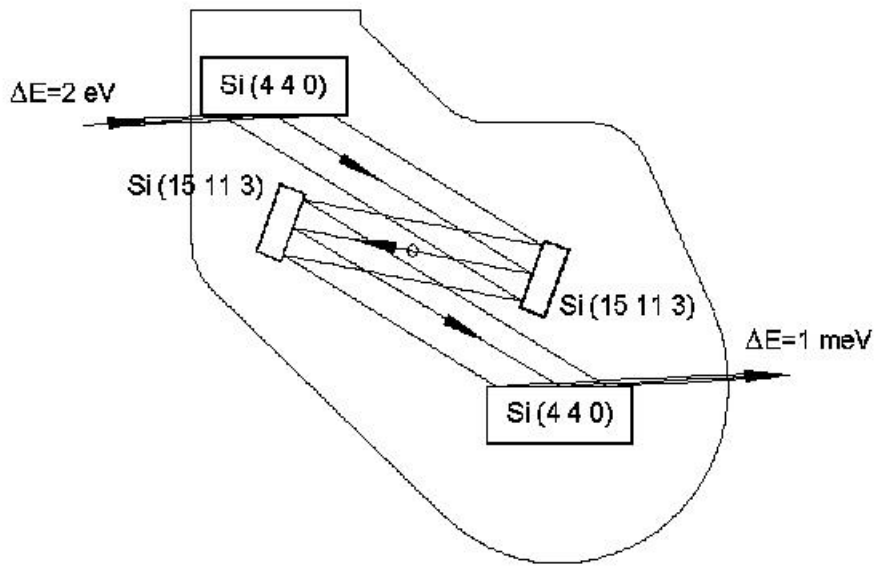

D. Shu, T. S. Toellner, and E. E. Alp, Nucl. Instrum. and Methods A 467-468, 771-774 (2001)

Weak-link-based Artificial Channel-Cut Crystal Mechanism

maximum displacement 94 µm (0.25 degree angular motion)

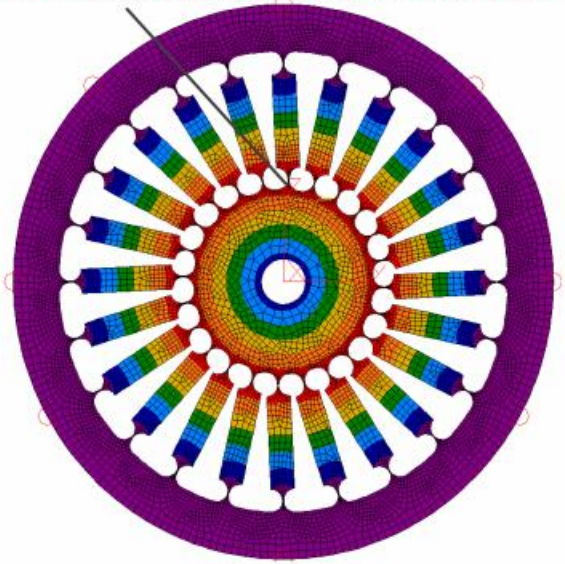

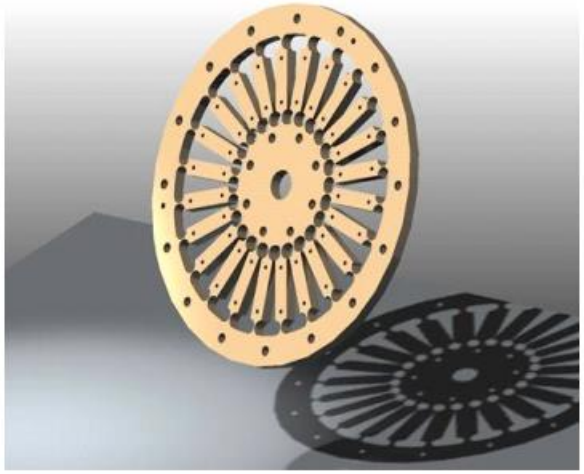

maximum von Mises stress 175 MPa

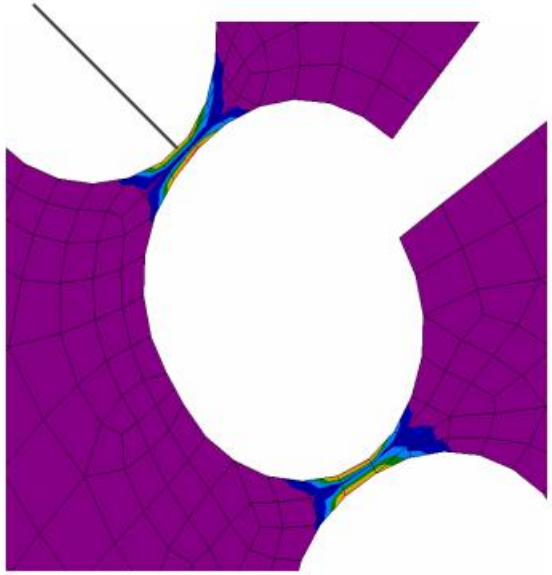

Unlike traditional kinematic linear spring mechanisms, the overconstrained weak-link mechanism provides much higher structural stiffness and stability. Using a laminar structure configured and manufactured by chemical etching and lithography techniques, we are able to design and build a planar-shape, high-stiffness, high-precision weak-link mechanism.

The precision of modern photochemical machining processes using lithography techniques makes it possible to construct a strain-free (or strain-limited) overconstrained mechanism on thin metal sheets. By stacking these thin-metal weak-link sheets with alignment pins, we can construct a solid complex weak-link structure for a reasonable cost.

D. Shu et al., SRI-2006 Conf. Proc. 879, AIP (2007) 1073-1076

Test of high-stiffness angular weak-link mechanism

- Sensitivity test with a laser Doppler encoder

  A test with 33 nrad average step size

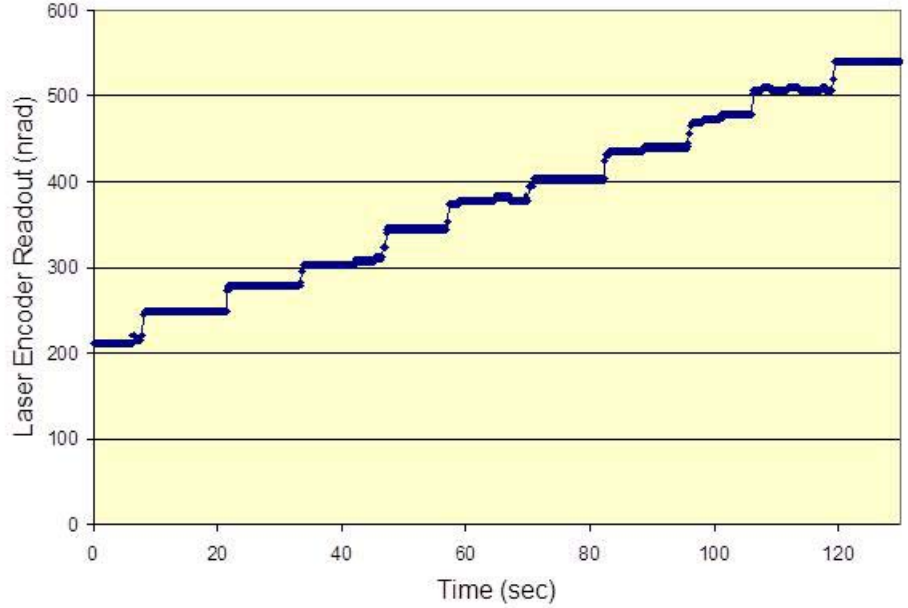

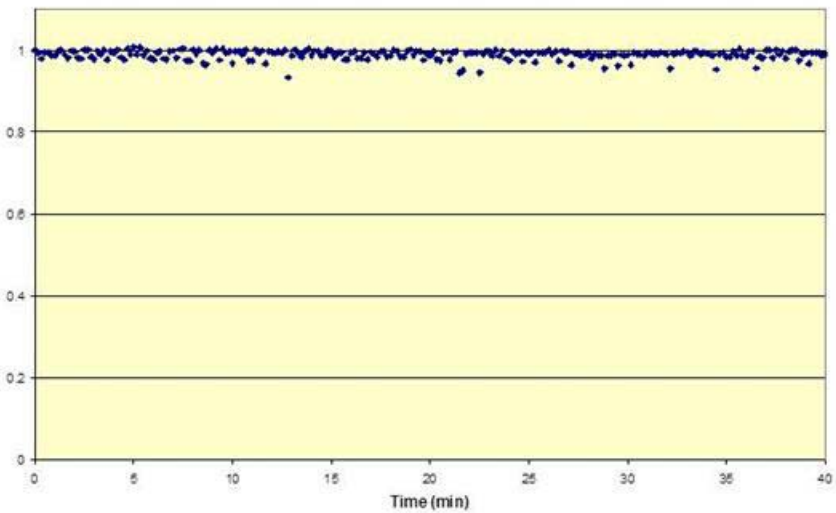

- Stability result from a x-ray experiment

  Relative intensity measured by an ionization chamber after the high-resolution monochromator (1-meV bandwidth) as a function of time. The data are corrected for the decaying current in the storage ring.

ACCM for high-resolution x-ray monochromators

References:

D. Shu, T. S. Toellner, and E. E. Alp, "Modular Overconstrained Weak-Link Mechanism for Ultraprecision Motion Control," Nucl. Instrum. Methods A 467-468, 771-774 (2001).

U.S. Patent granted No. 6,607,840, Redundantly constrained laminar structure as weak-link mechanisms, D. Shu, T. S. Toellner, and E. E. Alp, 2003.

D. Shu, T. S. Toellner, E. E. Alp, J. Maser, J. Ilavsky, S. D. Shastri, P. L. Lee, S. Narayanan, and G. G. Long, "Applications of Laminar Weak-Link Mechanisms for Ultraprecision Synchrotron Radiation Instruments", AIP CP879, 1073-1076 (2007).

ACCM for high-resolution x-ray monochromators

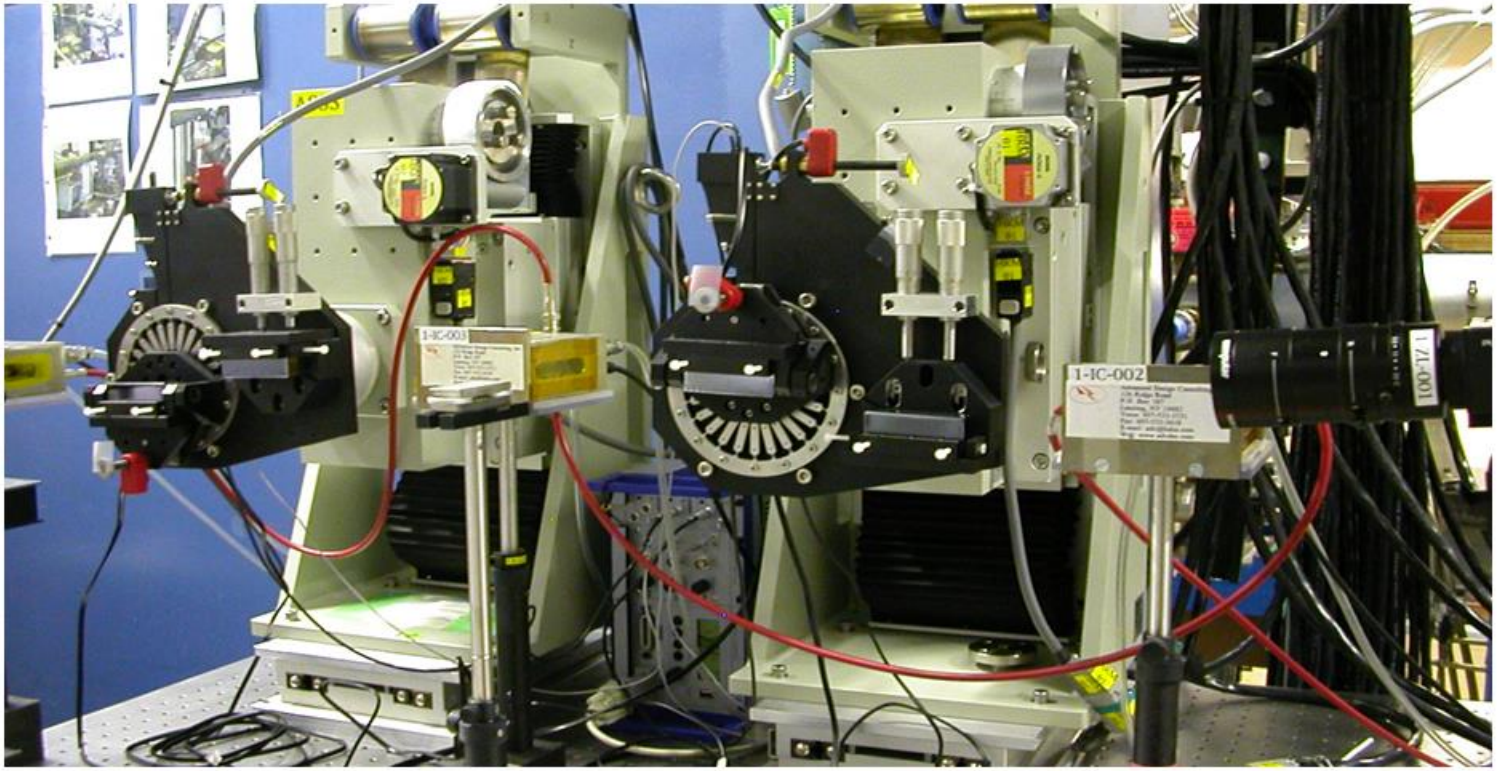

Photograph of a high-energy x-ray monochromator with four crystal reflections constructed at APS XOR beamline 1-ID-B. It shows a high-energy (50-100 keV) high-resolution x-ray monochromator with four crystal reflections constructed at APS beamline 1-ID-B, which has been used for resonant powder diffraction and stress/strain studies**.*

* Y. Zhang, A. P. Wilkinson, P. L. Lee, S. D. Shastri, D. Shu, D. –Y. Chung, M. G. Kanatzidis, J. Appl. Cryst. 38, 433-441 (2005).
** B. Jakobsen, H. F. Poulsen, U. Lienert, J. Almer, S. D. Shastri, H. Sorensen, C. Gundlach, W. Pantleon, Science 312, 889-892 (2006).

ACCM for high-resolution x-ray analysers

Artificial channel-cut crystal stage for the USAXS instrument crystal analyzer at APS 15-ID

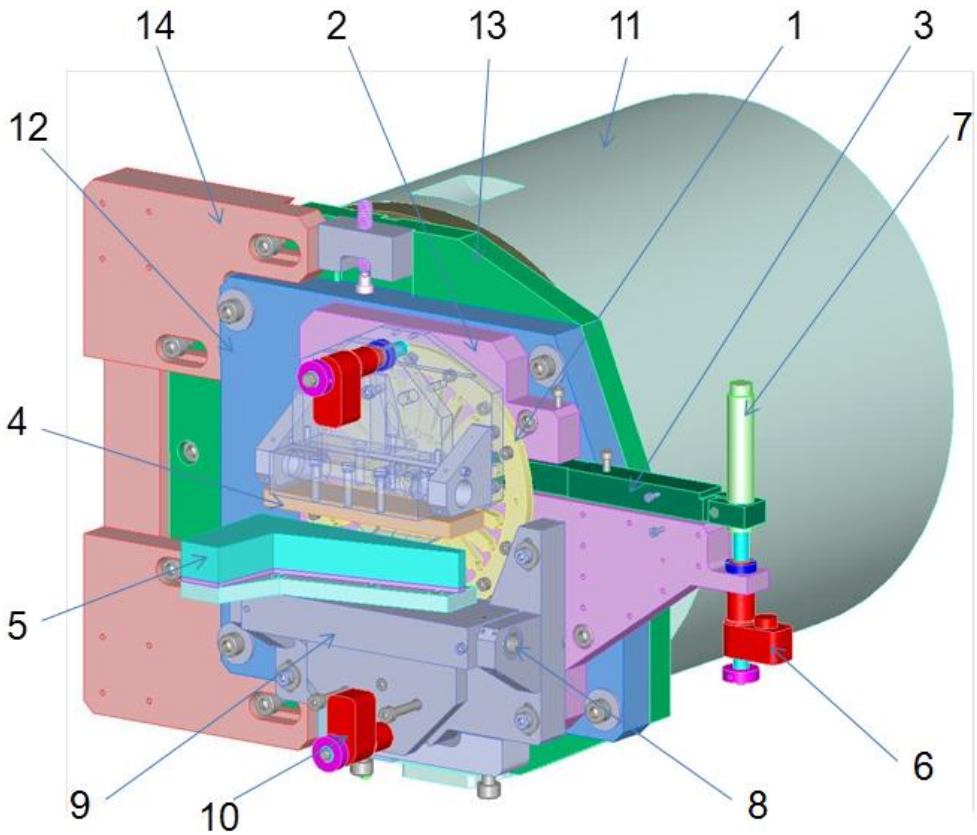

A 3D model of the artificial channel-cut crystal stage for the APS USAXS instrument crystal analyzer system: (1) high-stiffness, weak-link mechanism module; (2) base plate; (3) sine-bar; (4,5) two silicon single crystals; (6) Picomotor™; (7) Physik InstrumenteTM closed-loop controlled PZT; (8) commercial flexure bearing; (9) crystal holder; (10) PicomotorTM-driven structure; (11) Aerotech™ rotary stage; (12,13) adapter plates; (14) balancing plate.

J. Ilavsky, D. Shu, P.R. Jemian, and G.G. Long, AIP CP879, 1833-1836 (2007)

ACCM for high-resolution x-ray analysers

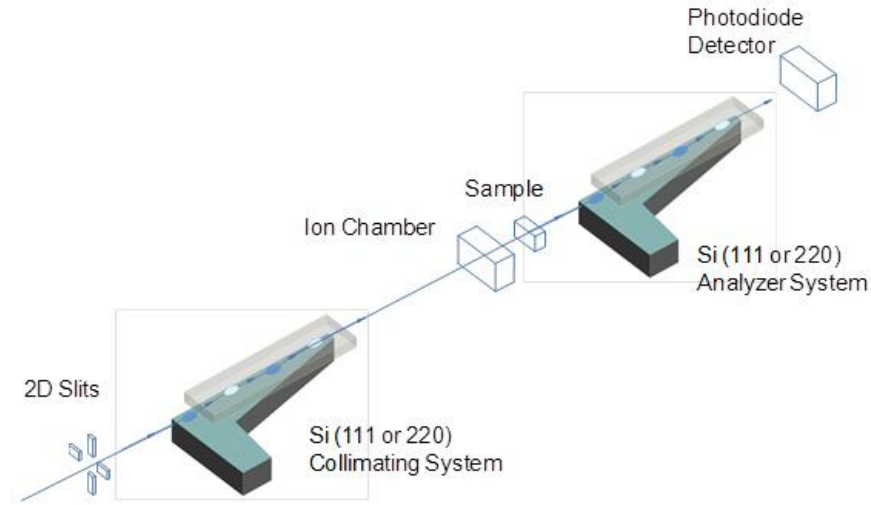

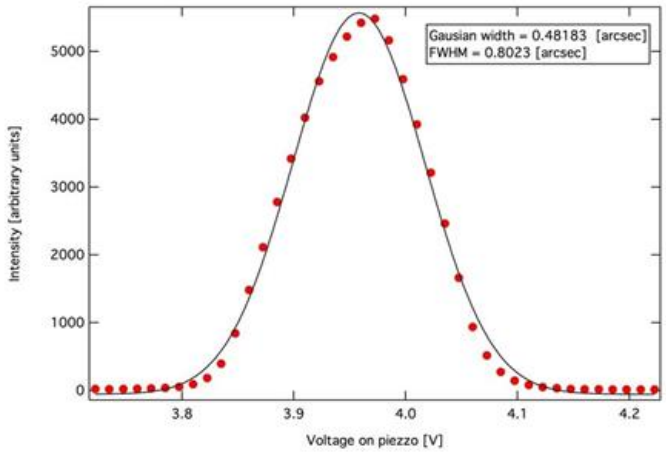

An X-ray rocking curve scan result using the artificial channel-cut crystal stage with a step size of about 300 nrad.

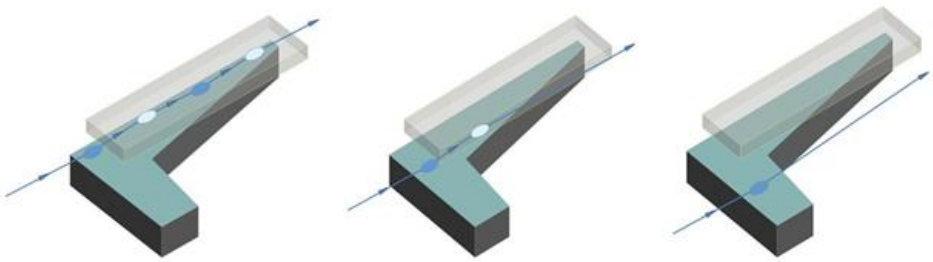

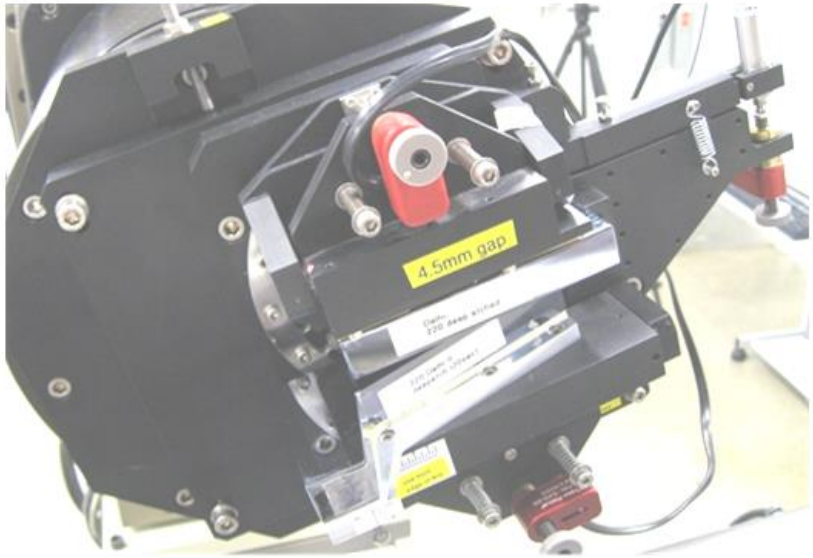

J. Ilavsky, D. Shu, P.R. Jemian, and G.G. Long, AIP CP879, 1833-1836 (2007)

Twelve-analyzer and detector system at APS 11-BM

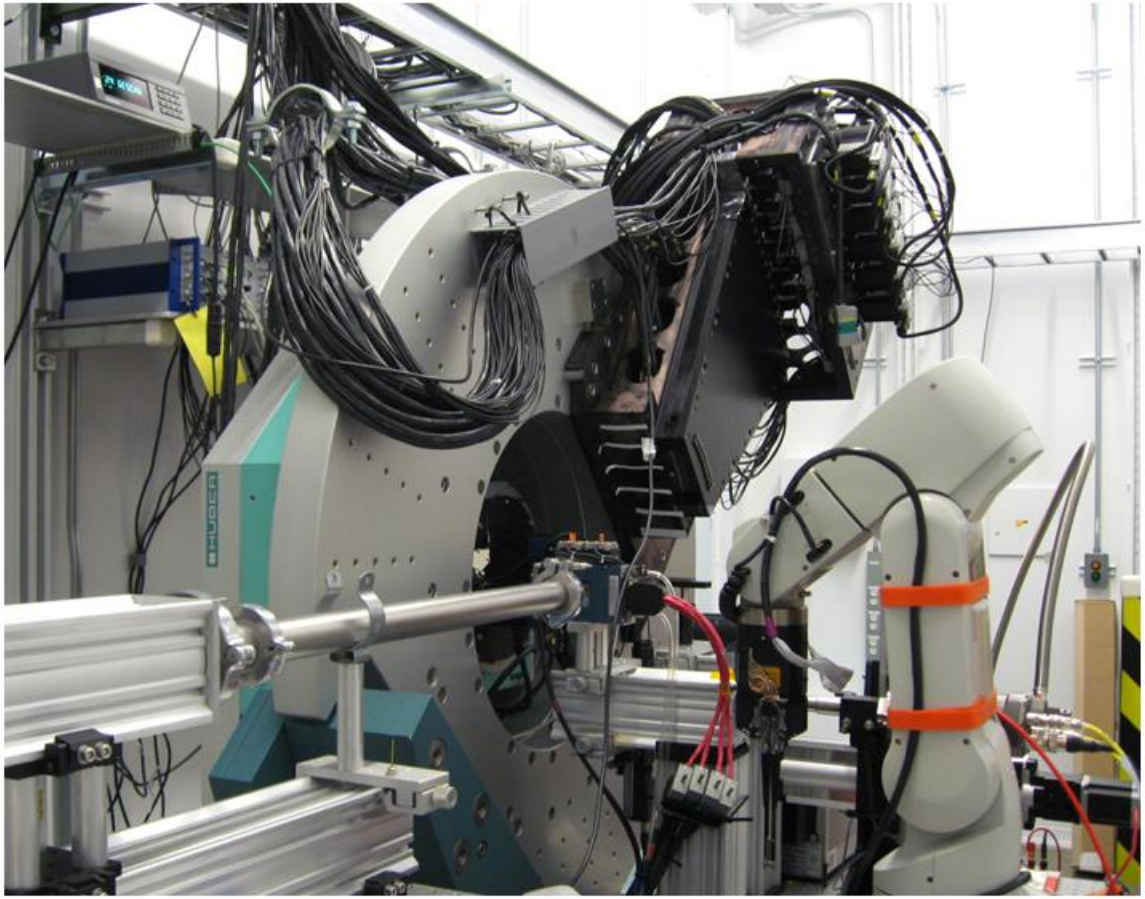

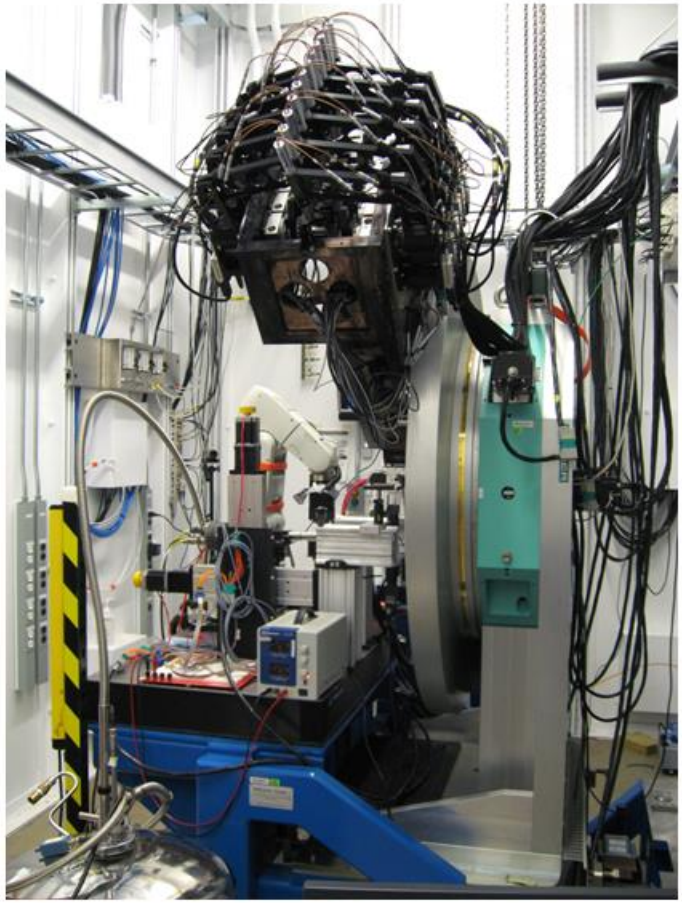

The high-resolution diffractometer has a dimension of 2600 mm (H) X 2100 mm (L) X 1700 mm (W). The main circle of the goniometer has a vertical mounting disk with an outside diameter of 1200 mm.

P. L. Lee et al., J. Sychrotron Rad. (2008) 15, 427-432

Twelve-analyzer and detector system at APS 11-BM

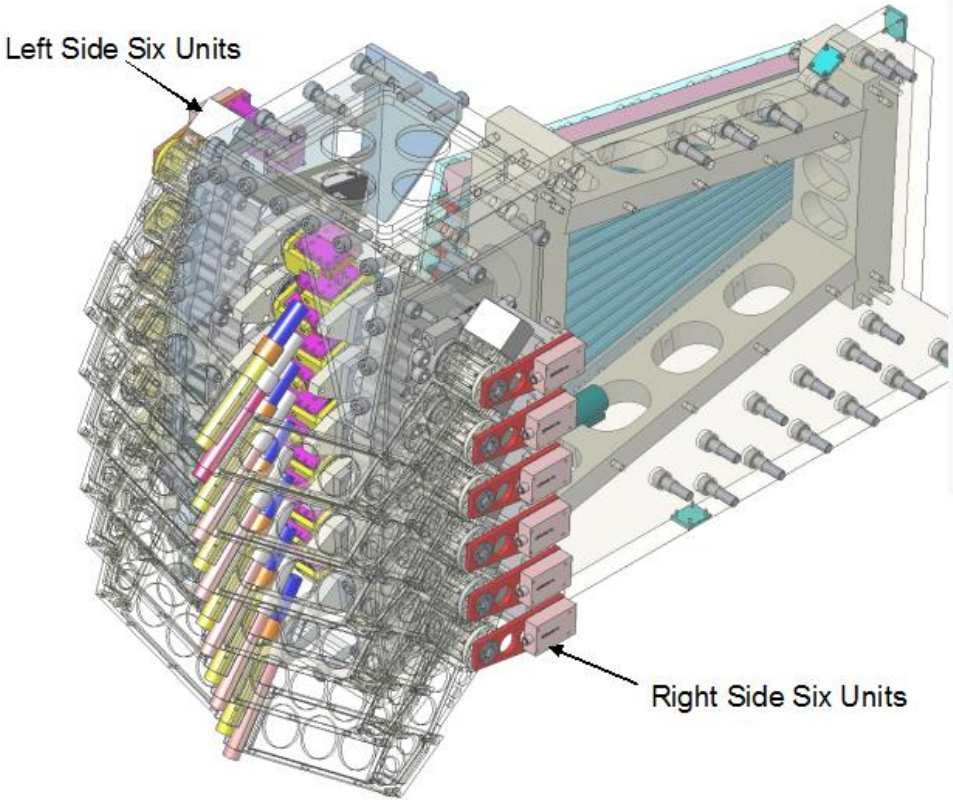

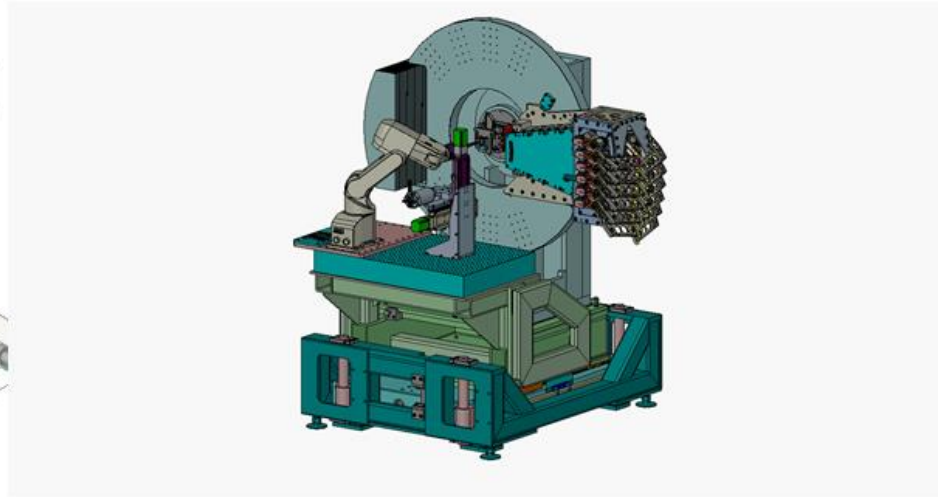

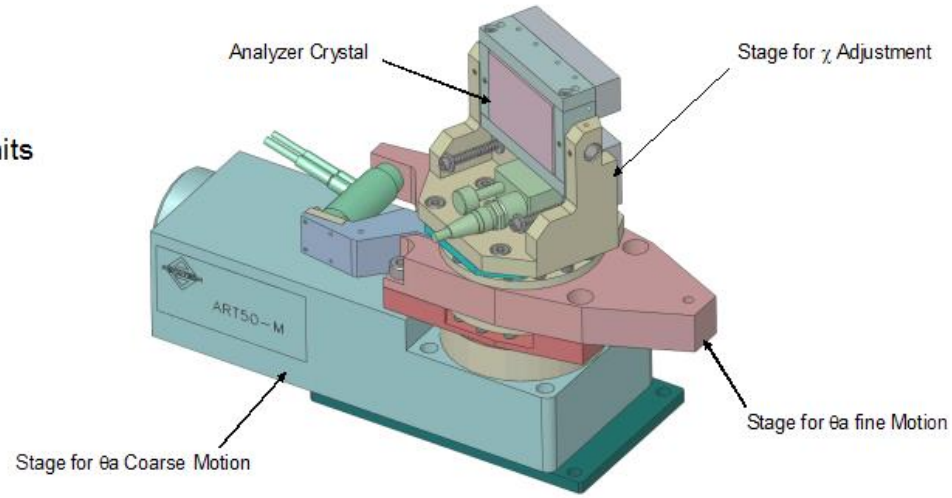

P. L. Lee et al., J. Sychrotron Rad. (2008) 15, 427-432

ACCM for high-resolution x-ray monochromator and analysers

Ultrahigh-Resolution Monochromator and Analyzer for CDFDW Inelastic X-ray Scattering Spectrometer at the APS 30-ID

In 2006, Yuri Shvyd"ko et al. observed three effects in Bragg diffraction of x-rays in backscattering geometry from asymmetrically cut crystals:

- *exact Bragg backscattering takes place not at normal incidence to the reflecting atomic planes,*
- *a well-collimated beam is transformed after the Bragg reflection into a strongly divergent beam with reflection angle dependent on x-ray wavelength (an effect of angular dispersion),*
- *parasitic Bragg reflections accompanying Bragg backreflection are suppressed.*

These effects offer a radically new means for monochromatization of x-rays not limited by the intrinsic width of the Bragg reflection, the so called CDW and CDFDW angular-dispersive monochromators configuration. The abbreviation CDFDW stands for: C – collimating crystal, D – dispersing-element crystal (two D-crystals are used in each CDDW), F- anomalous transmission filter, and W - wavelength-selector crystal. However, there are many optomechanical design challenges on the road for turning a CDDW optical configuration into a practical instrument

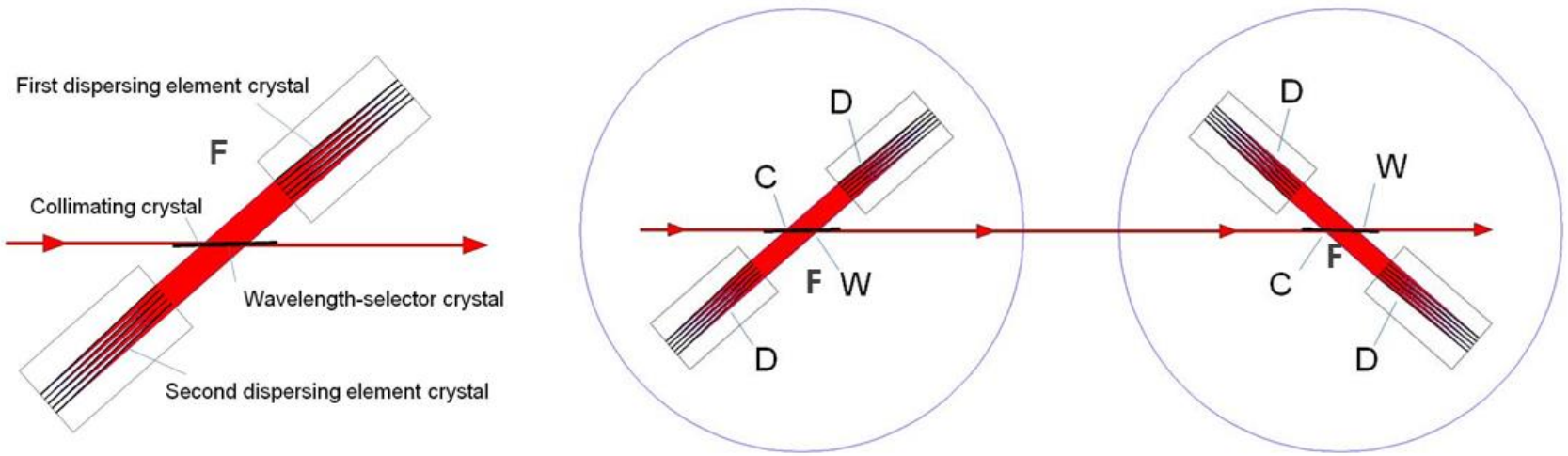

CDFDW Monochromator *CDFDW Analyzer*

Yuri Shvyd'ko, Stanislav Stoupin, Deming Shu, Stephen P. Collins, Kiran Mundboth, John Sutter, and Martin Tolkiehn, "High-contrast sub-millivolt inelastic X-ray scattering for nano- and mesoscale science," Nature Communications, (2014). DOI:10.1038/ncomms5219

ACCM for high-resolution x-ray monochromator and analysers

Ultrahigh-Resolution Monochromator and Analyzer for CDFDW Inelastic X-ray Scattering Spectrometer at the APS 30-ID

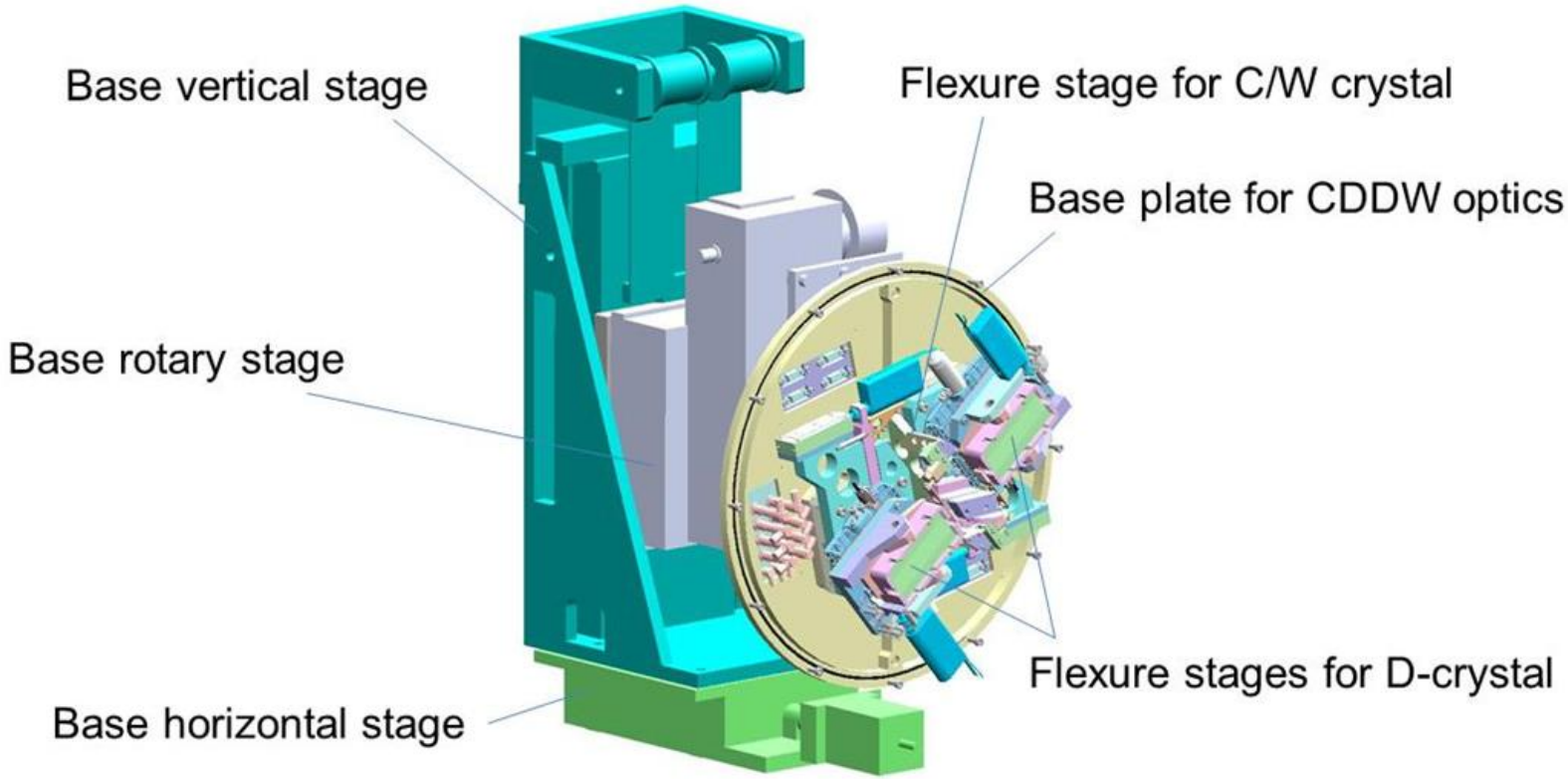

A 3-D model of the base stages for the alignment of the whole CDDW optics.

Yuri Shvyd'ko, Stanislav Stoupin, Deming Shu, Stephen P. Collins, Kiran Mundboth, John Sutter, and Martin Tolkiehn, "High-contrast sub-millivolt inelastic X-ray scattering for nano- and mesoscale science," Nature Communications, (2014). DOI:10.1038/ncomms5219

ACCM for high-resolution x-ray monochromator and analysers

Ultrahigh-Resolution Monochromator and Analyzer for CDFDW Inelastic X-ray Scattering Spectrometer at the APS 30-ID

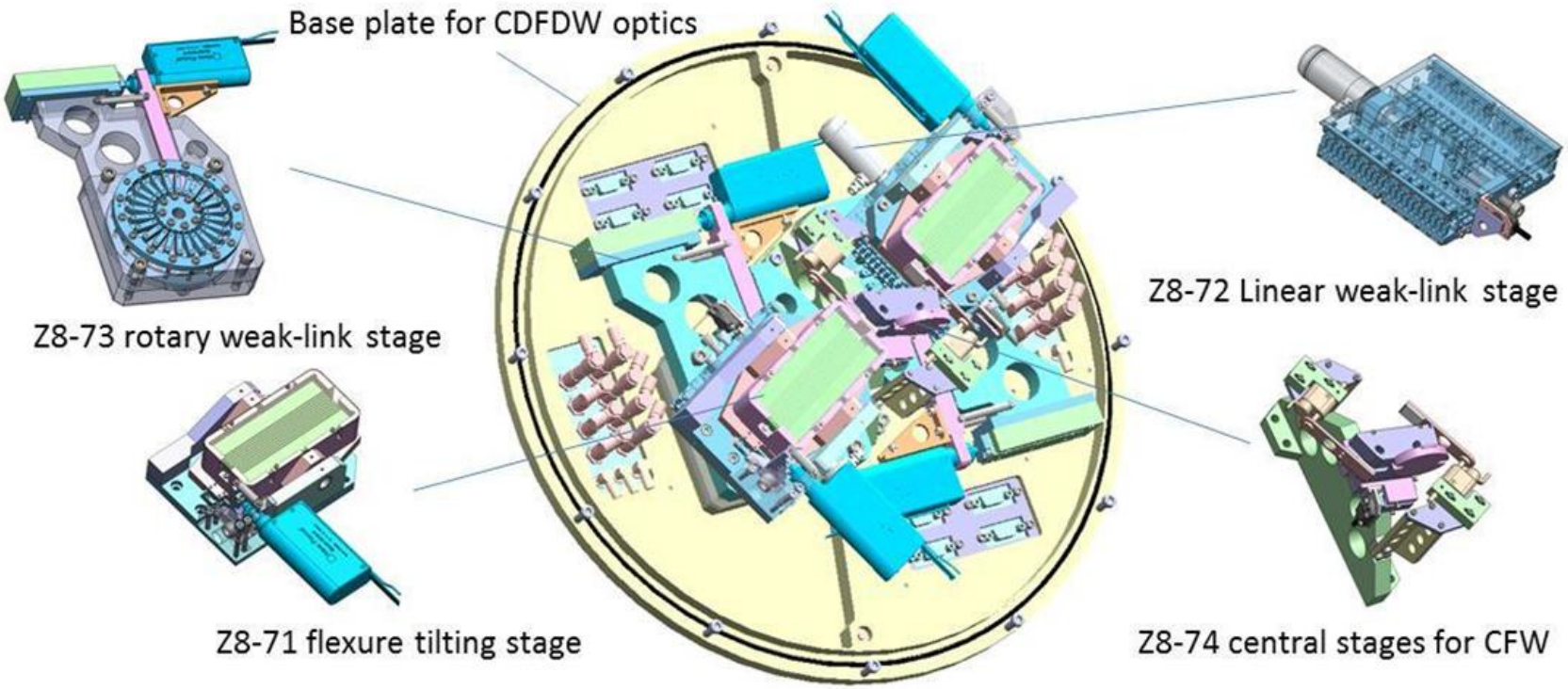

A 3-D model of the CDFDW x-ray monochromator for the prototype of the ultrahigh-resolution IXS spectrometer constructed at the APS.

Yuri Shvyd'ko, Stanislav Stoupin, Deming Shu, Stephen P. Collins, Kiran Mundboth, John Sutter, and Martin Tolkiehn, "High-contrast sub-millivolt inelastic X-ray scattering for nano- and mesoscale science," Nature Communications, (2014). DOI:10.1038/ncomms5219

ACCM for high-resolution x-ray monochromator and analysers

Ultrahigh-Resolution Monochromator and Analyzer for CDFDW Inelastic X-ray Scattering Spectrometer at the APS 30-ID

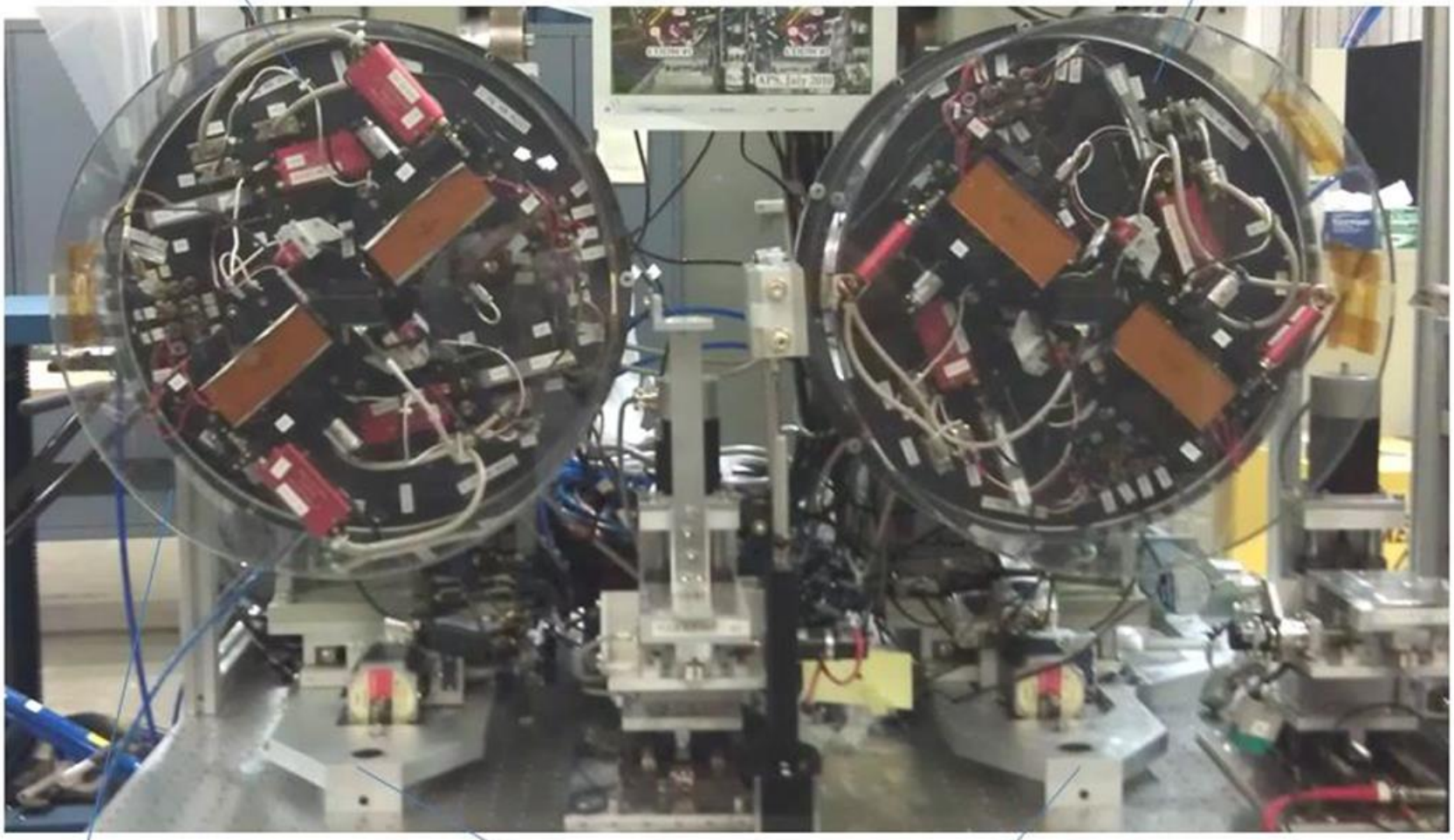

A photograph of the prototype of the ultrahigh-resolution IXS spectrometer designed, constructed, and tested at undulator-based beamline 30-ID at the APS.`

Yuri Shvyd'ko, Stanislav Stoupin, Deming Shu, Stephen P. Collins, Kiran Mundboth, John Sutter, and Martin Tolkiehn, "High-contrast sub-millivolt inelastic X-ray scattering for nano- and mesoscale science," Nature Communications, (2014). DOI:10.1038/ncomms5219

High-stiffness weak-link mechanism for linear motion reduction

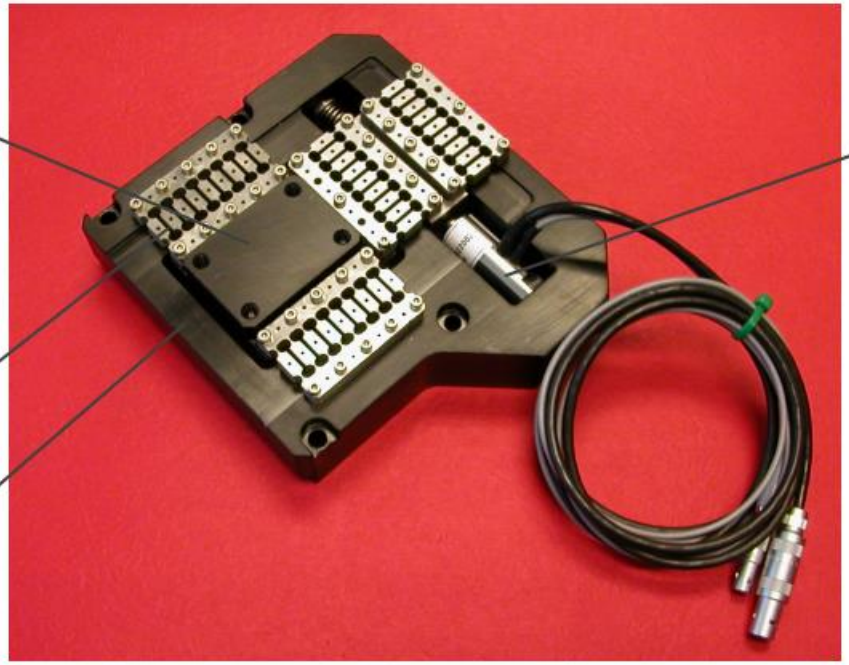

Using the same technique described in the section for the weak-link mechanism for a high-energy- resolution monochromator, we have developed a novel stage using a high-stiffness weak-link mechanism to perform linear motion closed-loop control at the sub-100-pm level with micron-level travel range. The structure consists of four groups of overconstrained weak-link parallelogram mechanisms made with lithography techniques. Driving sensitivity better than 30 pm was demonstrated with this weak-link linear-motion-reduction mechanism with a 1-micron travel range.

D. Shu, Y. Han, T. S. Toellner, and E. E. Alp, Proc. SPIE, Vol. 4771 (2002) 78-90

A one-dimensional linear actuator system with subnanometer closed-loop control resolution and centimeters travel range for an atomic force microscope

Prototype of a laser Doppler linear actuator system (LDLA) with sub-angstrom sensor resolution and positioning resolution over a 50-mm travel range.

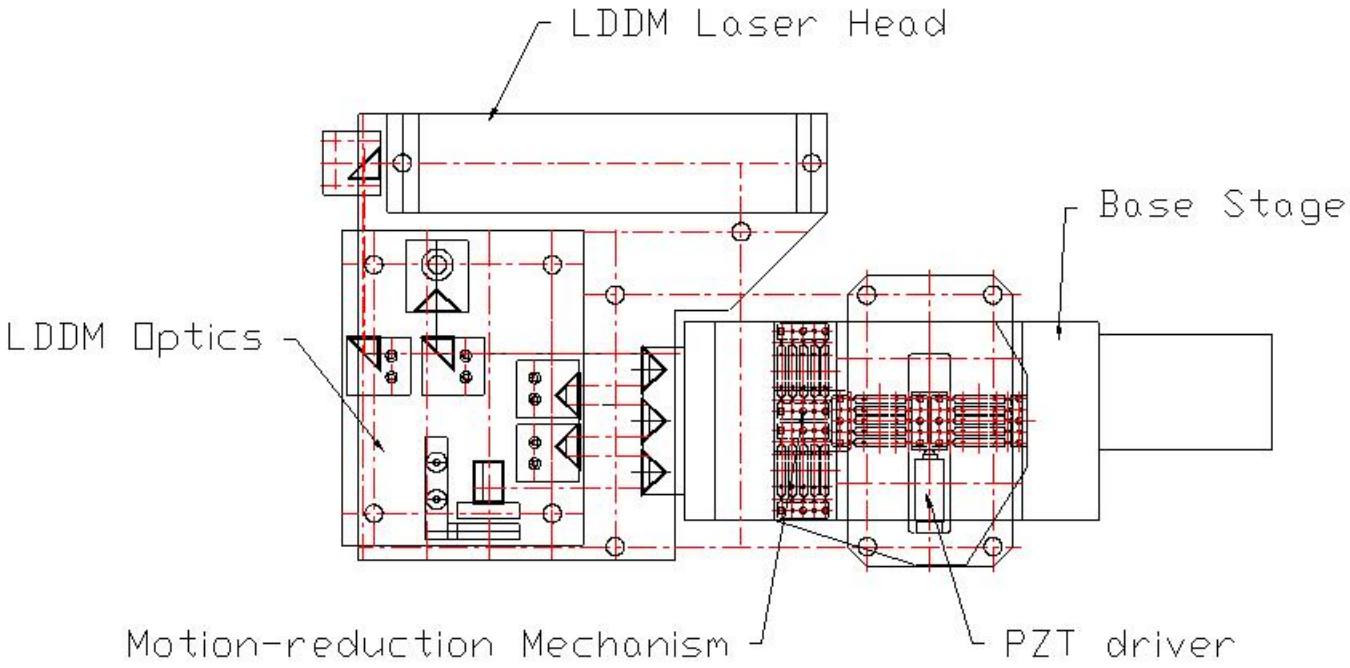

D. Shu, Y. Han, T. S. Toellner, and E. E. Alp, Proc. SPIE, Vol. 4771 (2002) 78-90

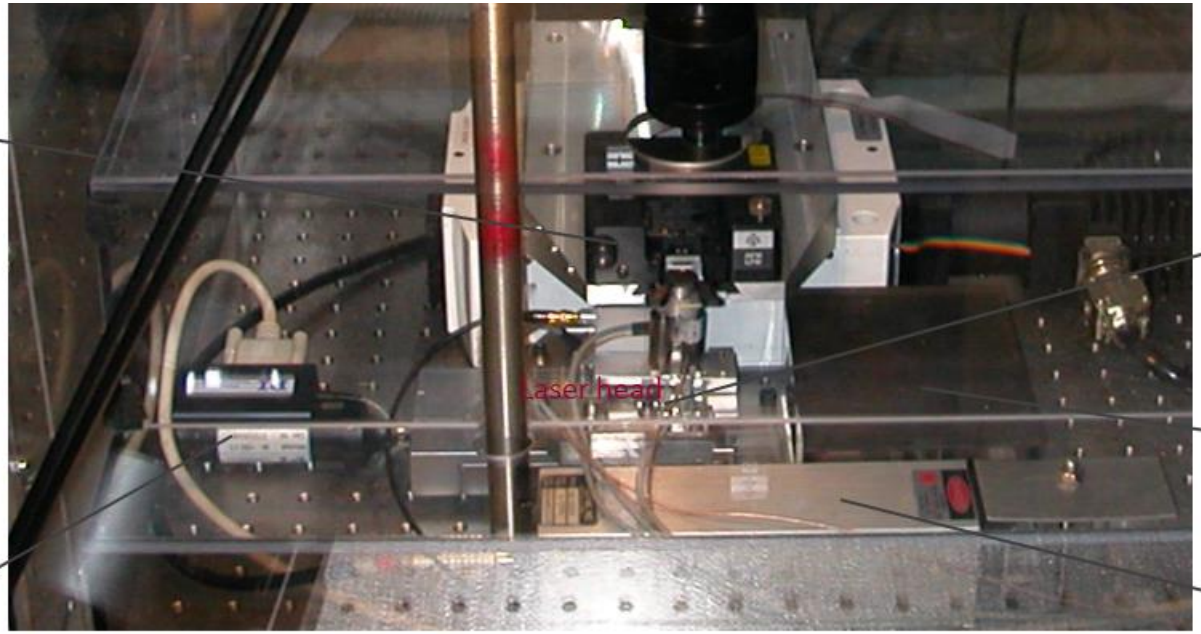

A one-dimensional linear actuator system based on the above high-stiffness weak-link technique and LDDM with multiple-reflection optics has been tested. This photo shows the one-dimensional laser Doppler linear actuator (LDLA) system for an atomic force microscope. In this coarse/fine closed-loop control setup, a PZT-driven motion-reduction mechanism was mounted on the top of a DC-motor-driven stage to drive the motion object (in this example, a sample holder for an atomic force microscope).

D. Shu, Y. Han, T. S. Toellner, and E. E. Alp, Proc. SPIE, Vol. 4771 (2002) 78-90

A one-dimensional linear actuator system with subnanometer closed-loop control resolution and centimeters travel range for an atomic force microscope

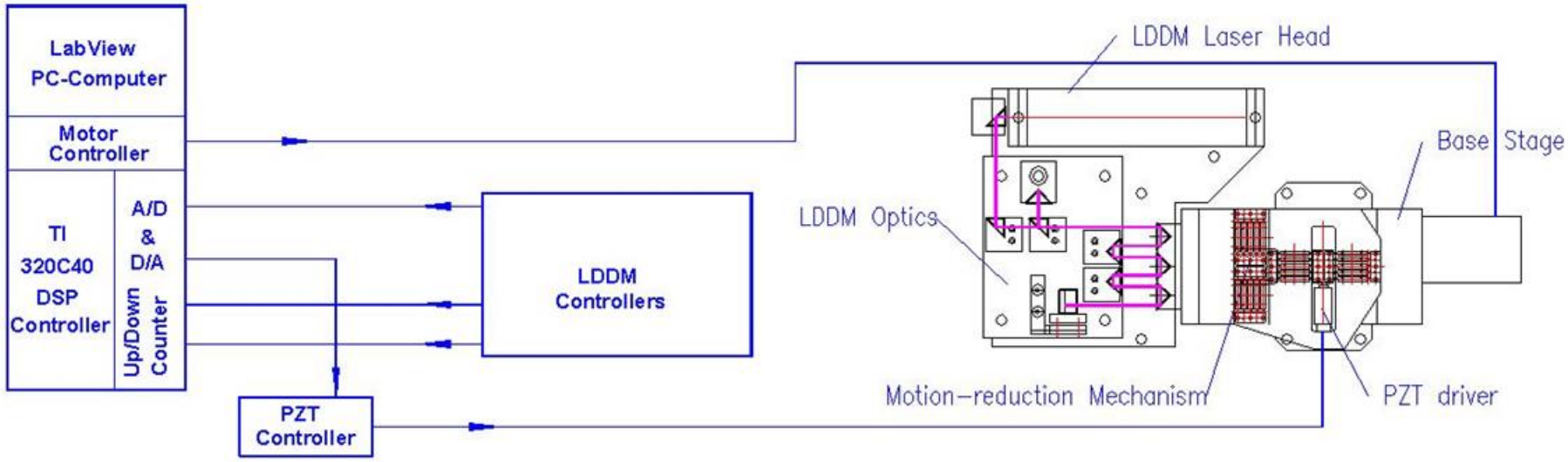

A laser Doppler displacement meter with an optical resolution extension assembly was used to measure the sample holder motion in the 25-mm range with sub-100-pm resolution. The LDDM position signal is fed back through a TI 320C40 DSP controller to control the PZT. The PZT drove the motion-reduction mechanism with sub-100-pm resolution to stabilize the motion. The DSP controller also provides digital filtering for the LDDM position signal. The system control computer synchronized the stage position and PZT feedback lock-in point with the LDDM position signal.

D. Shu, Y. Han, T. S. Toellner, and E. E. Alp, Proc. SPIE, Vol. 4771 (2002) 78-90

A one-dimensional linear actuator system with subnanometer closed-loop control resolution and centimeters travel range for an atomic force microscope

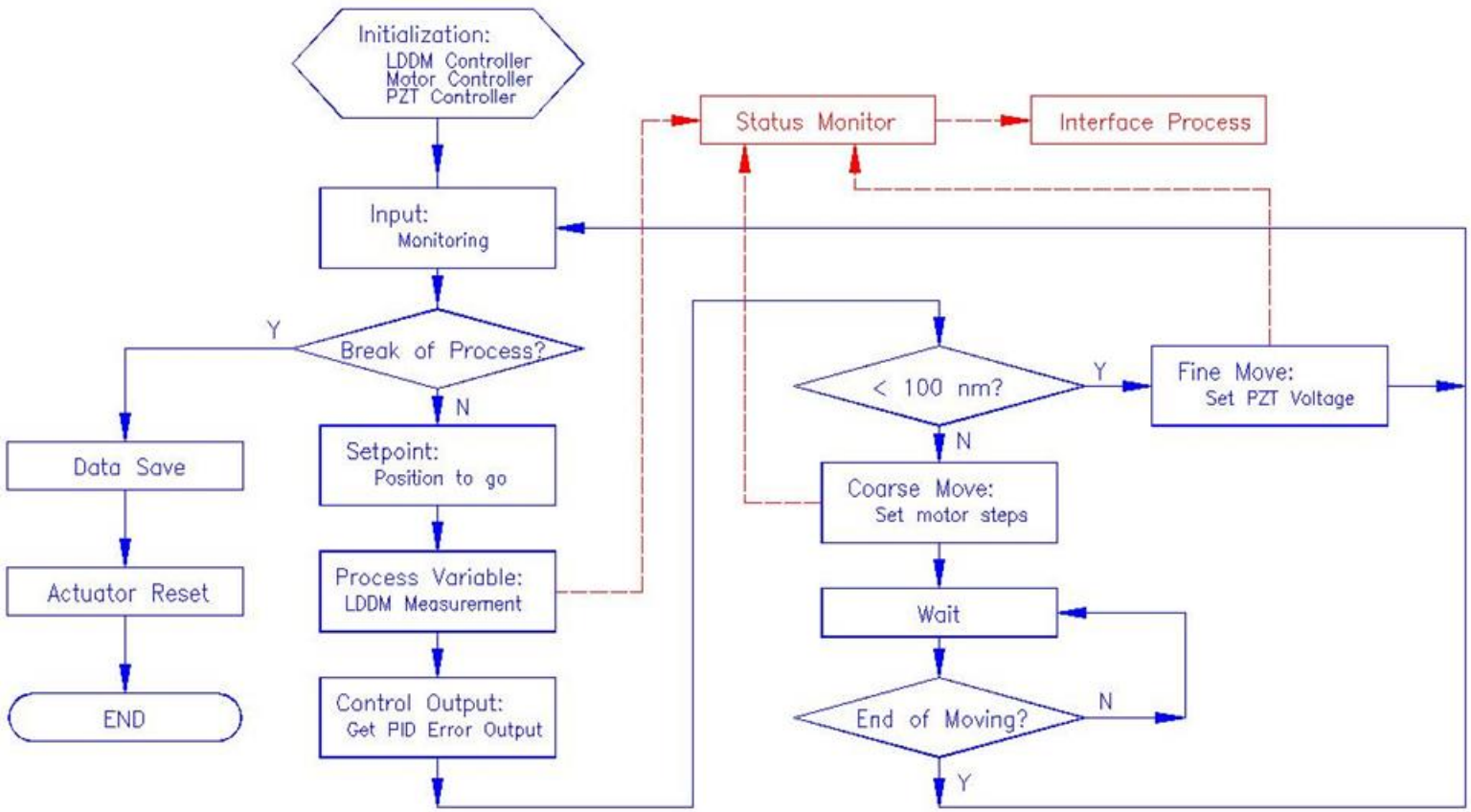

D. Shu, Y. Han, T. S. Toellner, and E. E. Alp, Proc. SPIE, Vol. 4771 (2002) 78-90

A one-dimensional linear actuator system with subnanometer closed-loop control resolution and centimeters travel range for an atomic force microscope

Test of a LDLA closed-loop feedback system

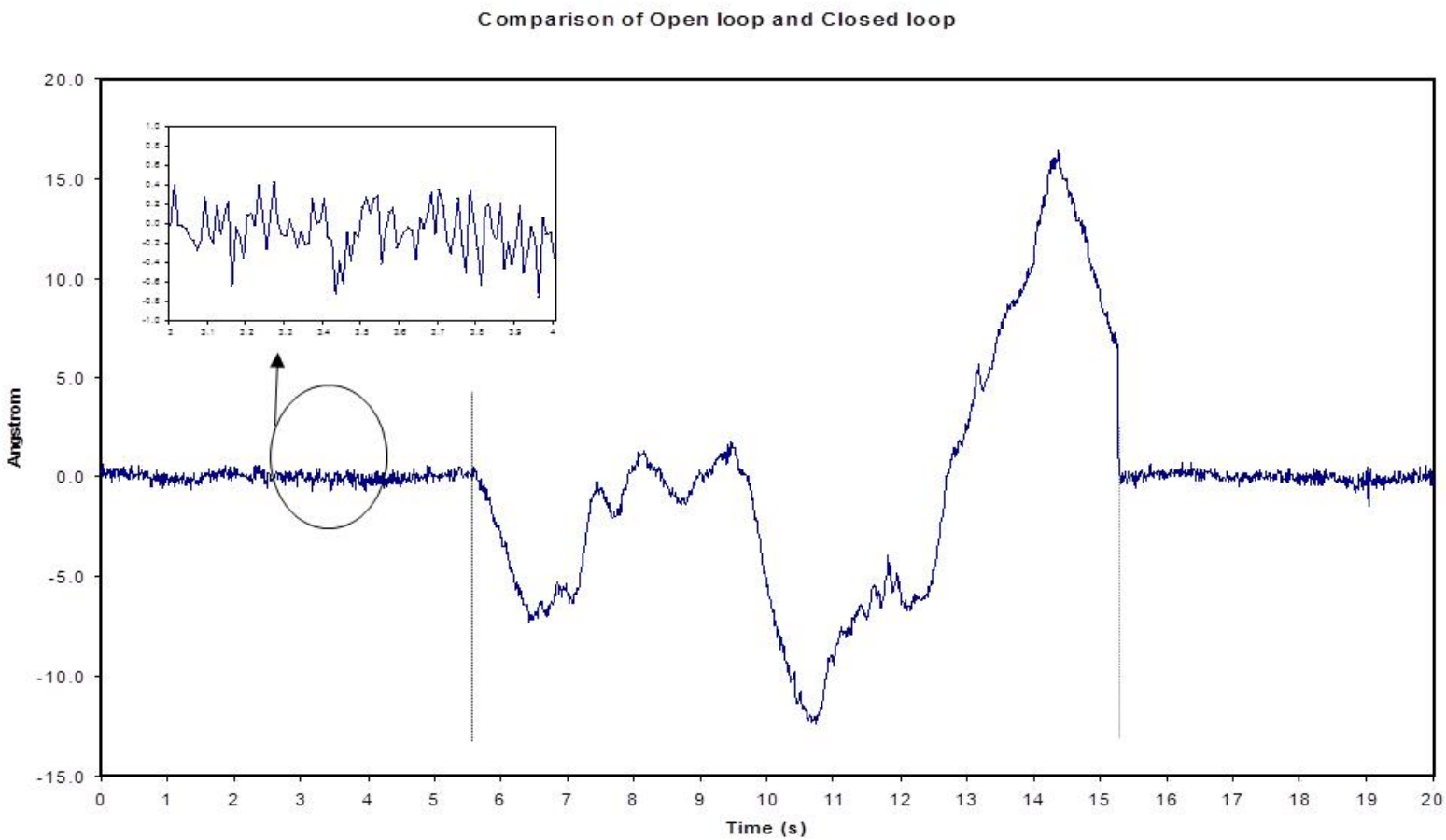

D. Shu, Y. Han, T. S. Toellner, and E. E. Alp, Proc. SPIE, Vol. 4771 (2002) 78-90

A one-dimensional linear actuator system with subnanometer closed-loop control resolution and centimeters travel range for an atomic force microscope

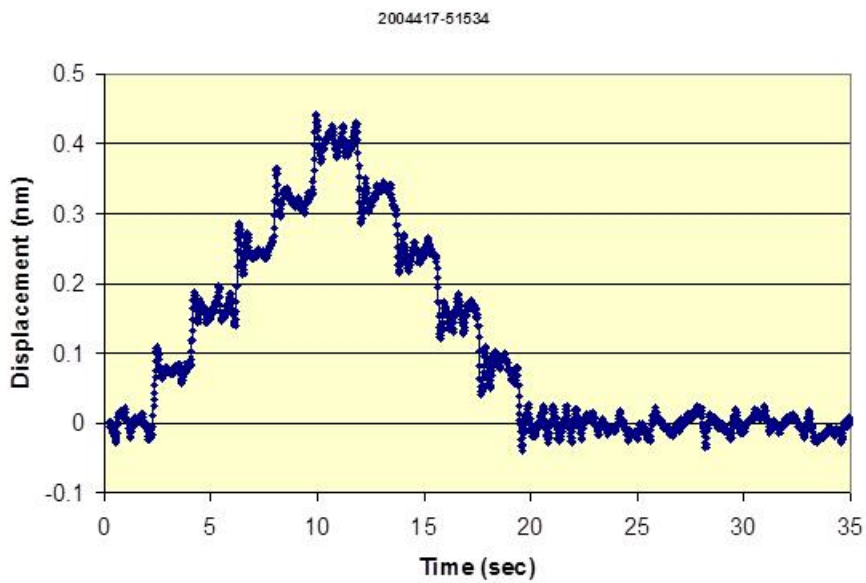

Resolution test of the one-dimensional laser Doppler linear actuator closed-loop control system. A series of 100-pm (left side) and 80-pm (right side) steps have been demonstrated.

D. Shu, Y. Han, T. S. Toellner, and E. E. Alp, Proc. SPIE, Vol. 4771 (2002) 78-90

Design of an X-ray Nanoprobe Prototype

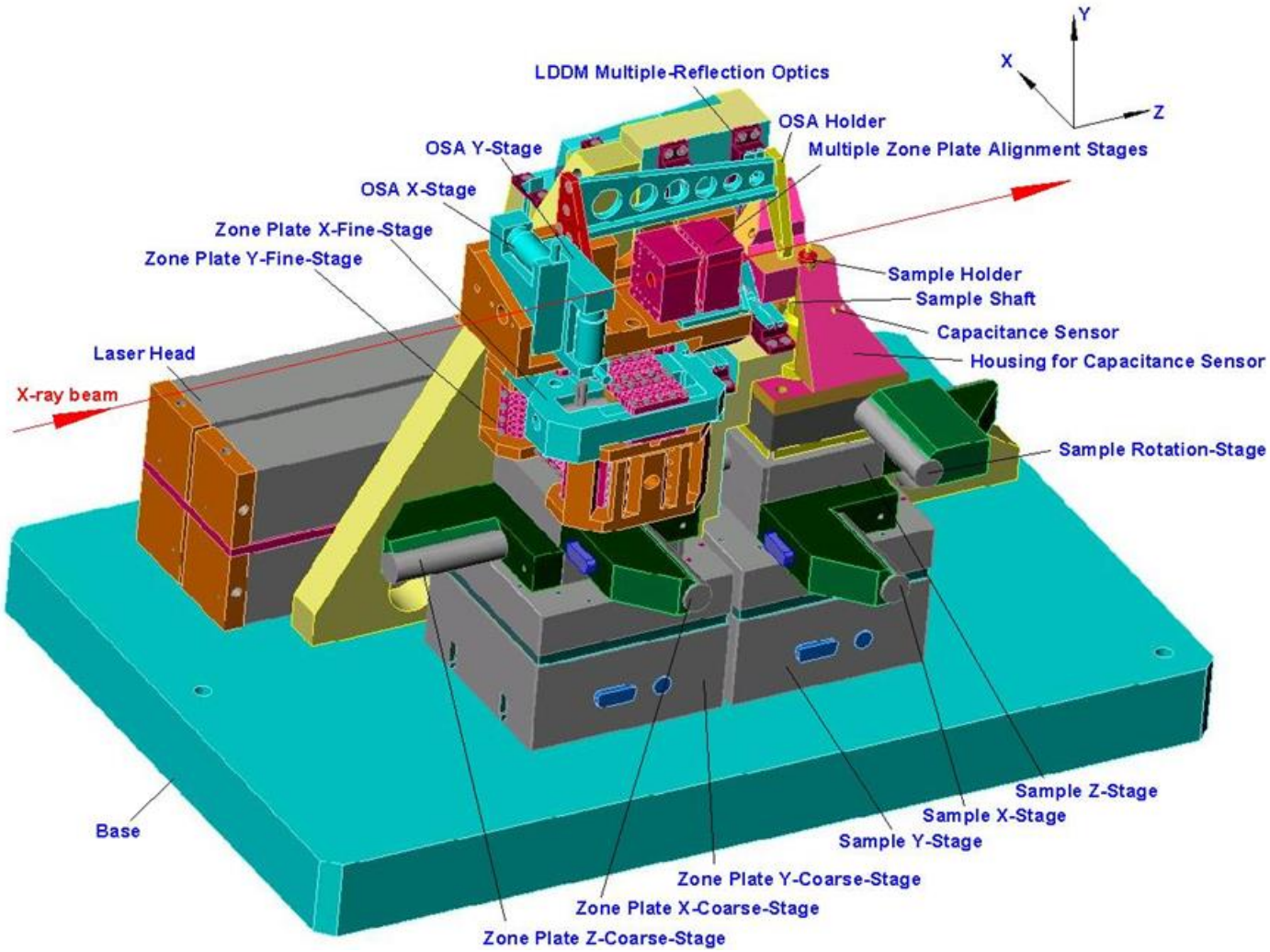

D. Shu et al., Proc. SPIE, Vol. 5877 (2005) 58770E, DOI: 10.1117/12.617723

Design of an X-ray Nanoprobe Prototype

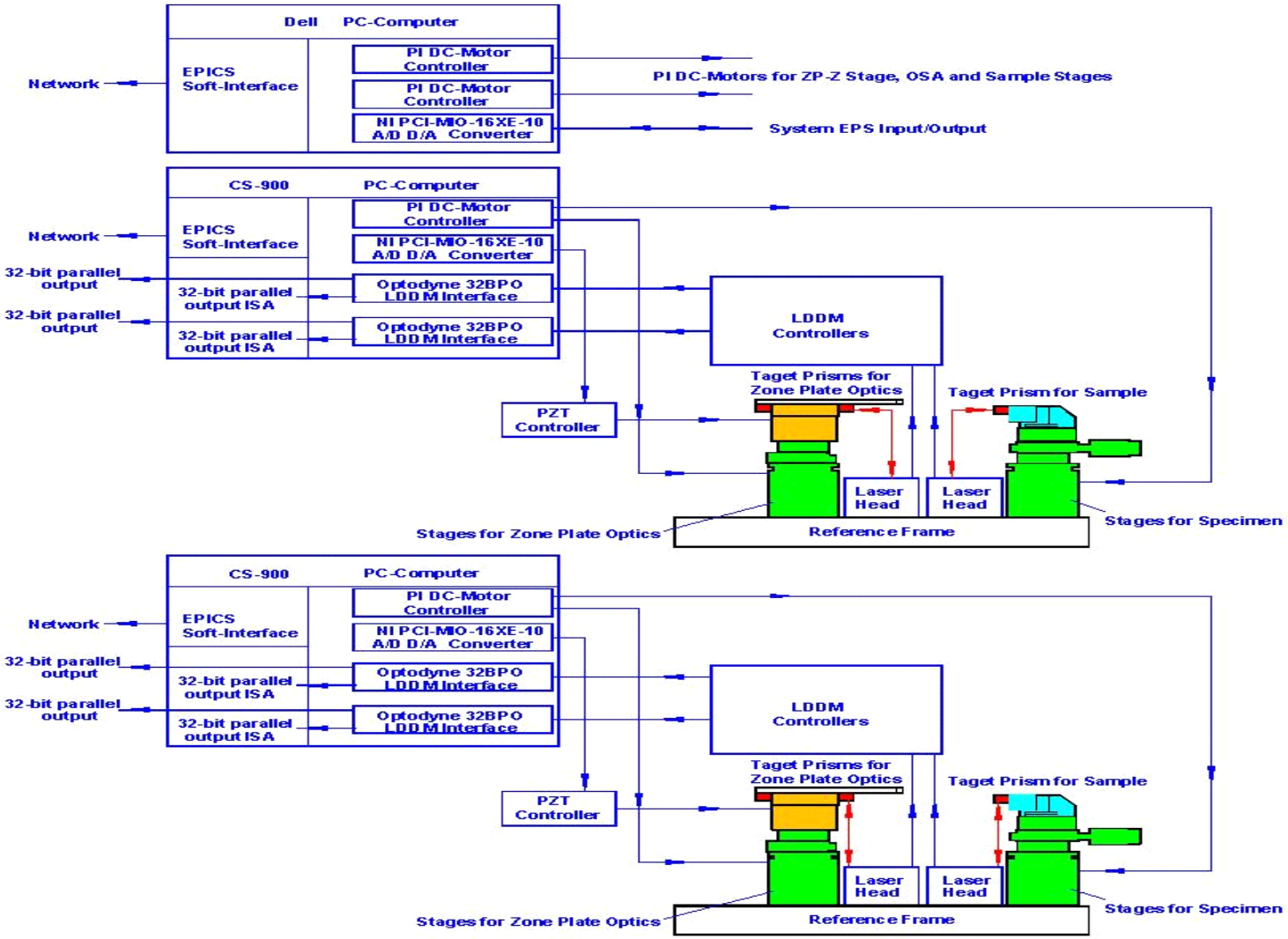

D. Shu et al., Proc. SPIE, Vol. 5877 (2005) 58770E, DOI: 10.1117/12.617723

Design of an x-ray nanoprobe prototype

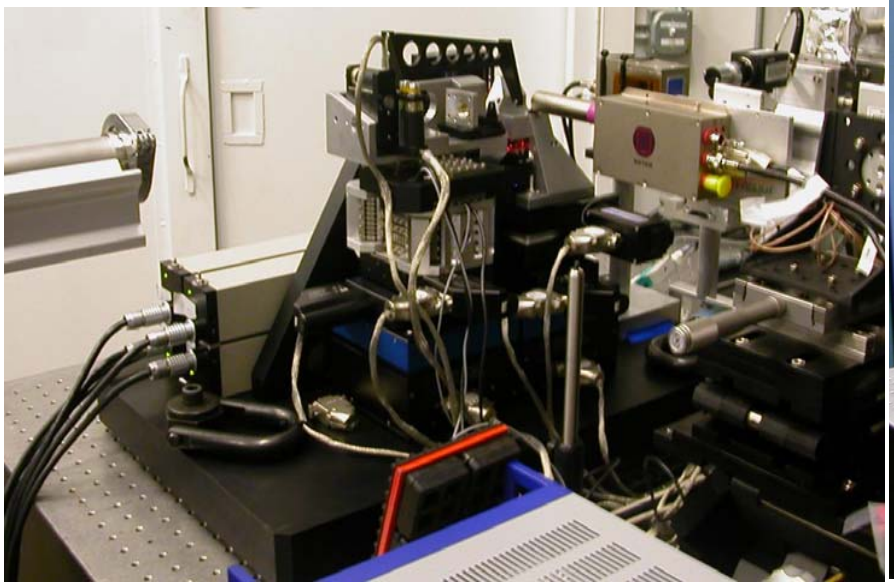

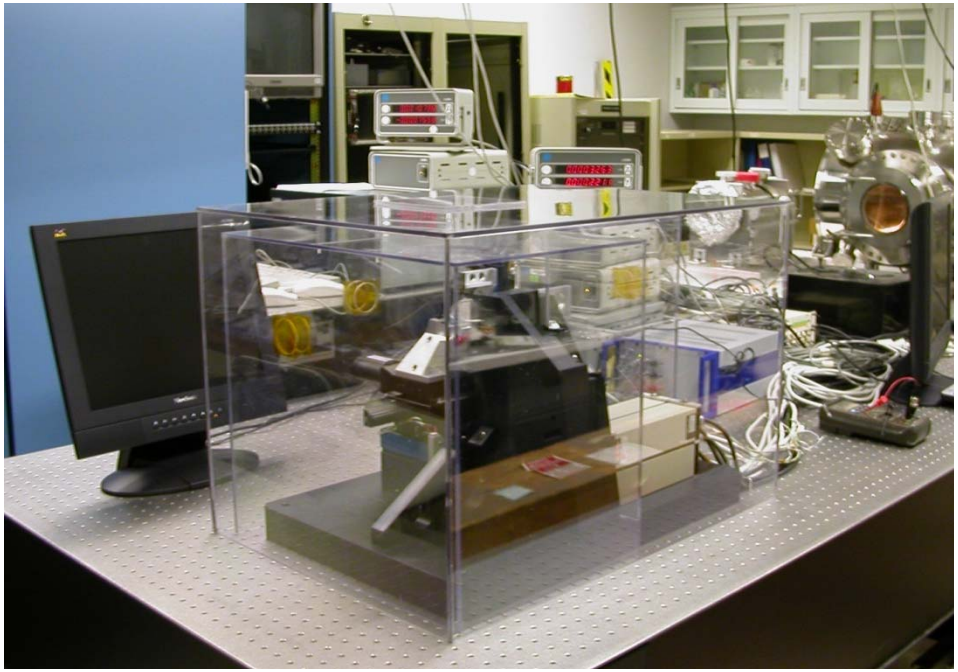

We started the x-ray nanoprobe prototype online commissioning in August 2003. These are photographs of the prototype at the APS 8-ID-E experimental station (left) and in a test laboratory (right).

D. Shu et al., Proc. SPIE, Vol. 5877 (2005) 58770E, DOI: 10.1117/12.617723

Design of an x-ray nanoprobe prototype

TABLE 1. Design specifications for the x-ray nanoprobe prototype laser Doppler encoder system

Overall Dimension (mm)	450 (X) x 450 (Y) x 650 (Z)
Encoder type	Two-dimensional differential laser Doppler encoder with multiple- reflection Optics [4,5,6,7]
Laser source	Frequency stabilized He-Ne Class II
Multiple-reflection optics path	16
Displacement resolution (nm)	0.125
Measurement range (mm)	12 (X) x 12 (Y) x 12 (Z)

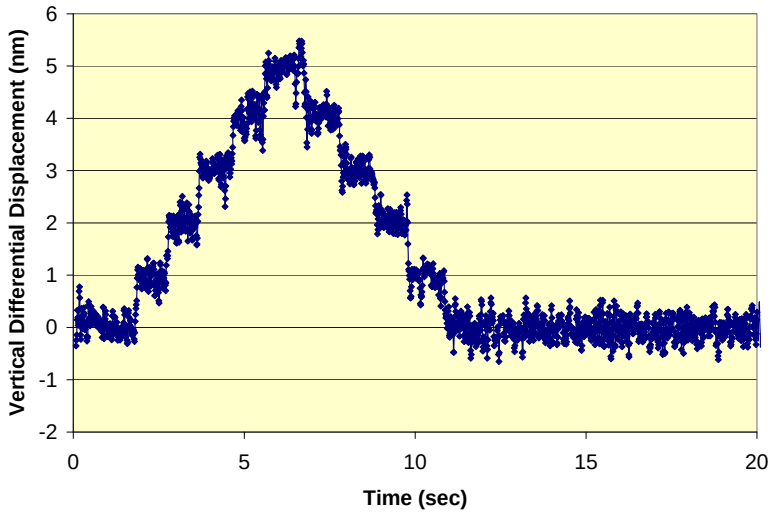

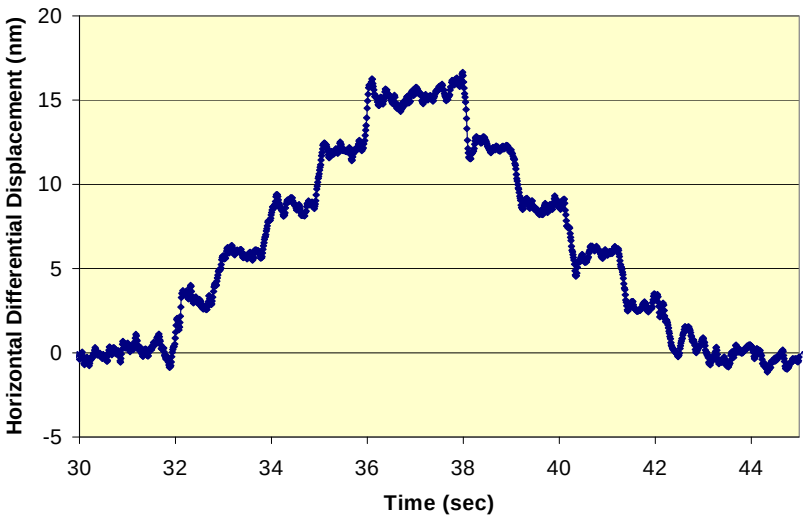

Closed-loop differential displacement test for the prototype scanning stage system for the x-ray nanoprobe at the APS 8-ID-E station, horizontal: left side; vertical: right side. A series of 1-nm and 3-nm differential vertical and horizontal displacement steps (between zone-plate holder and sample holder) have been demonstrated with closed-loop control.

D. Shu et al., Proc. SPIE, Vol. 5877 (2005) 58770E, DOI: 10.1117/12.617723

Design of an x-ray nanoprobe prototype

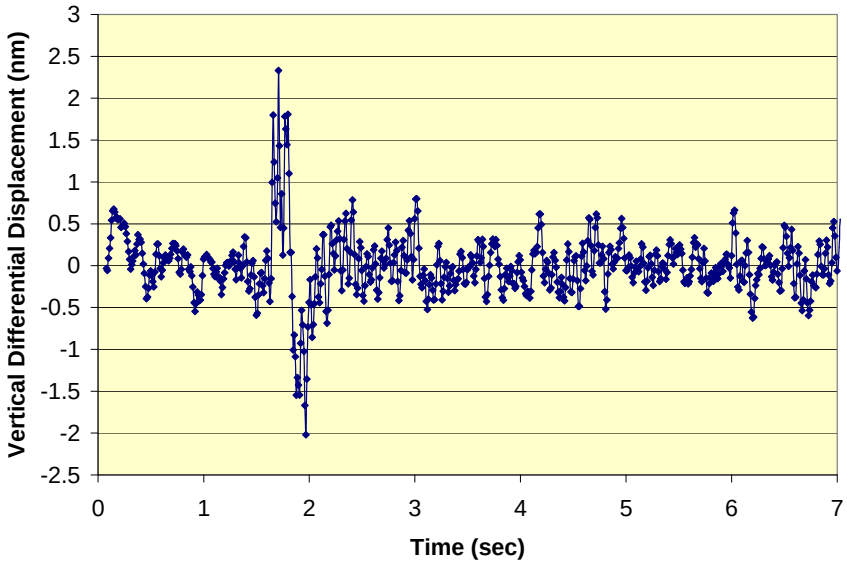

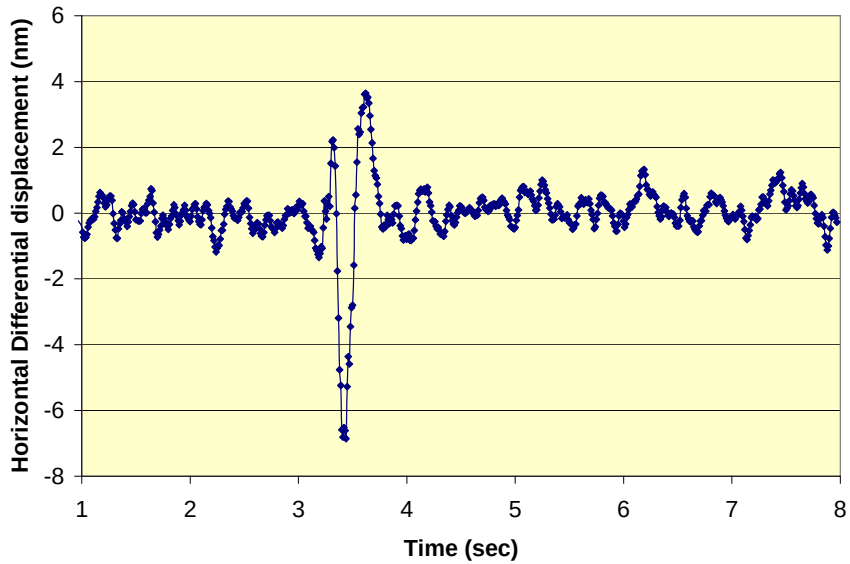

Active vibration control test for the prototype scanning stage system for the x-ray nanoprobe at the APS 8-ID-E station, vertical: left side; horizontal: right side. During this test, the closed-loop control system performed a damping action to a single external mechanical disturbance (an 80-kg mass dropped to the floor from a 0.2-m height at a distance of 3 m).

D. Shu et al., Proc. SPIE, Vol. 5877 (2005) 58770E, DOI: 10.1117/12.617723

Design of an x-ray nanoprobe prototype

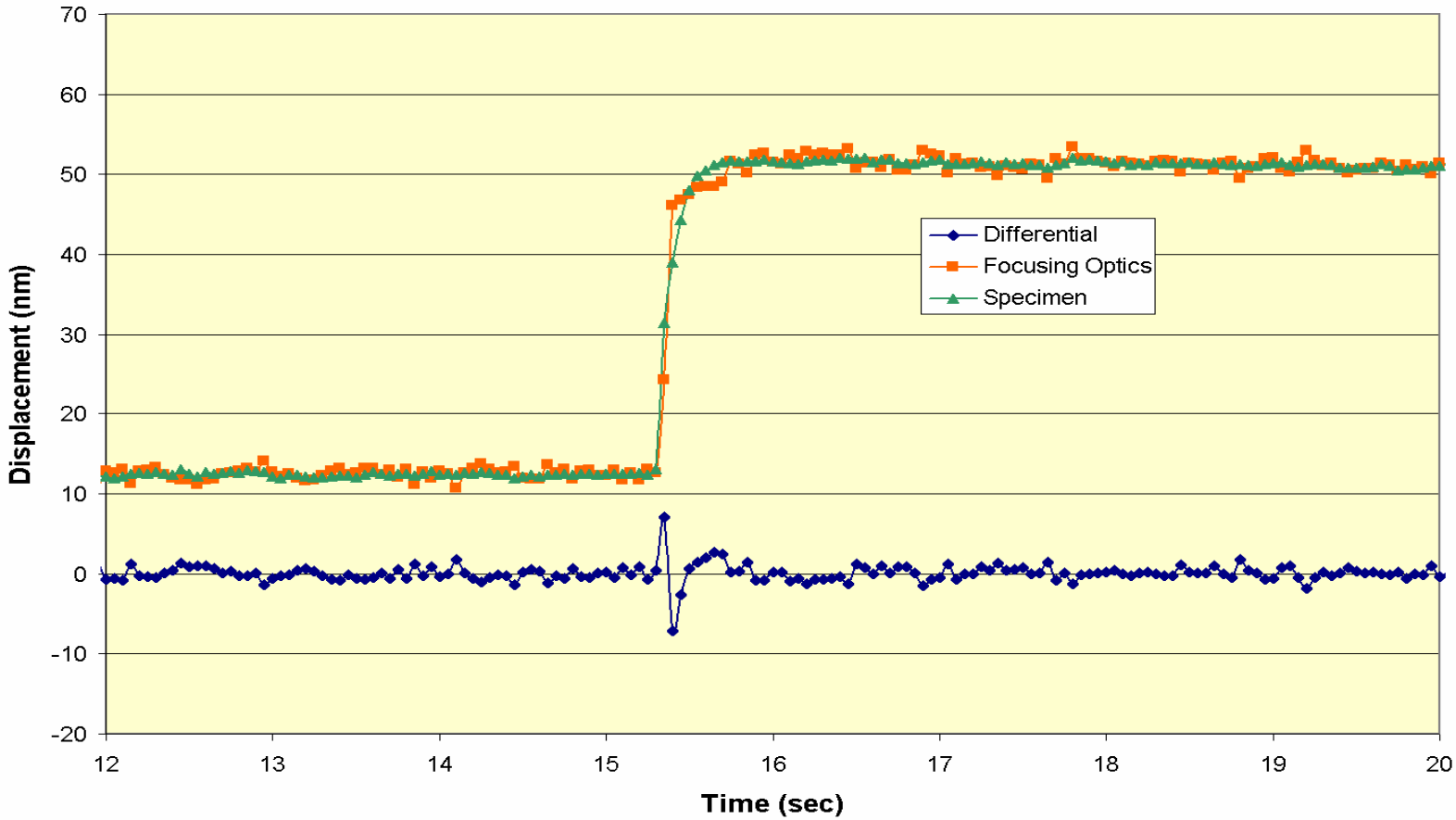

D. Shu et al., Proc. SPIE, Vol. 5877 (2005) 58770E, DOI: 10.1117/12.617723

Development of the Argonne CNM hard x-ray nanoprobe at APS sector 26

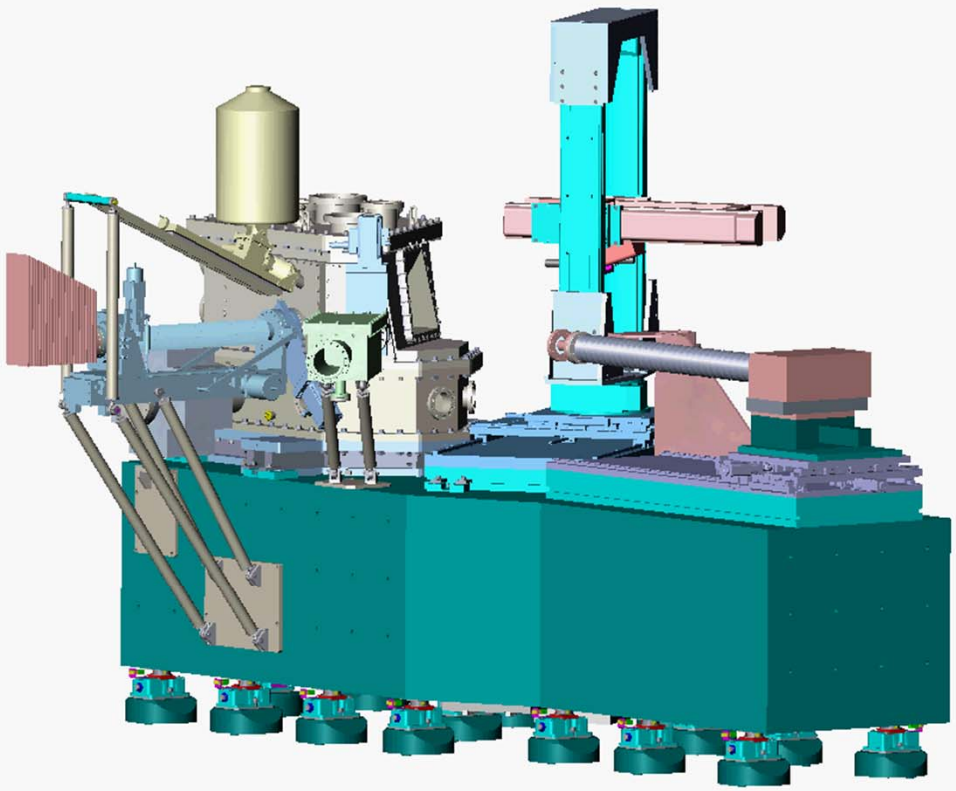

- ***The nanoprobe beamline provides fluorescence, diffraction, transmission, and tomographic imaging with a spatial resolution of as small as 30 nm.***
- ***Typical operation provides a spatial resolution of 50 nm in the spectral range of 8-12 keV.***

D. Shu et al., SRI-2006 Conf. Proc. 879, AIP (2007) 1321-1324

Mechanical general layout design for CNM nanoprobe instrument

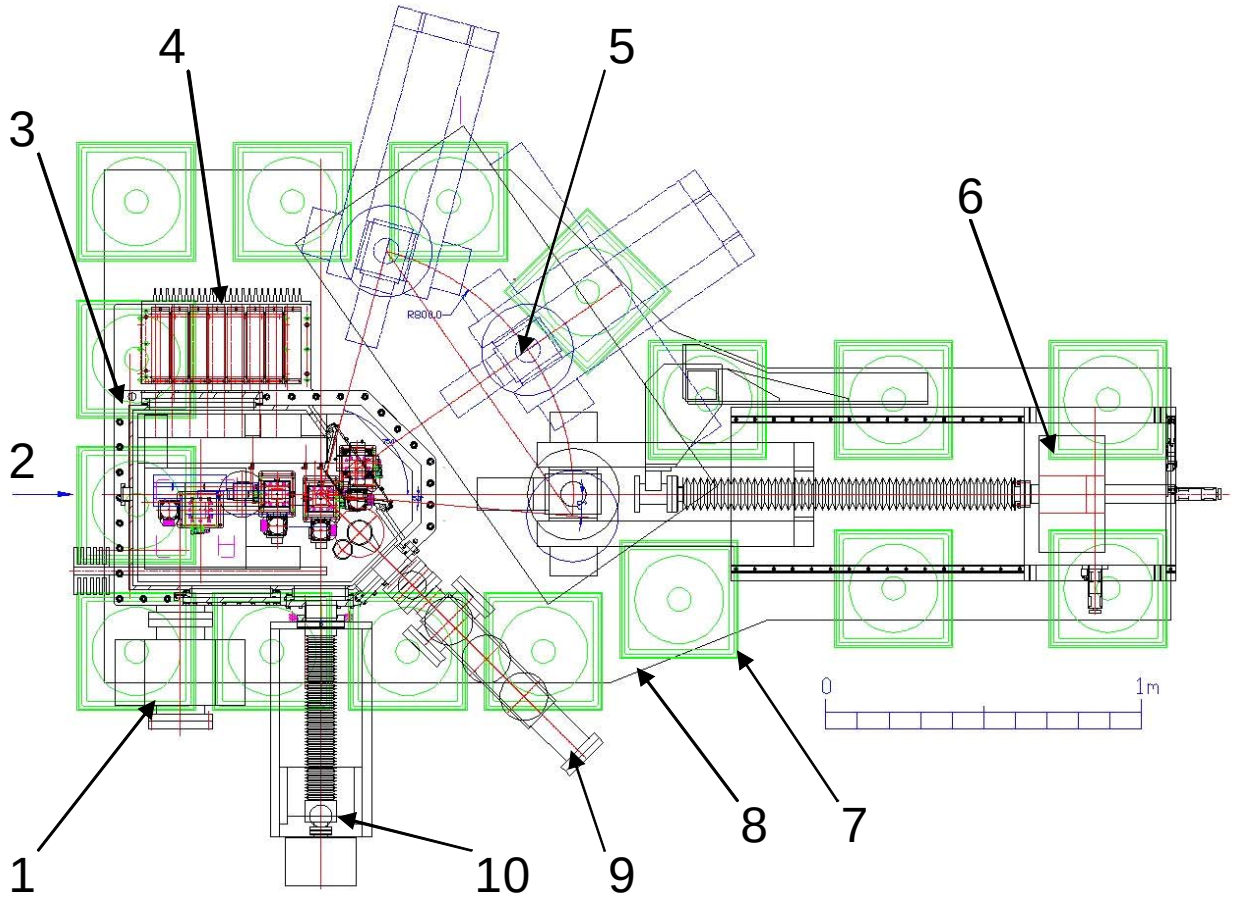

Top view of the hard x-ray nanoprobe instrument. (1) Ion pump; (2) Incident beam; (3) Instrument Chamber; (4) Laser head for LDDM; (5) Diffraction detector; (6) Transmission imaging detector; (7) Isolators below base; (8) Granite base; (9) Airlock for specimen exchange; (10) Fluorescence detector.

D. Shu et al., SRI-2006 Conf. Proc. 879, AIP (2007) 1321-1324

Mechanical general layout design for CNM nanoprobe instrument

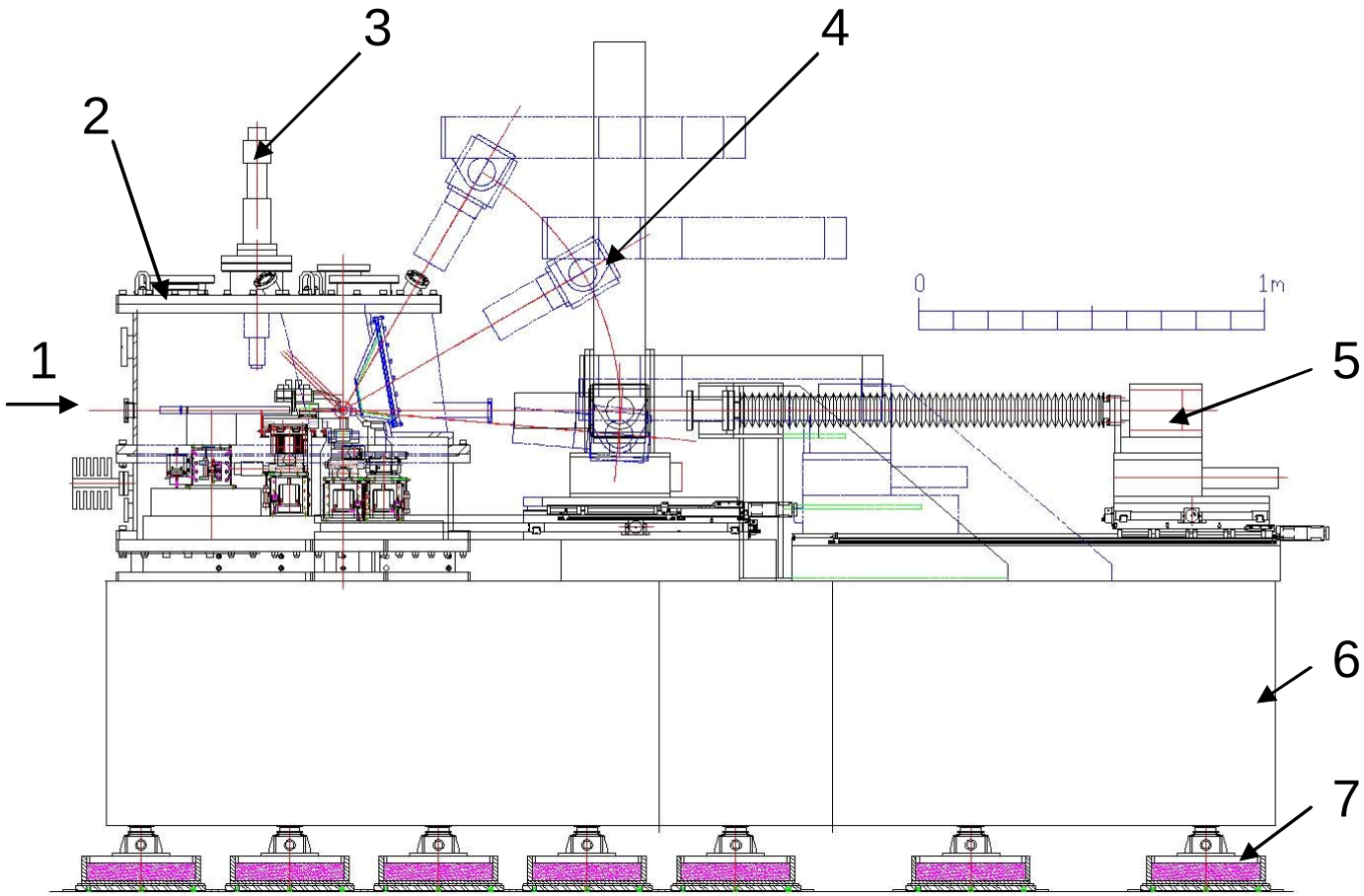

Side view of the hard x-ray nanoprobe instrument. (1) Incident beam; (2) Instrument chamber; (3) Optical microscope; (4) Diffraction detector; (5) Transmission imaging detector; (6) Granite base; (7) Isolators.

D. Shu et al., SRI-2006 Conf. Proc. 879, AIP (2007) 1321-1324

Positioning stage and encoder systems in central instrument chamber

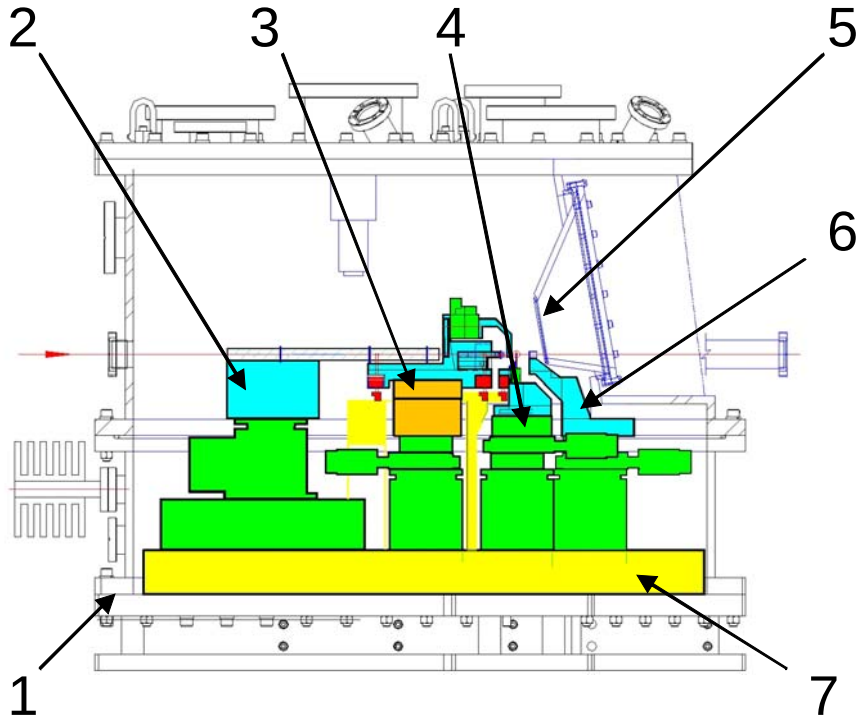

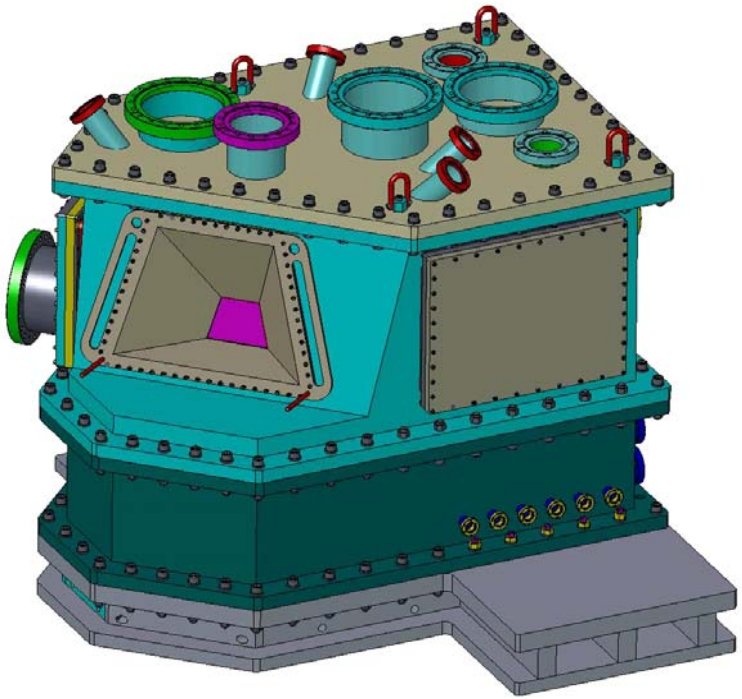

Left: A schematic side view of the nanoprobe instrument chamber. (1) Vacuum chamber; (2) CM; (3) FOM; (4) SM; (5) Beryllium window; (6) IOM; (7) Invar reference base. Right: A 3-D model of the nanoprobe instrument chamber.

D. Shu et al., SRI-2006 Conf. Proc. 879, AIP (2007) 1321-1324

Design challenges for the microdiffraction with nanoprobe

Limited by the geometric configuration of the nanoprobe instrument, it is not feasible to use a traditional goniometer to achieve the motions needed for a microdiffraction detector.

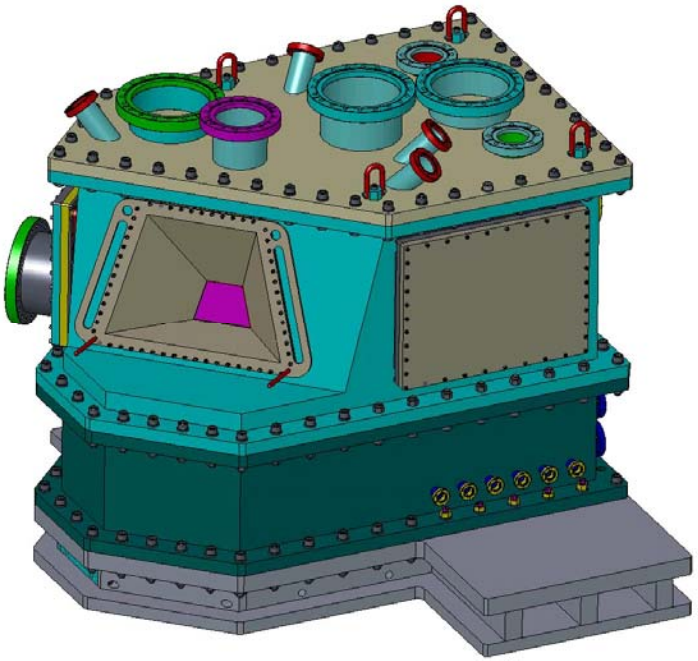

D. Shu et al., SRI-2006 Conf. Proc. 879, AIP (2007) 1321-1324

Commissioning of the Argonne nanoprobe instrument

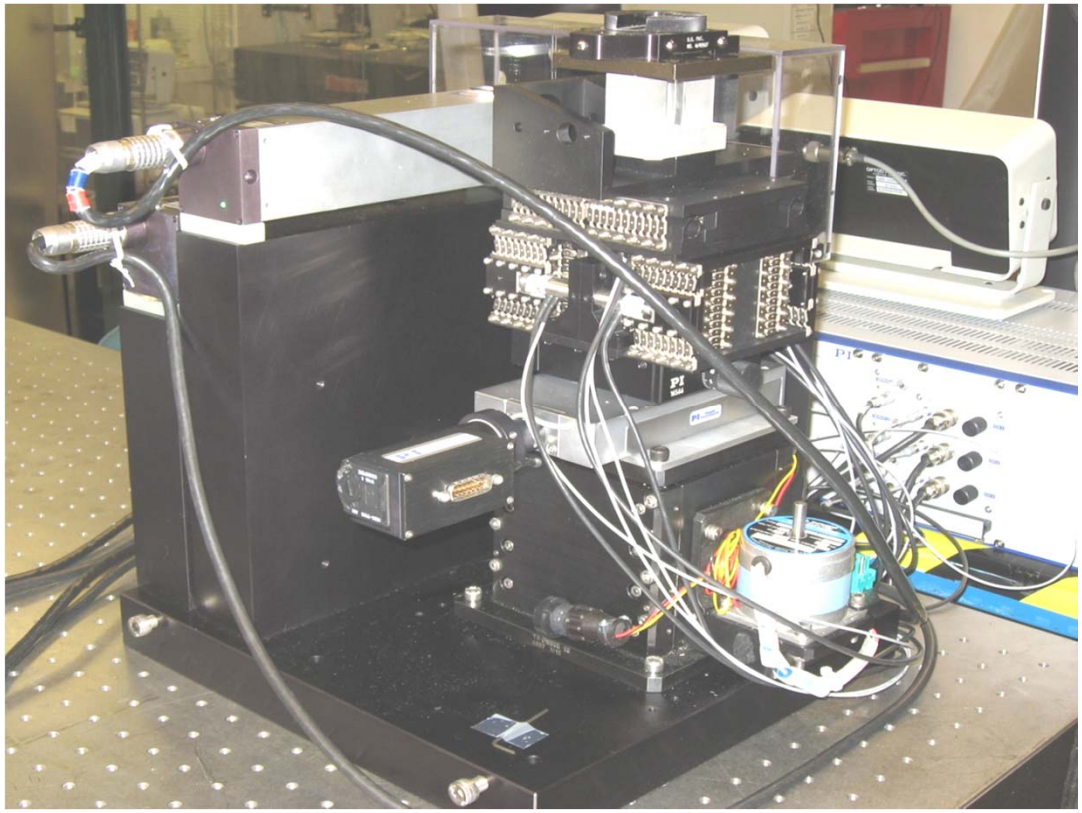

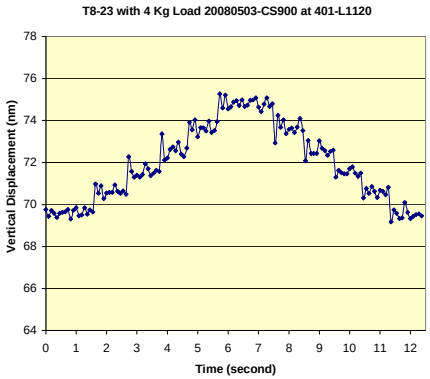

A nanopositioning diagnostic setup has been built to support the CNM nanoprobe instrument commissioning process at the APS. Its laser Doppler interferometer sytem provides subnanometer positioning diagnostic resolution with large dynamic range. A set of original APS designed ultraprecision PZT-driven weak-link stages with high stiffness motor-driven stages has been tested with this diagnostic setup.

D. Shu and J. Maser, Mechanical design of ultraprecision weak-link stages for nanometer-scale x-ray imaging, Proceedings of XRM-2008,.IOP Publishing, Journal of Physics: Conference Series 186 (2009) 012017.

D. Shu et al., Proc. SPIE, Vol. 5877 (2005) 58770E, DOI: 10.1117/12.617723

Commissioning of the CNM hard x-ray nanoprobe at APS sector 26

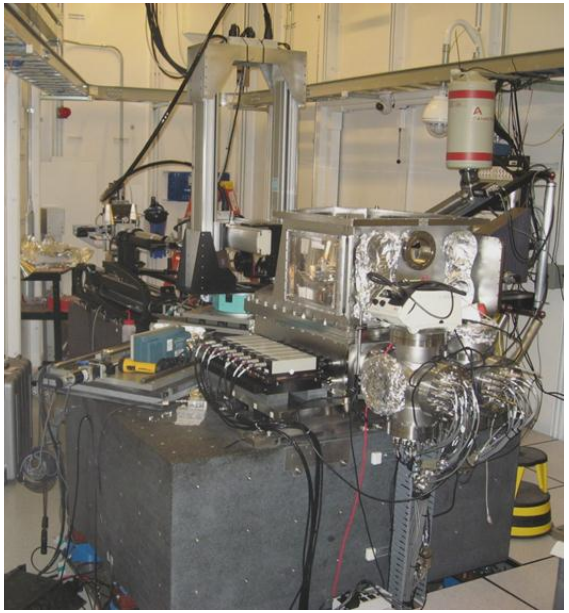

The nanoprobe beamline provides fluorescence, diffraction, transmission, and tomographic imaging with a spatial resolution of as small as 30 nm. Typical operation provides a spatial resolution of 50 nm in the spectral range of 8-12 keV.

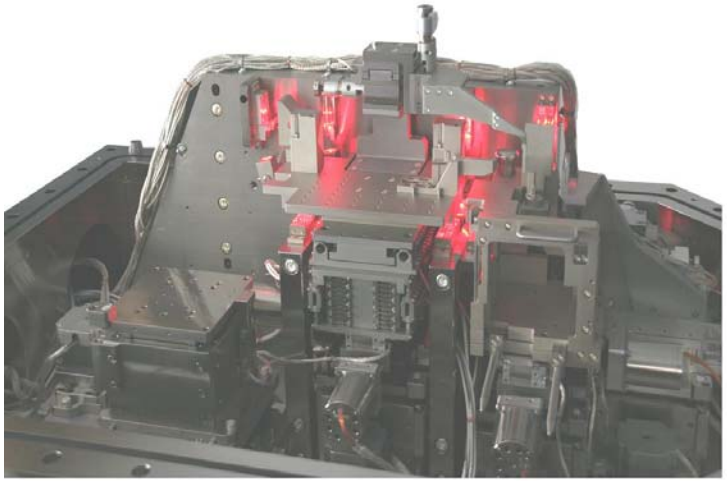

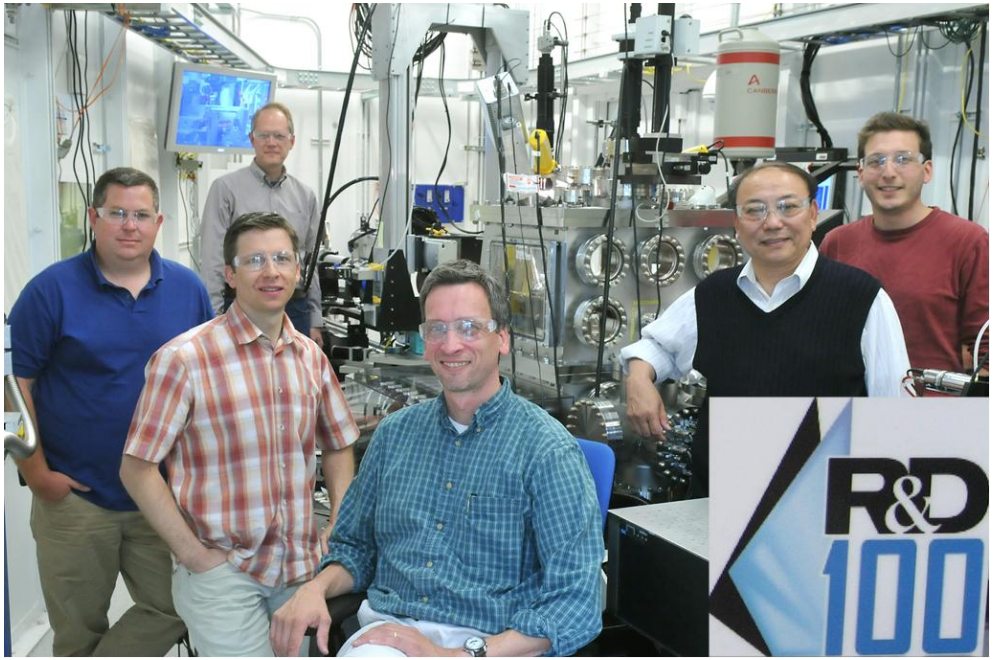

Courtesy of: xradia

2009

Mechanical design of an MLL multidimensional alignment system with nanometer-scale 2-D focusing

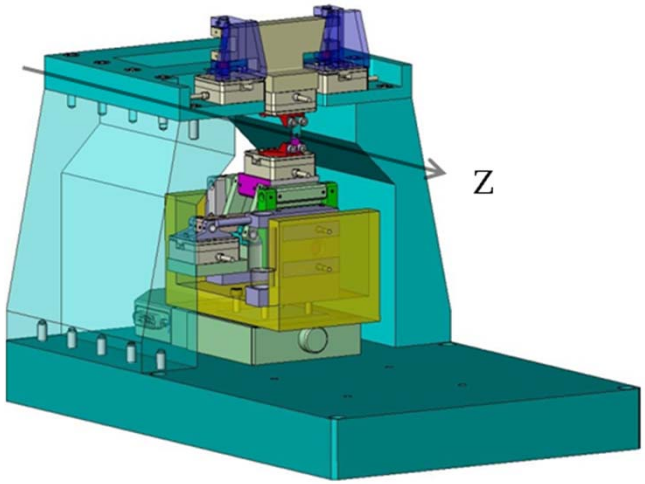

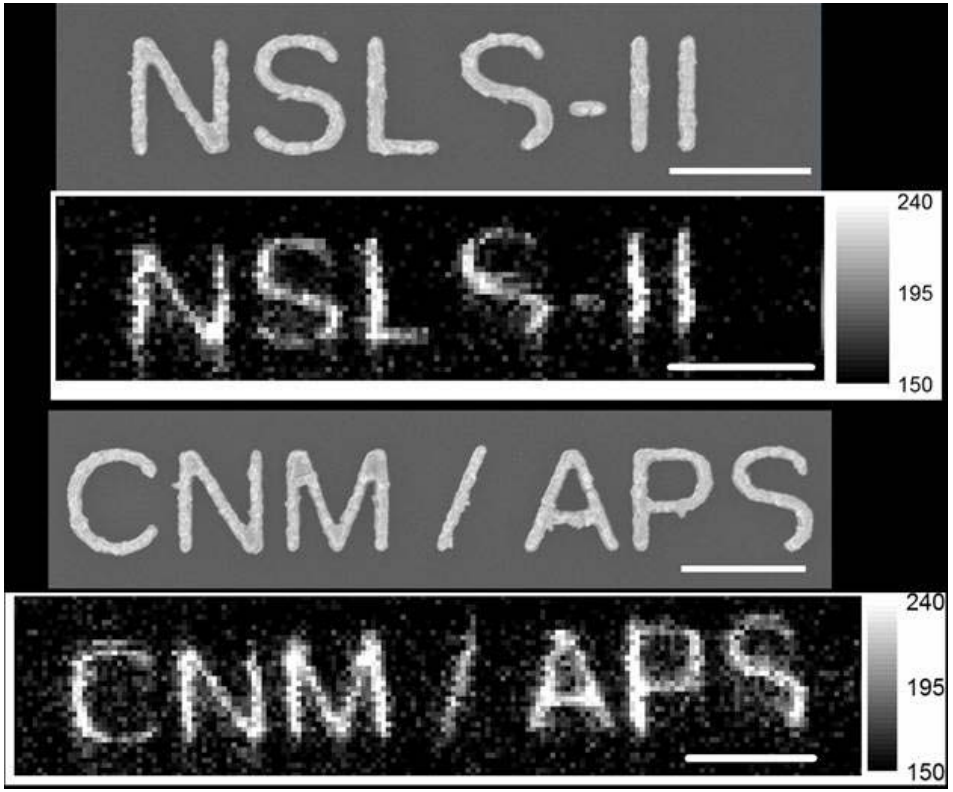

*MLL demonstrated of focusing of hard x-rays to a 2D focus of **25 nm horizontal x 27 nm vertical** FWHM at a photon energy of **12 keV**, and of 25 nm horizontal x 40 nm vertical FWHM at a photon energy of 19.52 keV.*

H. Yan, V. Rose, D. Shu, E. Lima, H. C. Kang, R. Conley, C. Liu, N. Jahedi, A. Macrander, G. B. Stephenson, M. Holt, Y. S. Chu, M. Liu, and J. Maser, Optics Express 15069 Vol.19, No.16 (2011)

UHV ACCM for x-ray double crystal monochromators

Design of the UHV X-ray Monochromator for XPCS at the APS 8-ID

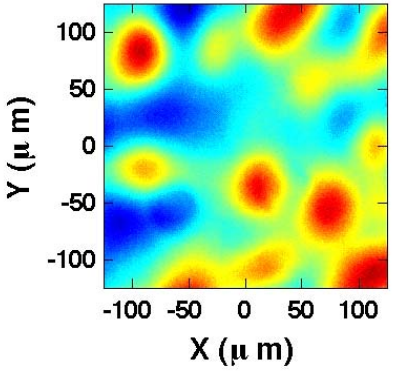

- X-ray photon correlation spectroscopy (XPCS) is a brilliance-limited technique, the monochromator must preserve the beam brilliance by having highly polished diffracting faces.

- The monochromator should also be mechanically stable so that spurious monochromator motions do not corrupt the fluctuating scattered x-ray signal arising from the sample.

- These requirements have not proven possible with either the original 8-ID-I "traditional" channel-cut design or an enhanced "Z-step" channel-cut crystal; they both produce spatially inhomogeneous (and statistically indistinguishable from each other) monochromatic beams.

S. Narayanan et al., J. Sychrotron Rad. (2008) 15, 12-18
D. Shu et al., proceedings of SPIE Vol. 6665, 66650O1-8 (2007)

UHV ACCM for x-ray double crystal monochromators

Design of the UHV X-ray Monochromator for XPCS at the APS 8-ID

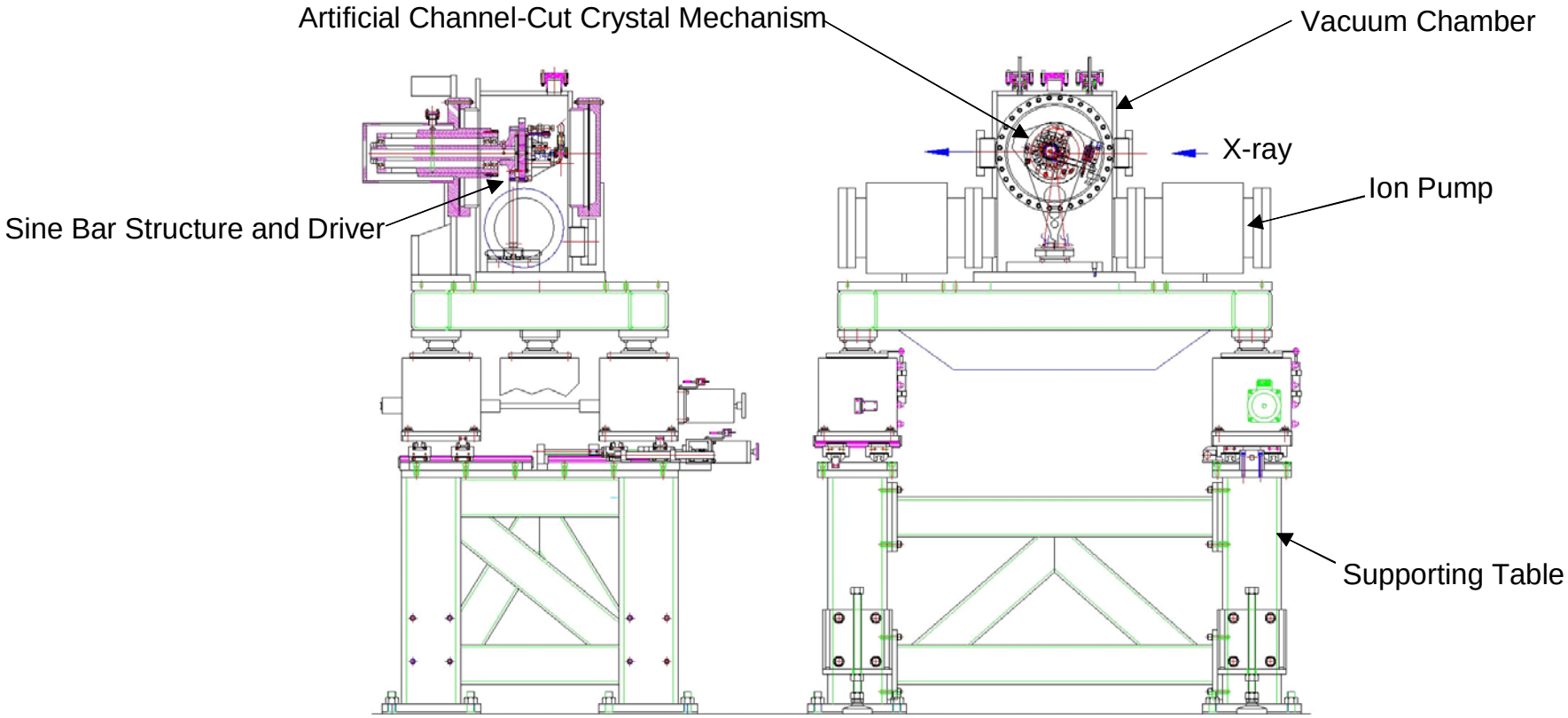

The 8-ID-I new monochromator consists of five sub-assemblies: a supporting table with five degrees of freedom motorized alignment capability, an UHV compatible vacuum chamber, a sine bar structure and its driver, an artificial channel-cut crystal mechanism, and two ion pumps.

S. Narayanan et al., J. Sychrotron Rad. (2008) 15, 12-18
D. Shu et al., proceedings of SPIE Vol. 6665, 66650O1-8 (2007)

UHV ACCM for x-ray double crystal monochromators

Design of the UHV X-ray Monochromator for XPCS at the APS 8-ID

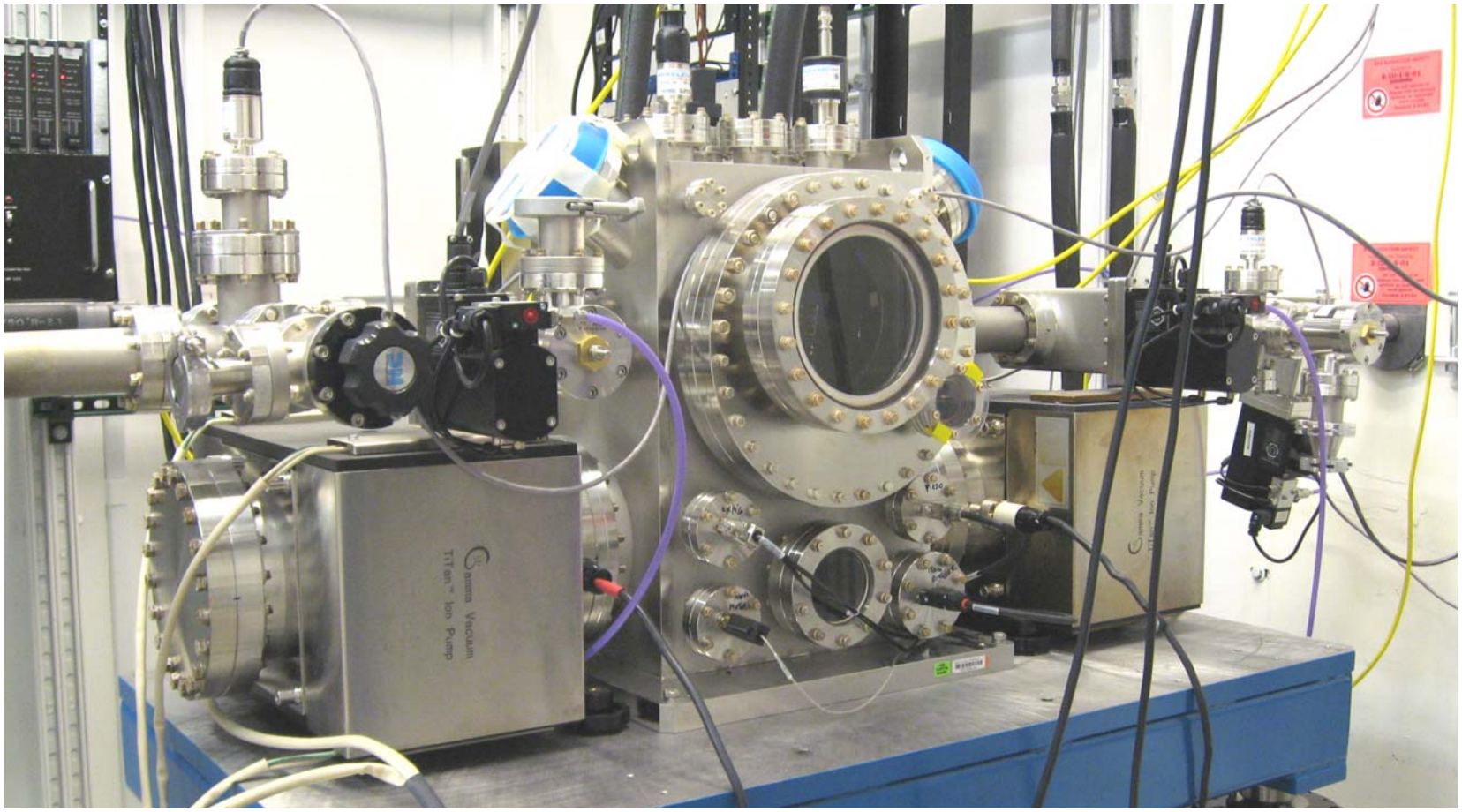

A photograph of the new 8-ID-I UHV-compatible artificial channel-cut x-ray monochromator.

S. Narayanan et al., J. Sychrotron Rad. (2008) 15, 12-18
D. Shu et al., proceedings of SPIE Vol. 6665, 66650O1-8 (2007)

UHV ACCM for x-ray double crystal monochromators

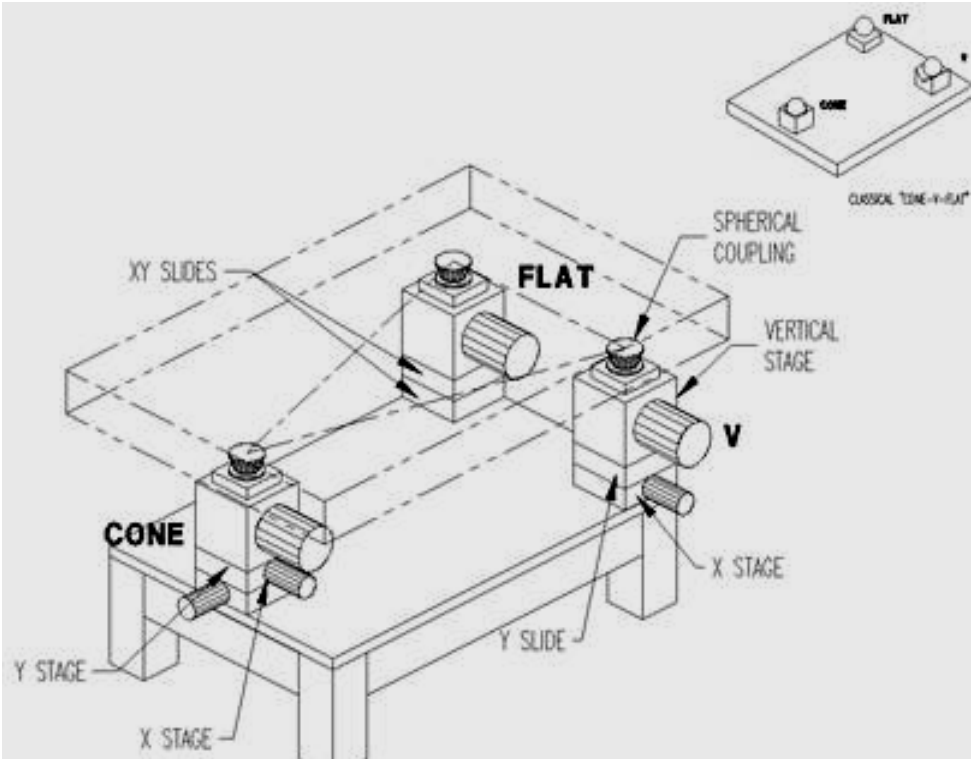

To provide five degrees of freedom alignment capability for the new monochromator crystal optics with the axis of the x-ray beam at the 8-ID-I experimental station, an APS designed standard kinematic mounting table is used as the base of the monochromator. The table's basic precision motion design uses the 3-point "cone-flat-V" kinematic mount concept obtained through the use of modular linear rolling stages and ball-bearing spherical joints as shown in the left side of Fig. 3. The "cone-flat-V" kinematic mount concept has the advantages of 3-point stability, reduced space usage, minimal motor drivers, free and unconstrained thermal expansion, and good positioning repeatability.

S. Narayanan et al., J. Sychrotron Rad. (2008) 15, 12-18
D. Shu et al., proceedings of SPIE Vol. 6665, 66650O1-8 (2007)

UHV ACCM for x-ray double crystal monochromators

TABLE 1. Design specifications of the supporting table for the new 8-ID-I monochromator

Motorized stages type	Stepping-motor-driven linear stages with spring-loaded linear potentiometer encoder
Horizontal travel range	25 mm
Horizontal positioning resolution	5 micron or better
Horizontal positioning reproducibility	20 micron or better
Vertical travel range	25 mm
Vertical positioning resolution	2 micron or better
Vertical positioning reproducibility	10 micron or better
Load capacity	1000 kg

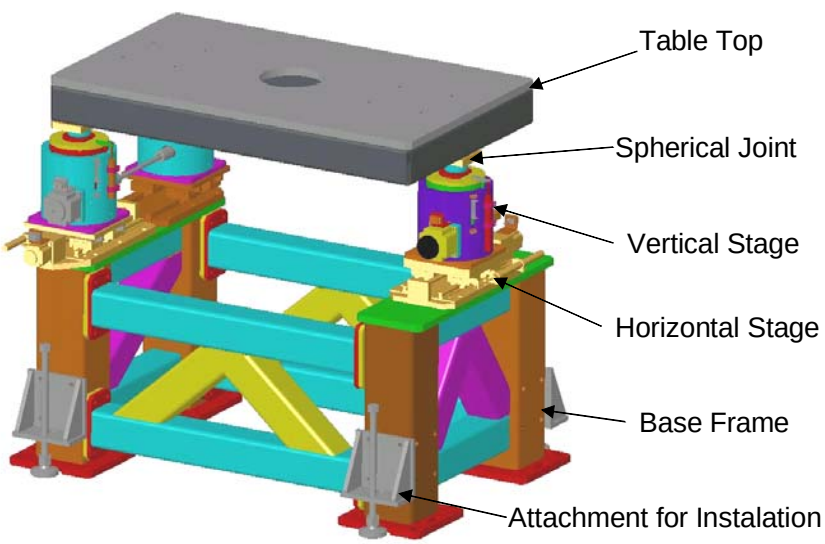

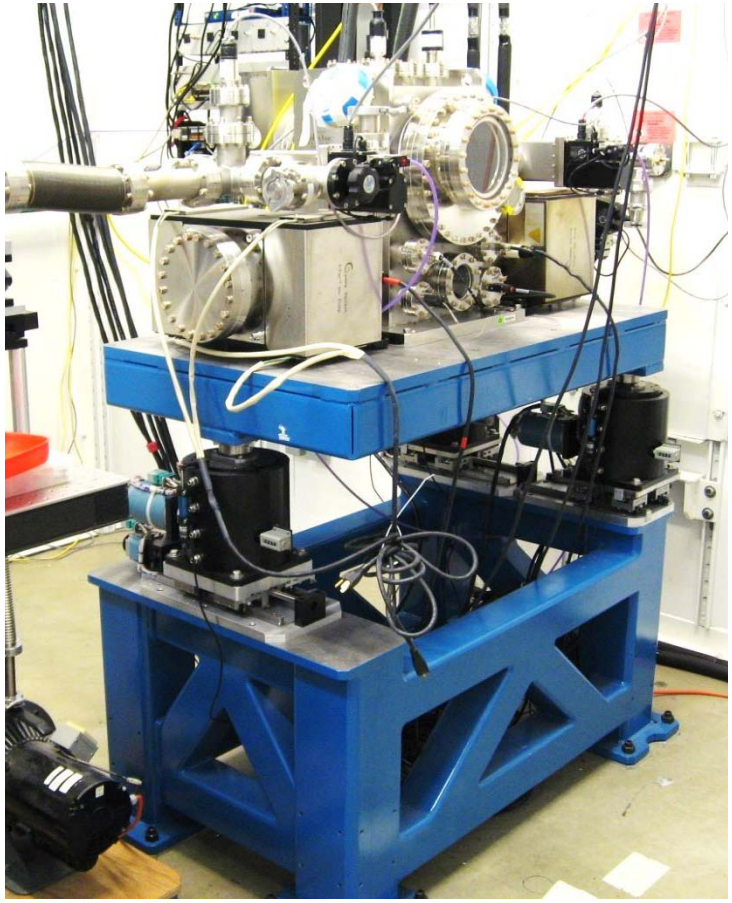

S. Narayanan et al., J. Sychrotron Rad. (2008) 15, 12-18
D. Shu et al., proceedings of SPIE Vol. 6665, 66650O1-8 (2007)

UHV ACCM for x-ray double crystal monochromators

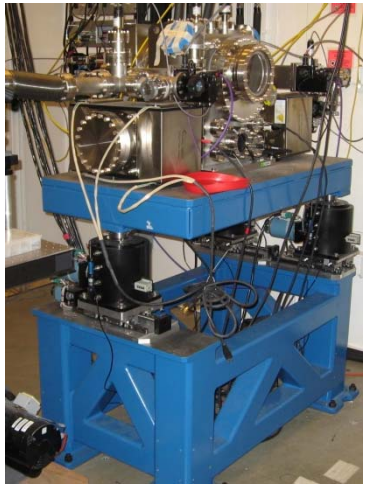

Linear potentiometer

A numbers of linear stages have been developed at the APS as the basic functional modules for the various supporting applications.

- Commercial cross-roller bearings and stepping motor driving system are used in most of the stages.
- Spring loaded linear potentiometers with 10-μm repeatability have been applied as absolute position sensors for all of the modules.
- For most of the heavy-load stages, a 200-μrad/25-mm straightness of trajectory has been achieved.
- For medium-load stages such as T2-24 vertical stage, a 10-μrad/5-mm straightness of trajectory was demonstrated in the test [1,2,3].

S. Narayanan et al., J. Sychrotron Rad. (2008) 15, 12-18
D. Shu et al., proceedings of SPIE Vol. 6665, 66650O1-8 (2007)

UHV ACCM for x-ray double crystal monochromators

Vacuum Chamber

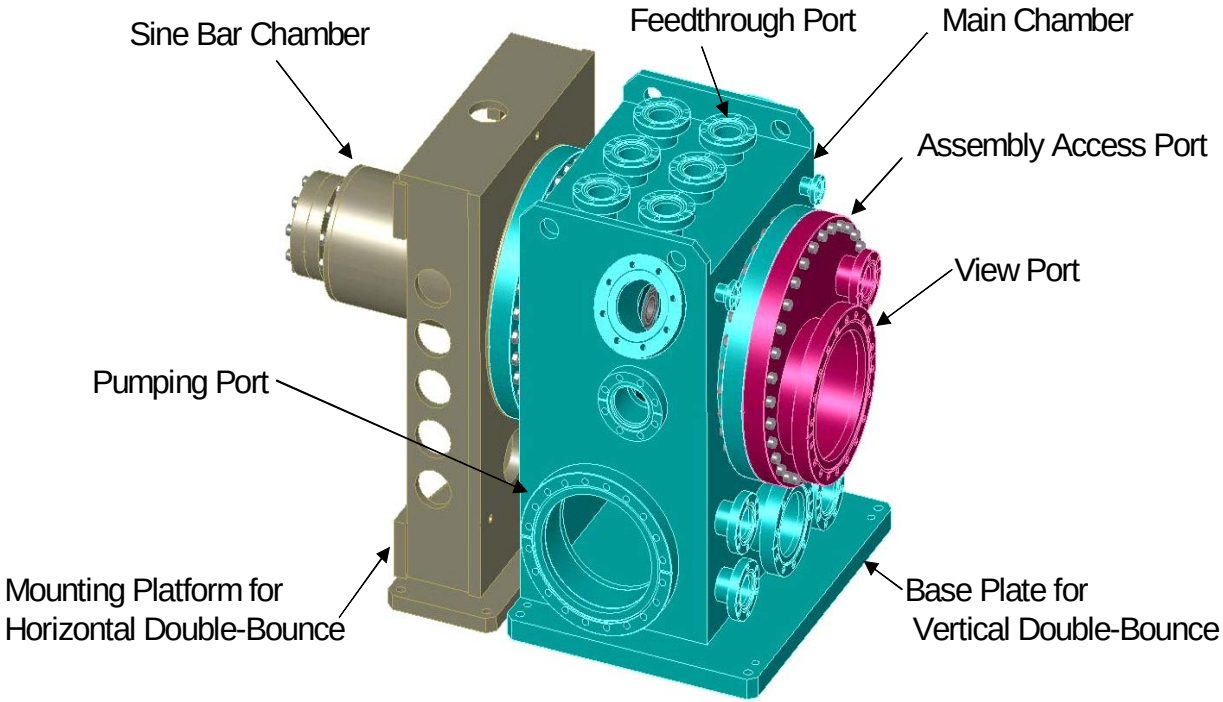

The vacuum chamber for the 8-ID-I new monochromator consists of three major sub-assemblies: a main chamber, a sine bar chamber, and a flange for the monochromator's assembly access with view port. The main chamber has a base mounting plate for the monochromator's vertical double-bounce operation configuration. On the sine bar chamber, there is another mounting platform, which is perpendicular to the main chamber base plate, for the monochromator's horizontal double-bounce operation configuration.

S. Narayanan et al., J. Sychrotron Rad. (2008) 15, 12-18
D. Shu et al., proceedings of SPIE Vol. 6665, 66650O1-8 (2007)

UHV ACCM for x-ray double crystal monochromators

Main Sine Bar Structure and Driver

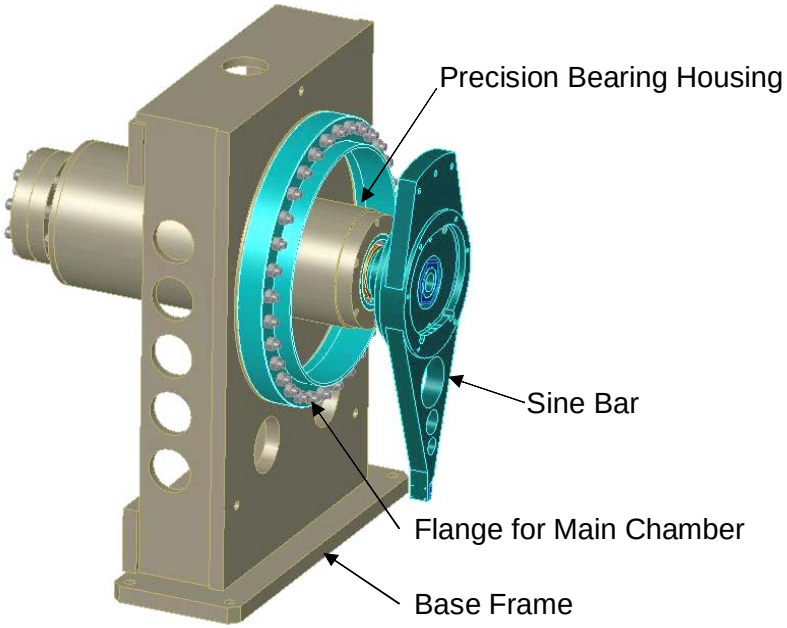

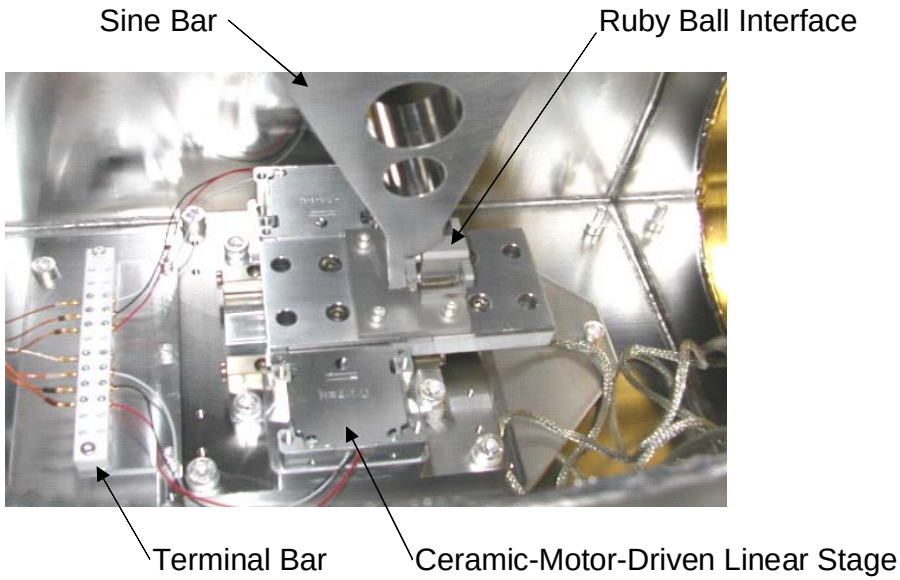

The main sine bar is assembled at the end of a precision hollow shaft supported by three sets of UHV-compatible precision bearings inside a precisely machined rigid housing, which permits stable angular rotation of the crystal optics. Using a ruby sapphire ball as a precision contact point, the sine bar arm is driven by a commercial ceramic-motor-driven linear stage [7-10] which has 0.01 micron linear positional resolution, yielding high angular resolution of the sine bar mechanism.

S. Narayanan et al., J. Sychrotron Rad. (2008) 15, 12-18
D. Shu et al., proceedings of SPIE Vol. 6665, 66650O1-8 (2007)

UHV ACCM for x-ray double crystal monochromators

Main Sine Bar Structure and Driver

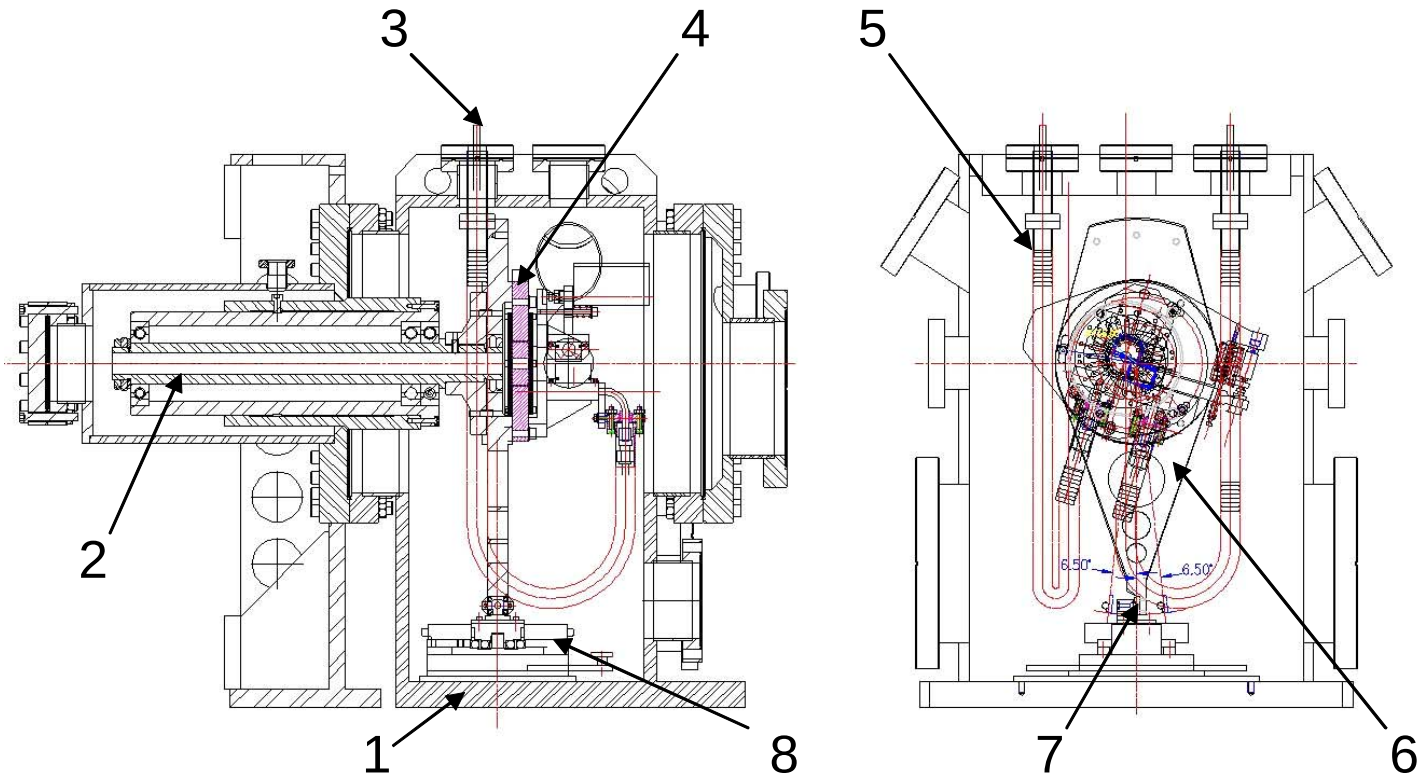

Detailed cross-sectional side and front views showing the mechanical and vacuum design of the artificial channel cut monochromator. In the center and right panels the “pink” x-ray beam is incident from the right and the monochromatic beam is transmitted to the left.

S. Narayanan et al., J. Sychrotron Rad. (2008) 15, 12-18
D. Shu et al., proceedings of SPIE Vol. 6665, 66650O1-8 (2007)

UHV ACCM for x-ray double crystal monochromators

Main Sine Bar Structure and Driver

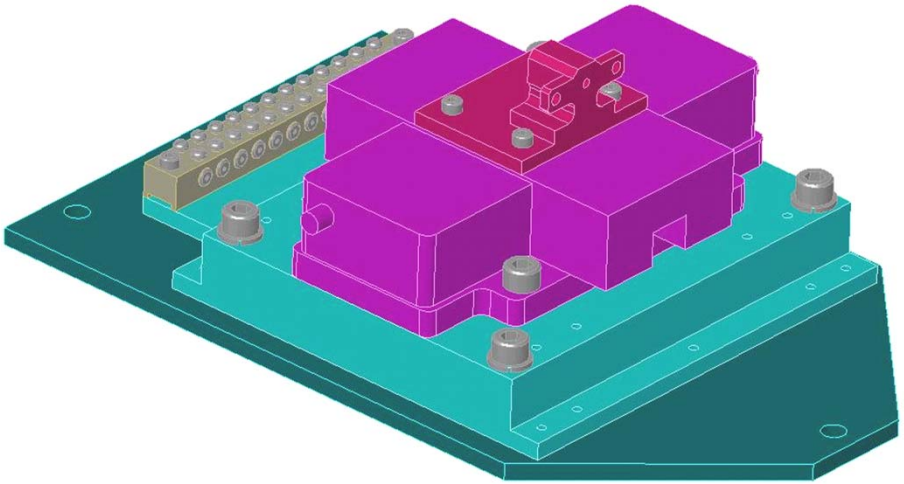

The main sine bar driver is an UHV-compatible linear slide assembly comprised of a precision slide from Alio Industries™, ceramic-motors from Nanomotion™, an encoder from Renishaw™, and an ACS Motion™ SPiiPlus stand-alone Ethernet servo controller. The combination delivers exceptionally precise closed-loop positioning in vacuum over extended length scales and velocity ranges.

S. Narayanan et al., J. Sychrotron Rad. (2008) 15, 12-18
D. Shu et al., proceedings of SPIE Vol. 6665, 66650O1-8 (2007)

UHV ACCM for x-ray double crystal monochromators

Water-cooling system

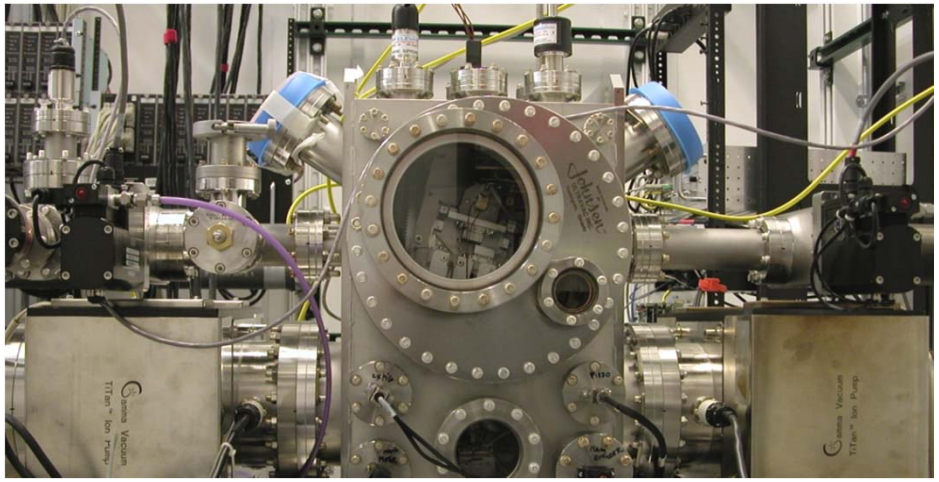

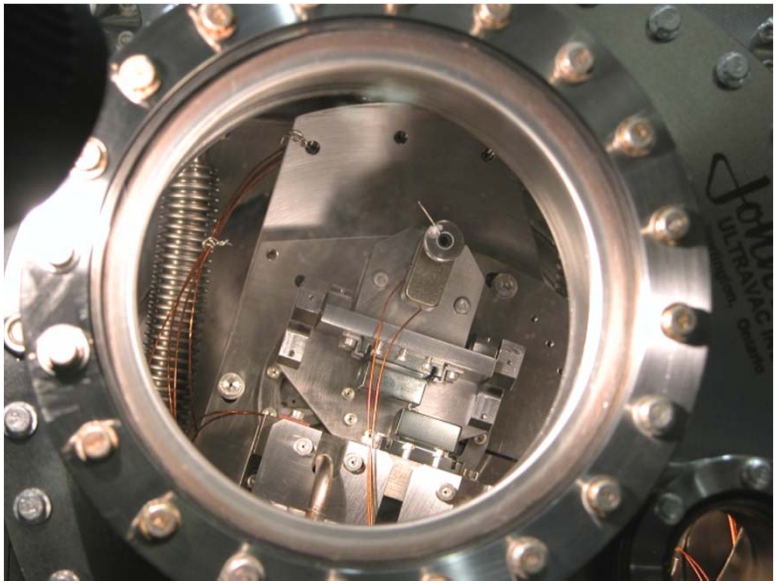

The artificial channel-cut crystal mechanism (ACCM) developed for the new 8-ID-I monochromator is the first such mechanism with UHV compatibility. Many mechanical details in this mechanism are carefully modified for UHV compatibility, such as using UHV-compatible materials and vented fasteners, prevention structures with locked gas packet, etc. As shown in Fig. 6, water cooling is provided for the first crystal by radiation resistant flexible cooling tubes shrouded by a vacuum bellows used in reverse pressure. With this style of water connection, the direct vacuum-to-water junction is avoided, eliminating the risk of water leak damaging the UHV environment.

S. Narayanan et al., J. Sychrotron Rad. (2008) 15, 12-18
D. Shu et al., proceedings of SPIE Vol. 6665, 66650O1-8 (2007)

UHV-Compatible Artificial Channel-Cut Crystal Mechanism

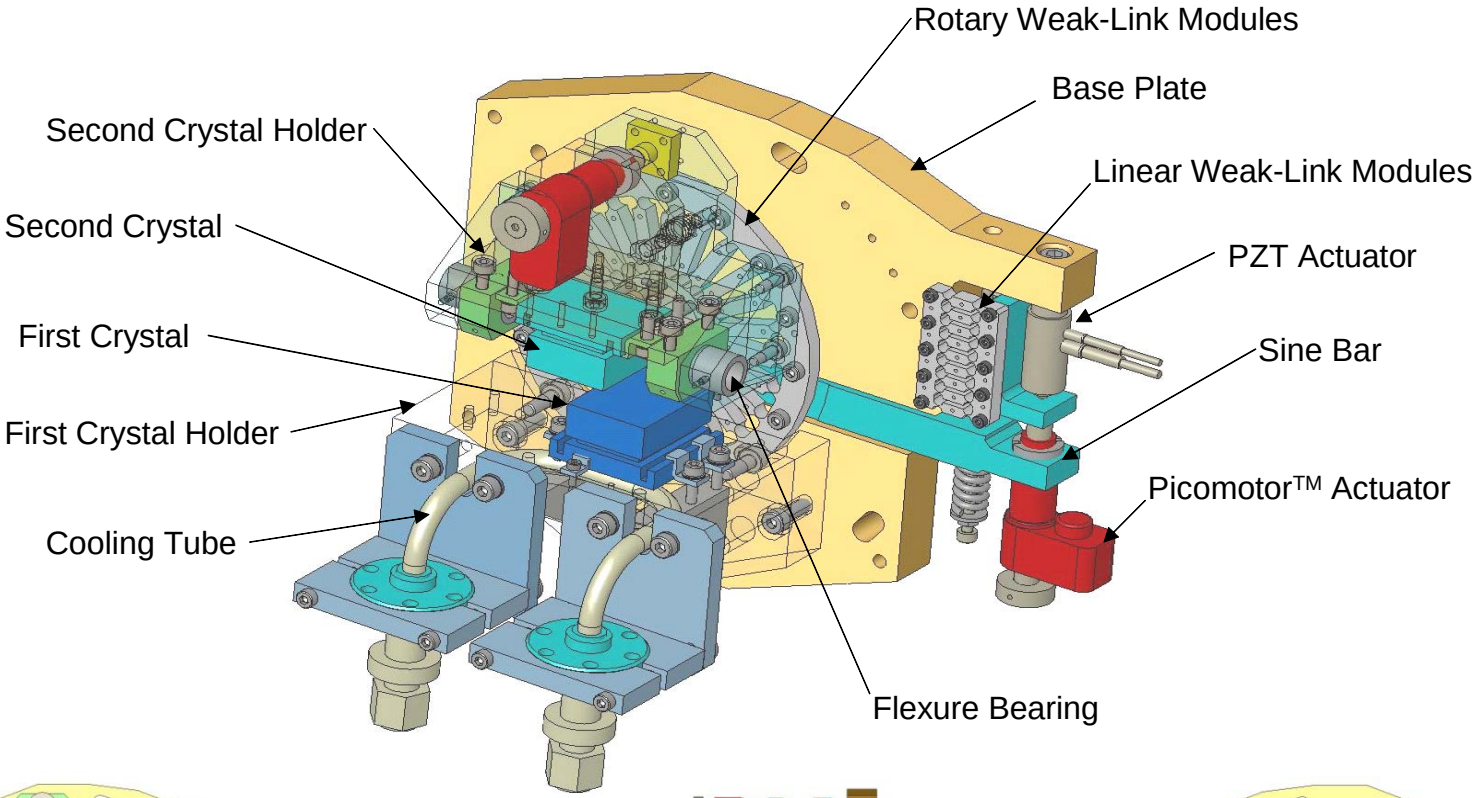

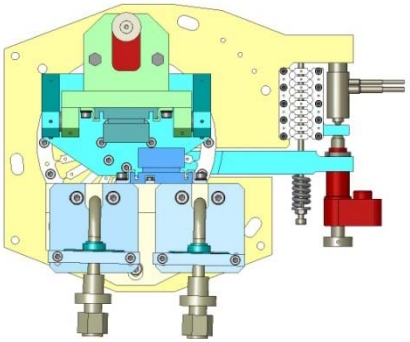

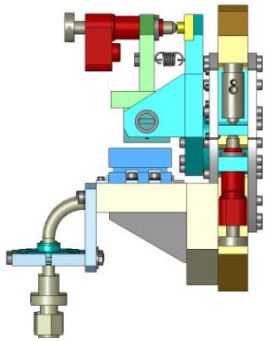

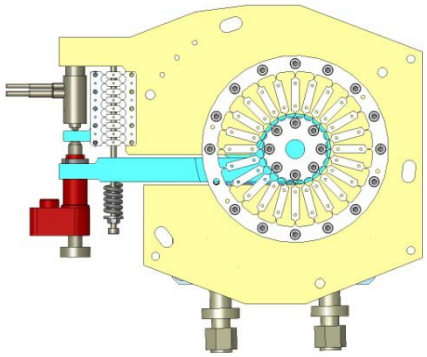

D. Shu, S. Narayanan, A. Sandy, M. Sprung, C. Preissner, and J. Sullivan, Precision Mechanical Design of an UHV-Compatible Artificial Channel-Cut X-ray Monochromator, Proceedings of SPIE 2007

UHV-Compatible Artificial Channel-Cut Crystal Mechanism

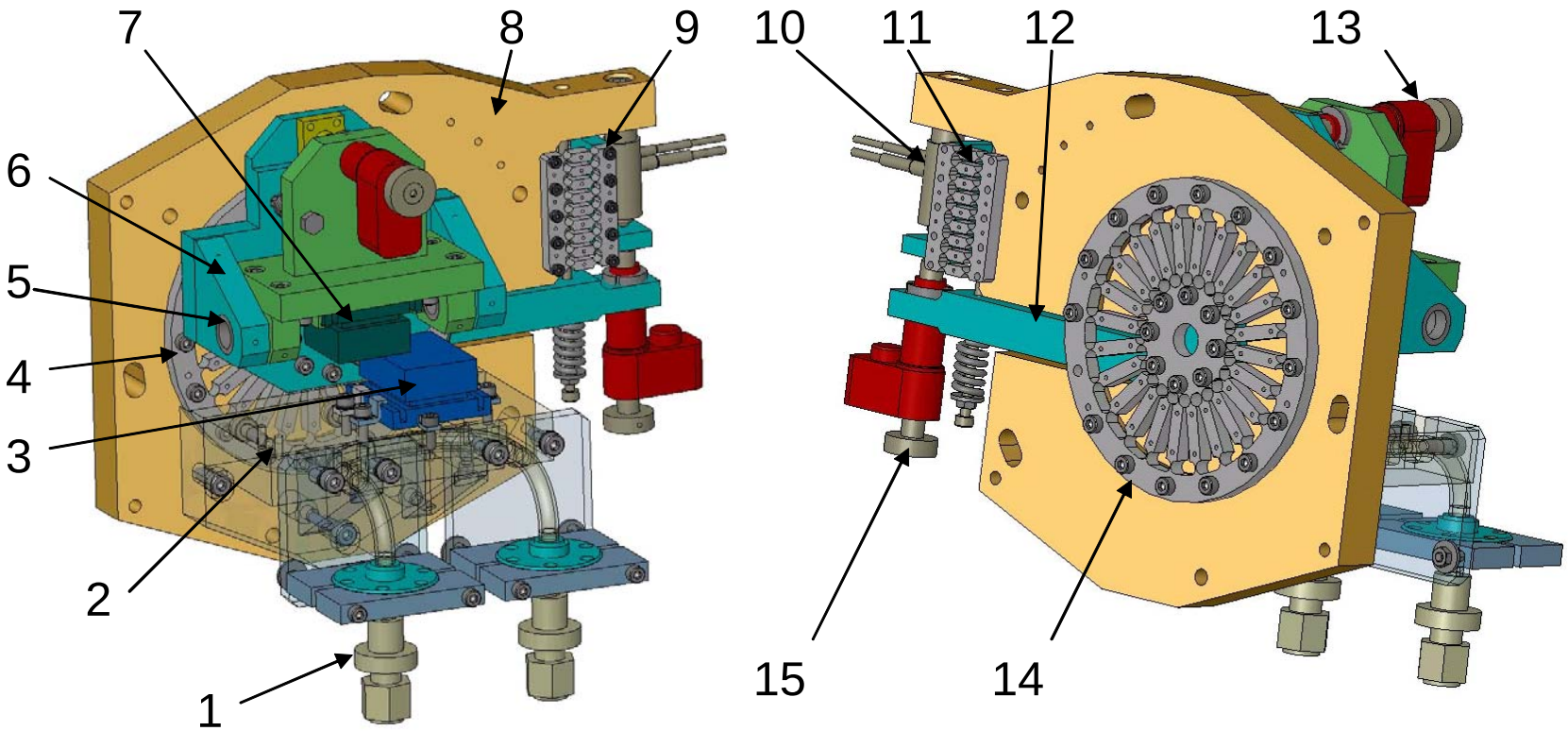

Front side and back side views of a 3-D model for a typical high-stiffness weak-link mechanism for an "artificial channel-cut crystal". (1) Cooling tube; (2) First crystal holder; (3) First crystal; (4) and (14) Rotary weak-link modules; (5) flexure bearing; (6) Second crystal holder; (7) Second crystal; (8) Base plate; (9) and (11) linear weak-link modules; (10) PZT actuator; (12) Sine bar: (13) and (15) PicomotorTM actuators. [9]

S. Narayanan et al., J. Sychrotron Rad. (2008) 15, 12-18
D. Shu et al., proceedings of SPIE Vol. 6665, 66650O1-8 (2007)

UHV ACCM for x-ray double crystal monochromators

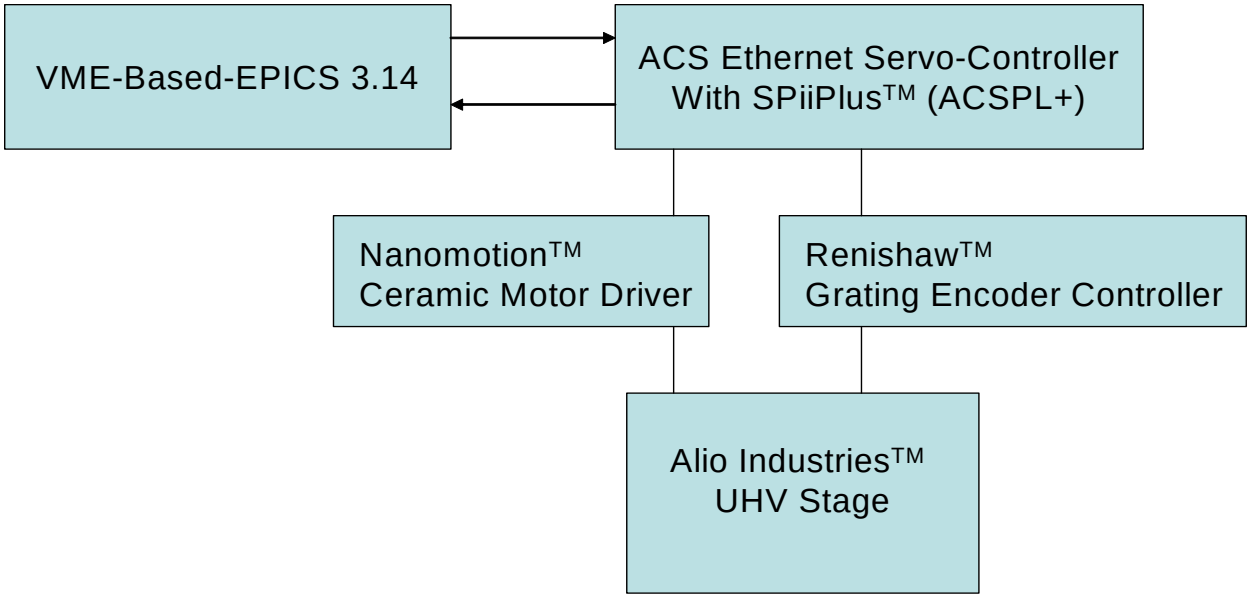

The new monochromator uses a customized UHV-compatible linear stage assembly to drive the main sine bar. It consists of a precision stage from Alio Industries™, piezoelectric actuators from Nanomotion™, an encoder from Renishaw™, and an ACS Motion™ SPiiPlus standalone Ethernet servo-controller. The combination delivers exceptionally precise closed-loop positioning in vacuum over extended length scales and velocity ranges. Since this new monochromator is an integral part of the APS 8-ID-I x-ray beamline instrument, it is important that this new assembly could be seamlessly integrated into APS beamline 8-ID's VME-based-EPICS control system.

S. Narayanan et al., J. Sychrotron Rad. (2008) 15, 12-18
D. Shu et al., proceedings of SPIE Vol. 6665, 66650O1-8 (2007)

UHV ACCM for x-ray double crystal monochromators

Test results of the UHV X-ray Monochromator for XPCS at the APS 8-ID

This new monochromator was installed in the APS beamline 8-ID-I in April 2006. Evidently, its transverse intensity profile is considerably more uniform than that produced by the traditional channel-cut monochromator previously installed in beamline 8-ID-I (left side of the figure). In particular, the variance of the recorded intensities in the center range |X| and |Y| < 67 microns is 50% less in the right side of the figure as compared with that in the left side of the figure.

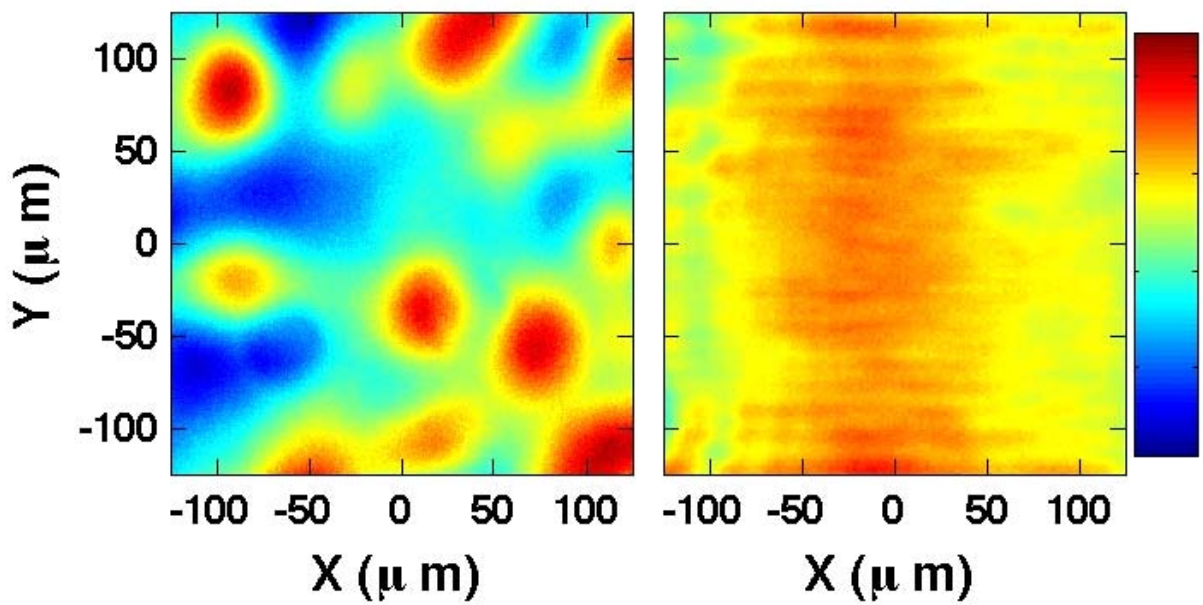

S. Narayanan et al., J. Sychrotron Rad. (2008) 15, 12-18
D. Shu et al., proceedings of SPIE Vol. 6665, 66650O1-8 (2007)

UHV ACCM for x-ray double crystal monochromators

Design of the UHV X-ray Monochromator for high pressure x-ray studies with diamond anvil cells at the APS HP-CAT 16-BM

HPCAT HIGH PRESSURE COLLABORATIVE ACCESS TEAM
at the Advanced Photon Source
GEOPHYSICAL LABORATORY, Carnegie Institution of Washington

- A wide variety of materials covering almost the entire periodic table have been used for high pressure study, which requires a wide x-ray energy monochromator at beamlines for different x-ray techniques, such as x-ray diffraction/scattering, spectroscopy, and imaging.

- The bending magnet radiation has wide energy spectrum with constant and smooth flux distribution. It is ideal for many applications to make measurements with wide energy range.

- An artificial channel-cut monochromator has been commissioned and is operational at APS HPCAT bending magnet beamline since 2008.

- The fixed vertical slits provide an exit beam at constant height when energy is scanned, which enables novel high pressure x-ray studies with diamond anvil cells.

W. Yang et al., proceedings of SRI-2008, Saskatoon, Canada, June 10-13 2008

UHV ACCM for x-ray double crystal monochromators

Design of the UHV X-ray Monochromator for high pressure x-ray studies with diamond anvil cells at the APS HP-CAT 16-BM

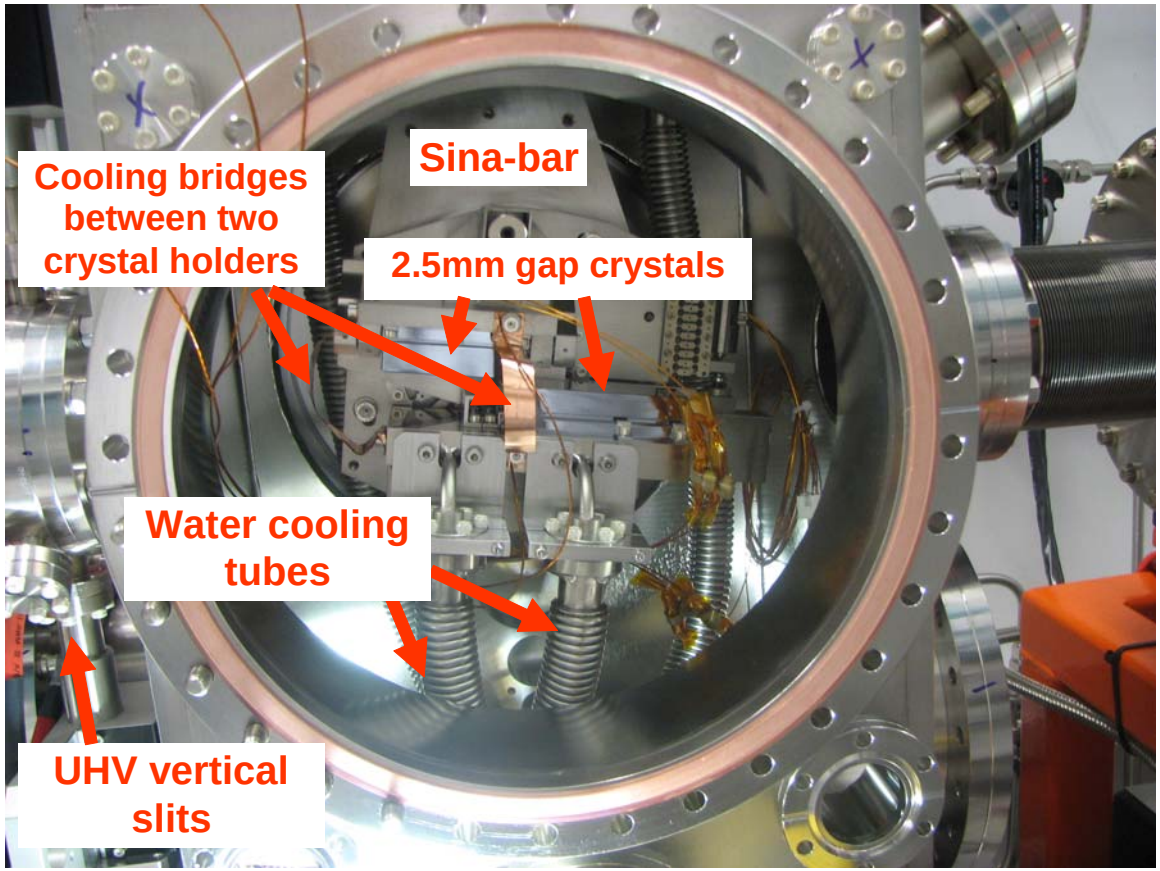

A UHV compatible high precision (10 nm) nanomotor (Nanomotion™) with long travel range (100 mm) is used to drive a 232 mm long sin-bar arm, which gives 40 nrad angular resolution and 24 degrees of total Bragg angle range. This angular range covers Si (111) reflection energy from 5 keV to 70 keV.

W. Yang et al., proceedings of SRI-2008, Saskatoon, Canada, June 10-13 2008

UHV ACCM for x-ray double crystal monochromators

Design of the UHV X-ray Monochromator for high pressure x-ray studies with diamond anvil cells at the APS HP-CAT 16-BM

- Both crystals are cut from the same Si (111) ingot. Fine tuning of second crystal is performed with ACCM mechanism. The ultimate aligning resolution for pitch and roll is 4nm (30 nrad) and 40 nm (300 nrad), respectively.

- A small gap of 2.5 mm was chosen for this monochromator with maximum 2 mm vertical acceptance of incident beam. Over the entire energy range, the exit beam height moves within ±140 microns. In order to fix the monochromatic beam height for the downstream optics, a pair of UHV compatible high precision vertical slits is installed after the second crystal with a narrower size to keep the exit beam position constant. This ensures the focused beam position after K-B mirrors at the same sample location, which is critical for high pressure study with diamond anvil cells.

- The ACCM mechanism ensures the two crystals have a fixed relative geometry. Once they are aligned, there will be no more tuning required between two crystals. High flexible stainless-steel formed bellows are used for water cooling system on the first crystal.

- A RTE-17 type chiller (ThermoFisher Scientific) is used for constant temperature water supply. Two copper belts are used to connect the two crystal holders to remove the heat load from second crystal, thus shorten the warm-up time.

W. Yang et al., proceedings of SRI-2008, Saskatoon, Canada, June 10-13 2008

UHV ACCM for x-ray double crystal monochromators

Operation status of the UHV X-ray Monochromator for high pressure x-ray studies with diamond anvil cells at the APS HP-CAT 16-BM

An e-mail from HP-CAT beamline scientist (Dr. Wenge Yang) on April 17, 2014:

- *The artificial channel cut monochromator at 16-BM-D has been working very well. We are able to do spectroscopy scan over wide energy range.*

- *After initial alignment of the second crystal (both theta and chi direction), we do not need to adjust these two motors for wide enegy range we usually use (5-40 keV). I attach one figure with the entire spectrum scan with energy 5-70 keV and second figure for the energy calibration for energy 5 keV to 40 keV. For both work, we do not need to retune the second crystal angles.*

- *We have replaced the nanomotion stage with a high resolution stepping motor stage with encoder on it. The energy resolution is good enough. We are using Si (111) crystal with stepping motor travel range 100 mm. So we can have energy range from 5keV to beyond 70 keV for the BM beamline.*

UHV ACCM for x-ray double crystal monochromators

Design of the UHV X-ray Monochromator for high pressure x-ray studies with diamond anvil cells at the APS HP-CAT 16-BM

An e-mail from HP-CAT beamline scientist (Dr. Wenge Yang) on April 17, 2014:

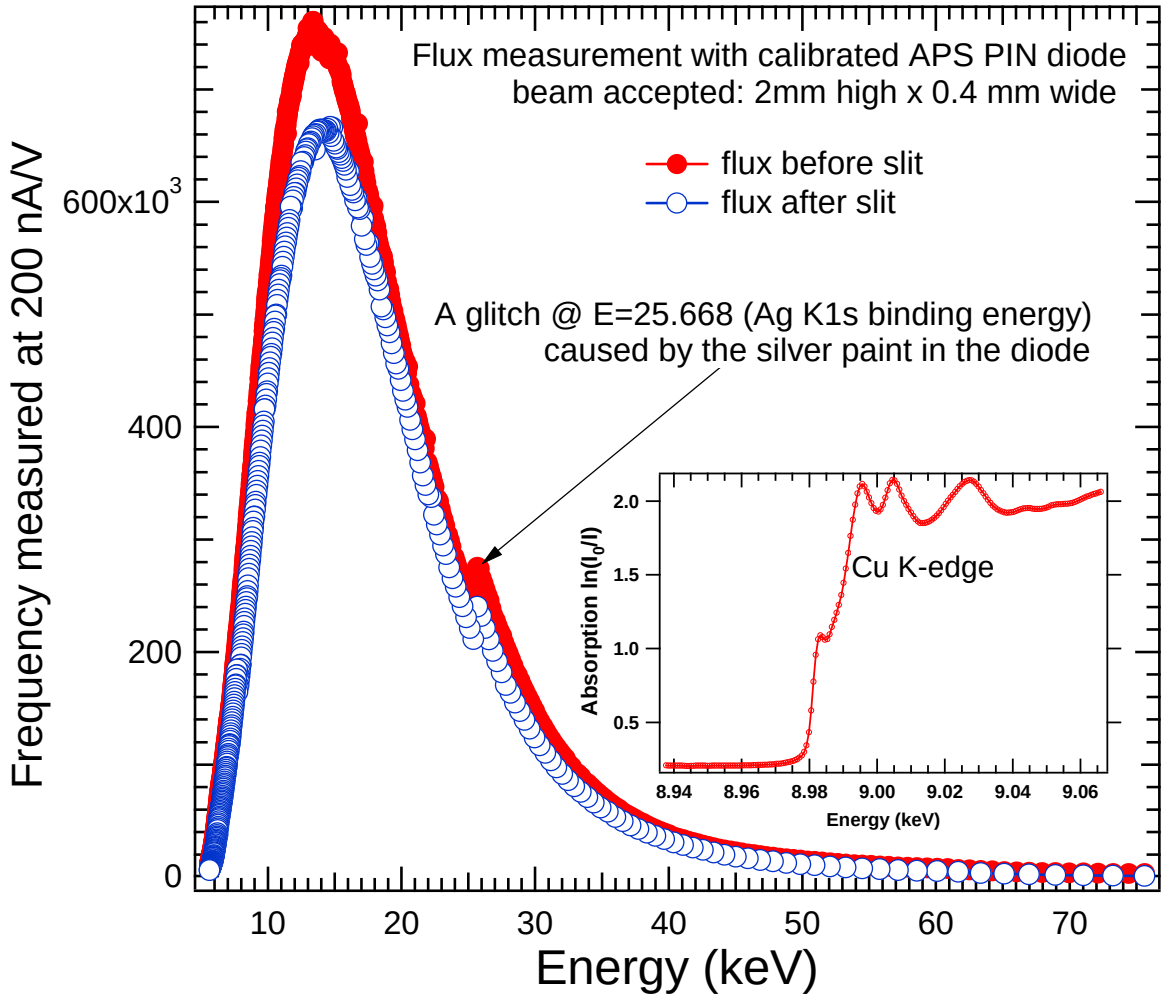

Fig. 2 The intensity measurement over entire energy range. The energy was calibrated based on 16 XANES characteristic peak energies like one as insert from fine energy scan near Cu edge.

UHV ACCM for x-ray double crystal monochromators

Design of the UHV X-ray Monochromator for high pressure x-ray studies with diamond anvil cells at the APS HP-CAT 16-BM

An e-mail from HP-CAT beamline scientist (Dr. Wenge Yang) on April 17, 2014:

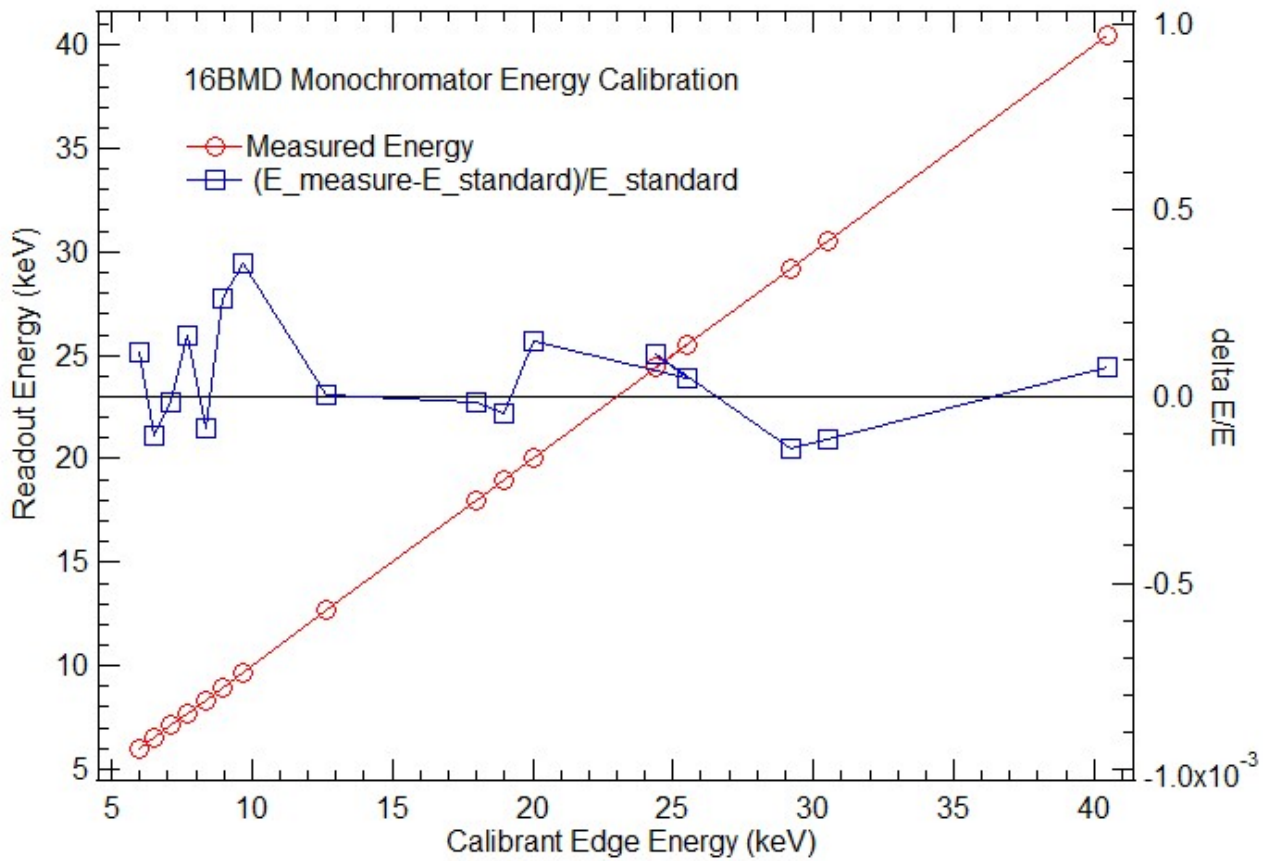

UHV ACCM for x-ray double crystal monochromators at LCLS/SLAC

- Two APS designed UHV-compatible artificial channel-cut monochromators have been constructed and installed at LCLS/SLAC for XPCS and other applications.

- First monochromator for LCLS/SLAC has been commissioned and characterized at Aug. 27, 2010.

- The water-cooled UHV-compatible artificial channel-cut crystal monochromator was originally developed by APS scientists and engineers to meet the challenging stability and optical requirements of the XPCS program at XSD beamline 8-ID-I at the APS.

- Using a laminar structure configured and manufactured by chemical etching and lithography techniques, we were able to design and build a planar-shape, high-stiffness, high-precision weak-link module. The precision and stability of this mechanism allowed us to align or adjust an assembly of crystals to achieve the same performance as does a single channel-cut crystal, so we called it an "artificial channel-cut crystal."

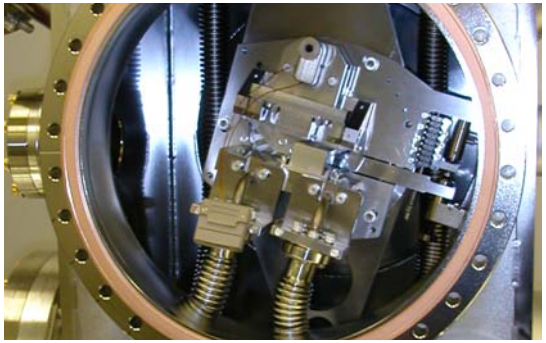

A photograph of the APS 8-ID UHV-compatible artificial channel-cut crystal monochromator. Two similar monochromators were constructed and installed at LCLS/SLAC for XPCS and other applications.

APS Science 2010, ANL-10/35, ISSN 1931-5007, p134

Design of a diamond-crystal monochromator for the LCLS hard x-ray self-seeding project

- *To longitudinally improve the coherent quality of the x-ray radiation produced by the LCLS FEL and reduce the level of the spikiness in their spectrum and temporal structures, a proposal was made at DESY in August 2010 to remove one 3.4-m-long LCLS undulator section near U15 and replace it with a weak electron delay (a small four-dipole chicane) and a diamond crystal in order to monochromatize and self-seed the LCLS hard x-ray radiation when using the 20-pC low-charge operating mode.*
- *As the result of collaborations between the APS, Argonne National Laboratory, and the LCLS at SLAC National Accelerator Laboratory, we have designed and constructed a diamond crystal monochromator for the LCLS hard x-ray self-seeding (HXRSS) project.*
- *In January 2012, the monochromator was installed in the tunnel of LCLS, and the HXRSS commissioning team started the self-seeding test soon after.*

A Better and Brighter Linac Coherent Light Source

The APS has been an enthusiastic participant in development of the Linac Coherent Light Source (LCLS), the free-electron laser (FEL) light source constructed by and at the SLAC National Accelerator Laboratory. APS expertise in undulator insertion devices helped the LCLS attain its place as the first and so far only U.S. source of highly focused, laser-like x-ray beams. Now the LCLS and the APS have extended the collaboration to realize a long-standing objective for light-source scientists: a self-seeded FEL x-ray laser pulse that focuses to an even higher intensity in a much narrower band of x-ray wavelengths.

The LCLS operates in the self-amplified spontaneous emission (SASE) regime, which amplifies the spontaneous emission of electrons produced at the beginning of the undulator string. As the

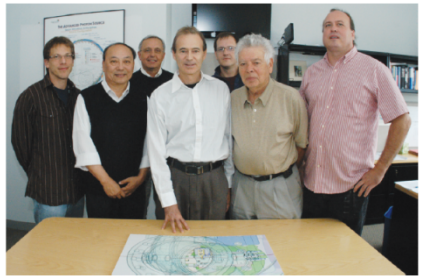

The APS participants in the LCLS self-seeding project are, left to right, Ryan Lindberg (ASD), Deming Shu (AES), Yuri Shvyd'ko (XSD), Alexander Zholents (ASD), Stanislav Stoupin (XSD), Emil Trakhtenberg (AES), and William Berg (ASD).

J. Amann, W. Berg, V. Blank, F.-J. Decker, Y. Ding, P. Emma, Y. Feng, J. Frisch, D. Fritz, J. Hastings, Z. Huang, J. Krzywinski, R. Lindberg, H. Loos, A. Lutman, H.-D. Nuhn, D. Ratner, J. Rzepiela, D. Shu, Yu. Shvyd'ko, S. Spampinati, S. Stoupin, S. Terentyev, E. Trakhtenberg, D. Walz, J. Welch, J. Wu, A. Zholents and D. Zhu, „Demonstration of self-seeding in a hard-X-ray free-electron laser", NATURE PHOTONICS, DOI: 10.1038/NPHOTON.2012.180.*

Alexander A. Zholents, "What's Next? The FEL Manifesto," Synch. Rad. News 25(6), 27 (2012)

Monochromator UHV enclosure and its space limits

- *Since the space available for the HXRSS diamond monochromator is considerably limited by its surrounding components and the existing girder system, a compact vacuum enclosure was designed with ultra-high-vacuum (UHV) compatibility as required by LCLS vacuum system.*
- *The monochromator vacuum enclosure hosts a 10" flange for a 4-axis diamond positioning system, a beryllium window for x-ray diagnostics, a 75 l/s ion pump, two 1.33" O.D. viewports, and a pair of all-metal valves connected to the LCLS vacuum system.*
- *The distance between the flanges of two valves for bellows is limited to less than 264 mm.*
- *The monochromator vacuum enclosure is mounted to the original girder system through a base plate with alignment mechanisms.*

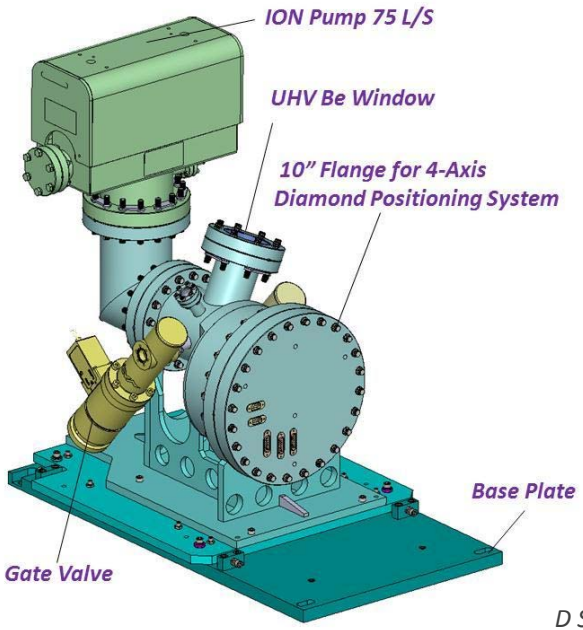

D Shu, Y Shvyd'ko, J Amann, P Emma, S Stoupin, and J Quintana, "Design of a diamond-crystal monochromator for the LCLS hard x-ray self-seeding project", J. Phys. Conf. Ser. 425 052004 (2013)

Monochromator UHV enclosure and its space limits

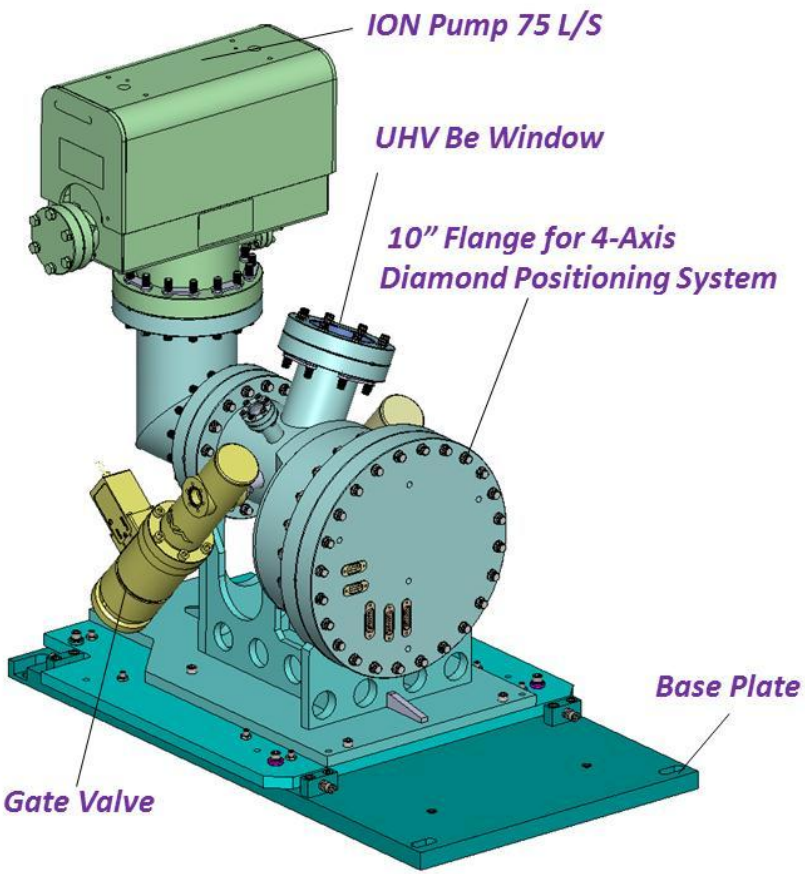

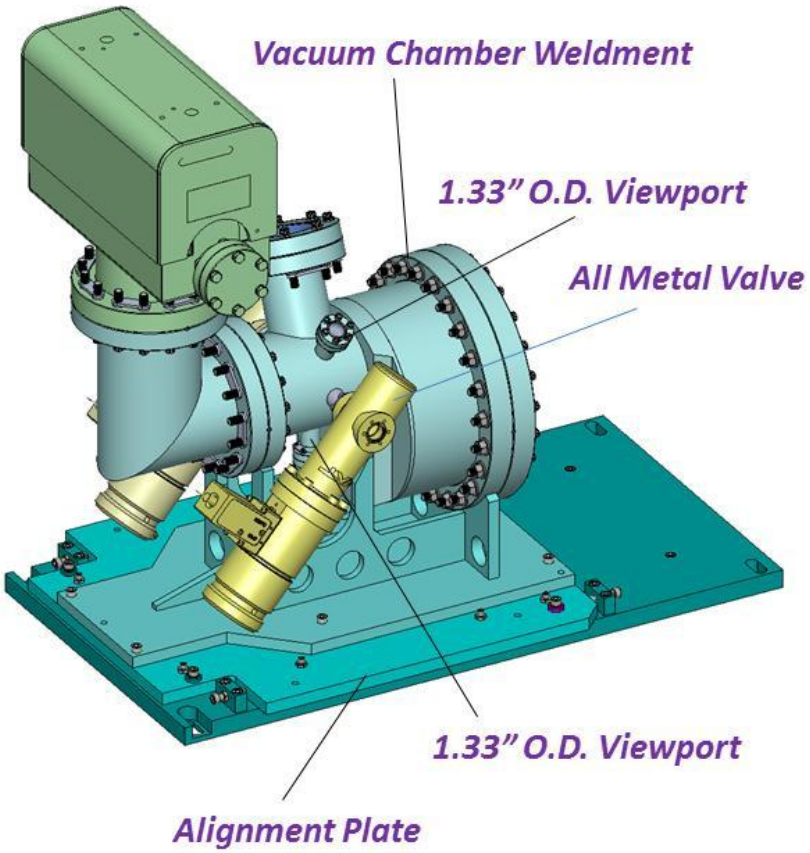

3-D models for the HXRSS diamond monochromator UHV enclosure.The monochromator vacuum enclosure hosts a 10" flange for a 4-axis diamond positioning system, a beryllium window for x-ray diagnostics, a 75 l/s ion pump, two 1.33" O.D. viewports, and a pair of all-metal valves connected to the LCLS vacuum system.

D Shu, Y Shvyd'ko, J Amann, P Emma, S Stoupin, and J Quintana, "Design of a diamond-crystal monochromator for the LCLS hard x-ray self-seeding project", J. Phys. Conf. Ser. 425 052004 (2013)

Design of the precision motion control in UHV

- *A 4-axis precision stage system for diamond crystal manipulation is mounted on a 10" base flange.*
- *The base flange is equipped with electric feedthroughs for various in-vacuum motors and optical encoders closed-loop controlled from controllers outside vacuum.*
- *Precision mounting holes are also prepared on the base flange for diamond-crystal position survey and alignment from outside vacuum.*

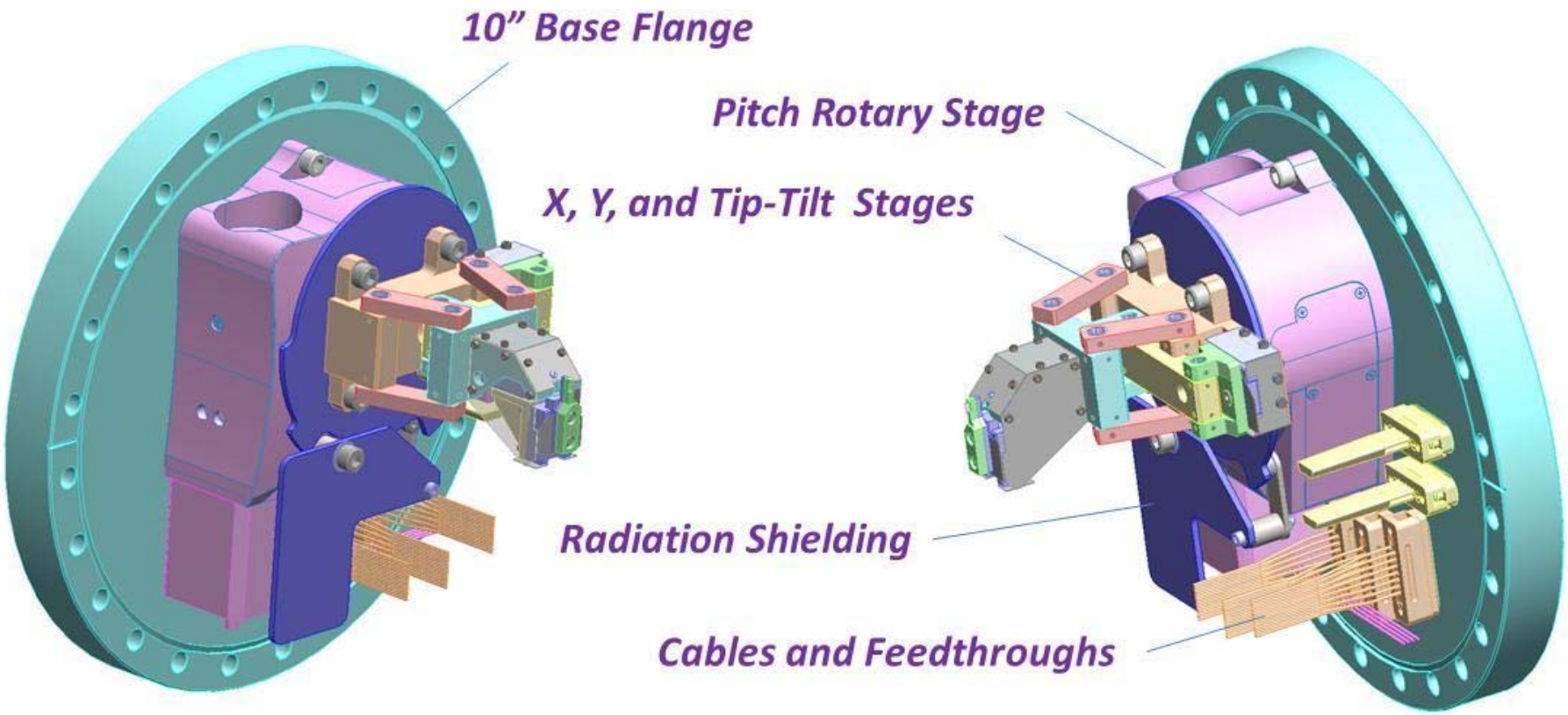

D Shu, Y Shvyd'ko, J Amann, P Emma, S Stoupin, and J Quintana, "Design of a diamond-crystal monochromator for the LCLS hard x-ray self-seeding project", J. Phys. Conf. Ser. 425 052004 (2013)

Design of the precision motion control in UHV

Design specifications for the HXRSS diamond monochromator 4-axis precision stage system.

Parameter	Value	Units
X position control range	-1/+3	mm
Y_{roll} position control range	+1.5/-8.5	mm
X and Y_{roll} position resolution and stability (rms)	< 0.05	mm
crystal extraction position (approx.)	-8.5	mm
crystal pitch angle hard limit range	42 – 98	deg
crystal pitch angle limit switch range	45 – 95	deg
crystal pitch angle operation range	47 – 93	deg
pitch angle stability (rms)	< 0.005	mrad
crystal roll angle control range	±2.5 – ± 3	deg
crystal roll angle resolution and stability (rms)	<0.010	mrad
Vacuum	UHV	
F-F distance w/valves	264	mm

D Shu, Y Shvyd'ko, J Amann, P Emma, S Stoupin, and J Quintana, "Design of a diamond-crystal monochromator for the LCLS hard x-ray self-seeding project", J. Phys. Conf. Ser. 425 052004 (2013)

Design of the precision motion control in UHV

Pitch rotary stage

- *The monochromator pitch stage controls the Bragg angle of the diamond crystal.*
- *It is a customized Micos™ PRS-110 UHV-compatible stepping-motor-driven rotary stage with a 0.0001-degree resolution optical angular encoder.*
- *The pitch stage is specified to have a better than 0.0002-degree unidirectional repeatability with closed-loop control.*
- *Molybdenum radiation shielding plates are applied to the rotary stage to protect the optical encoder and electronics components in the stage.*

D Shu, Y Shvyd'ko, J Amann, P Emma, S Stoupin, and J Quintana, "Design of a diamond-crystal monochromator for the LCLS hard x-ray self-seeding project", J. Phys. Conf. Ser. 425 052004 (2013)

Design of the precision motion control in UHV

Tip-tilt and linear stages

- *The monochromator tip-tilt stage provides a roll adjustment for the diamond crystal alignment .*
- *The 4-bar flexural bearing structure is modified from an original APS design for a compact multi-dimensional alignment apparatus developed for multilayer Laue lenses (MLLs) with nanometer-scale 2-D focusing [2].*
- *The 4-bar flexural bearing structure is operated by a SmarAct™ PZT-driven linear stage to provide a precise angular positioning around the Yroll-axis, which is rotating with the pitch stage, and agrees with the Y-axis while the pitch angle (equal to the x-ray grazing incidence angle to the diamond crystal) is at the 90-degree position as shown in the figure .*
- *The X and Y_{roll} linear stages, mounted on top of the 4-bar flexural bearing structure, provide the linear motion required by the HXRSS system.*
- *During the self-seeding test, the X and Y_{roll} linear stages align the diamond crystal to the test position. The X and Y_{roll} linear stages can retract the diamond crystal holder to a safe position in the LCLS normal operation condition with safety interlock control.*

D Shu, Y Shvyd'ko, J Amann, P Emma, S Stoupin, and J Quintana, "Design of a diamond-crystal monochromator for the LCLS hard x-ray self-seeding project", J. Phys. Conf. Ser. 425 052004 (2013)

Design of the precision motion control in UHV

Tip-tilt and linear stages

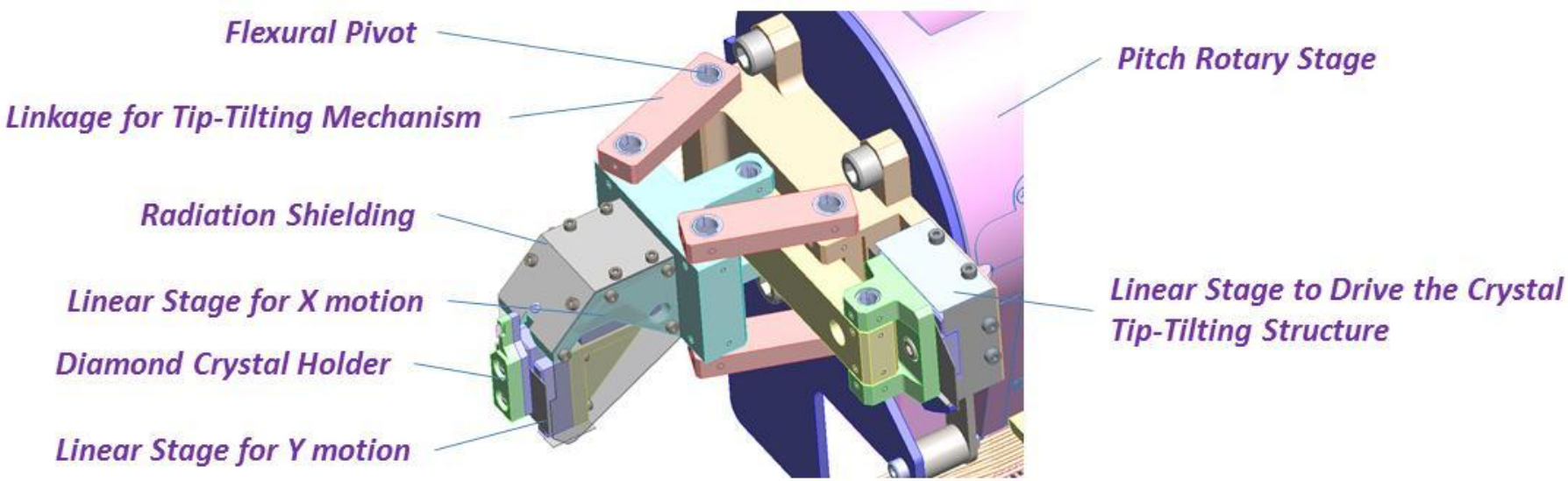

3-D models for the HXRSS diamond monochromator tip-tilt and linear stages.

D Shu, Y Shvyd'ko, J Amann, P Emma, S Stoupin, and J Quintana, "Design of a diamond-crystal monochromator for the LCLS hard x-ray self-seeding project", J. Phys. Conf. Ser. 425 052004 (2013)

Tip-Tilt Stage for Diamond Crystal Positioning

The same mechanism has been used for APS/NSLS-II MLL hard x-ray optics alignment apparatus

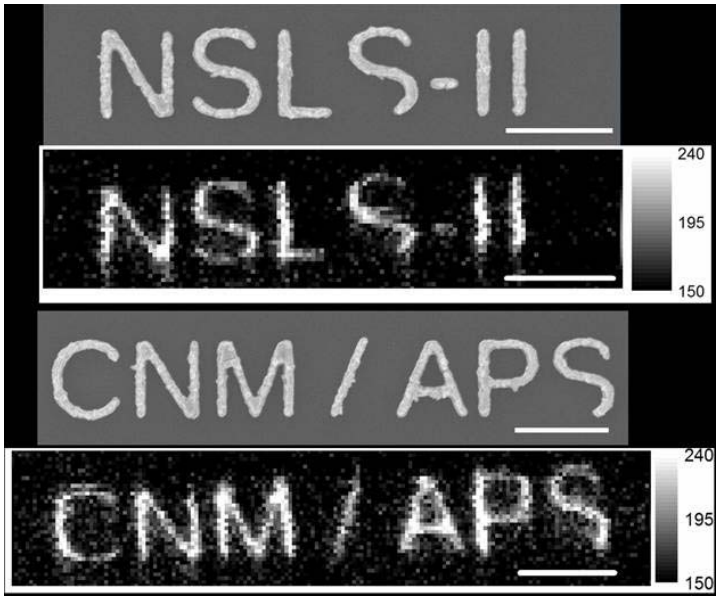

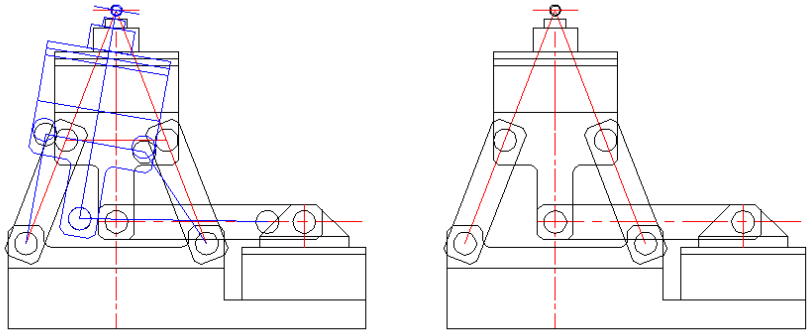

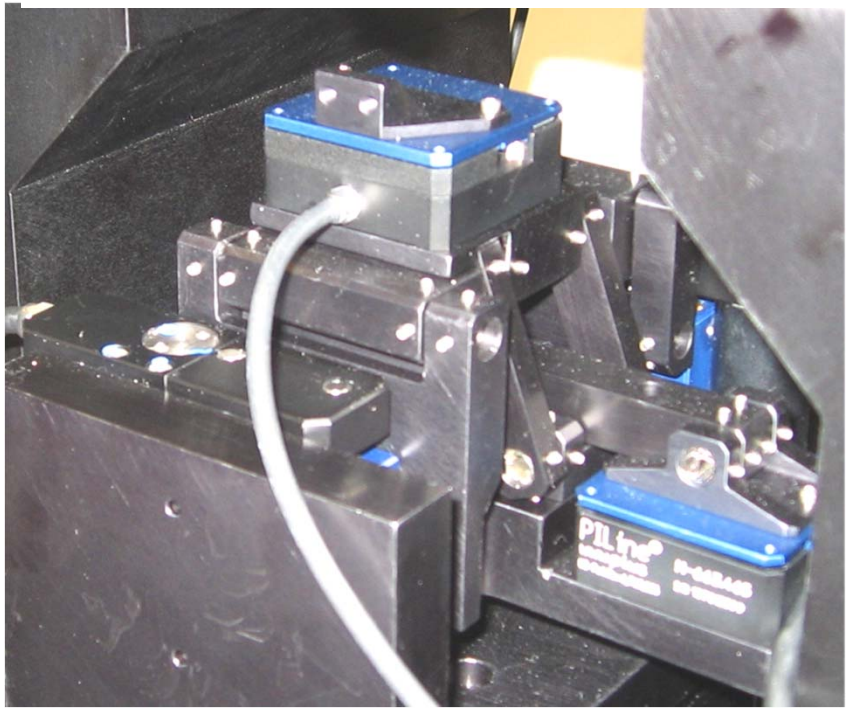

MLL demonstrated of focusing of hard x-rays to a 2D focus of 25 nm horizontal x 27 nm vertical FWHM at a photon energy of 12 keV, and of 25 nm horizontal x 40 nm vertical FWHM at a photon energy of 19.52 keV.

H. Yan, V. Rose, D. Shu, E. Lima, H. C. Kang, R. Conley, C. Liu, N. Jahedi, A. Macrander, G. B. Stephenson, M. Holt, Y. S. Chu, M. Liu, and J. Maser, Optics Express 15069 Vol.19, No.16 (2011)

Linear Stage to Drive the Crystal Tip-Tilting Structure

SmarAct SLC-2430

SLC-2430

Basic Data

- Dimensions: 30x24x10.5mm³
- Travel: about 16mm
- Blocking force: min. 3.0N
- Weight: about 36g

Movement

- Velocity: max. 8mm/s
- Step width: bewteen 50nm and 500nm
- Scanning range: about 750nm
- Resolution: sub-nanometer

Load

- Load: 50N
- horizontal and vertical application possible

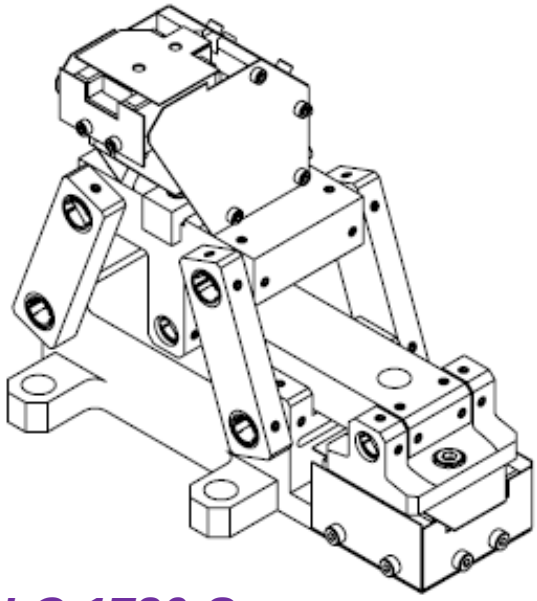

Linear Stage for Crystal X motion *SmarAct SLC-1720-S*

- Dimensions: 22 x 17 x 8.5 mm³
- Travel: about 12 mm
- Weight: about 13 g
- Allowable load: 40 N
- Integrated nanosensor
- Options:
  - Vacuum compatibility: HV, UHV
  - Non-magnetic

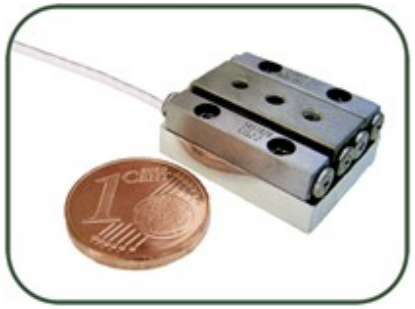

- Velocity: max. 8mm/s
- Step width: bewteen 50nm and 500nm
- Scanning range: about 750nm
- Resolution: sub-nanometer

Load

- Load: 40N
- horizontal and vertical application possible

Courtesy of: SmarAct

Thin diamond crystal plate handling

- The HXRSS monochromator is using a 0.1- to 0.15-mm-thick, very high quality thin diamond-crystal plate with (001) orientation [3].
- Since the crystal holder is close to the electron beam in the linear accelerator, it is best that the diamond holder be made of low-Z materials to meet radiation safety requirements. Highly ordered pyrolytic graphite (HOPG) was chosen to form the diamond-crystal holder.
- The diamond holder was designed to minimize the strain in the diamond crystal induced by the holder structure. The diamond holder consists of two parts: a main body and a back plate.
- A precision slot is machined on the main body with a trapezoid shape, which is matched with the diamond-crystal shape to prevent the crystal sliding out of the holder. With an optimized sliding fit, the diamond crystal is held in the holder with a stable and near strain-free condition.
- The diamond crystal and its HOPG holder were manufactured by TISNCM [3].

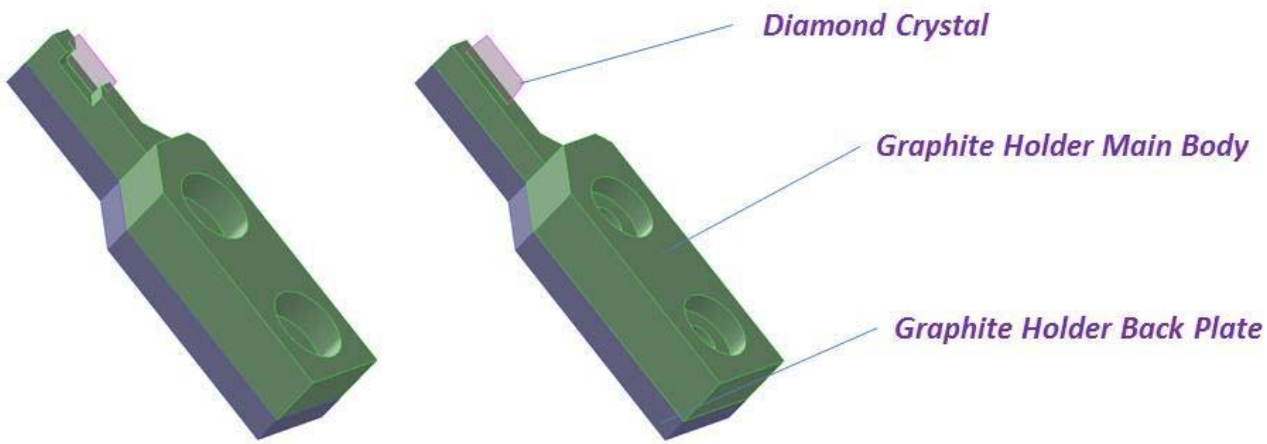

D Shu, Y Shvyd'ko, J Amann, P Emma, S Stoupin, and J Quintana, "Design of a diamond-crystal monochromator for the LCLS hard x-ray self-seeding project", J. Phys. Conf. Ser. 425 052004 (2013)

UHV ACCM for x-ray double crystal monochromators at EXFEL

Argonne Work For Others (WFO) project 857Y2 with EXFEL
for Cryo-cooling UHV ACCM design collaboration

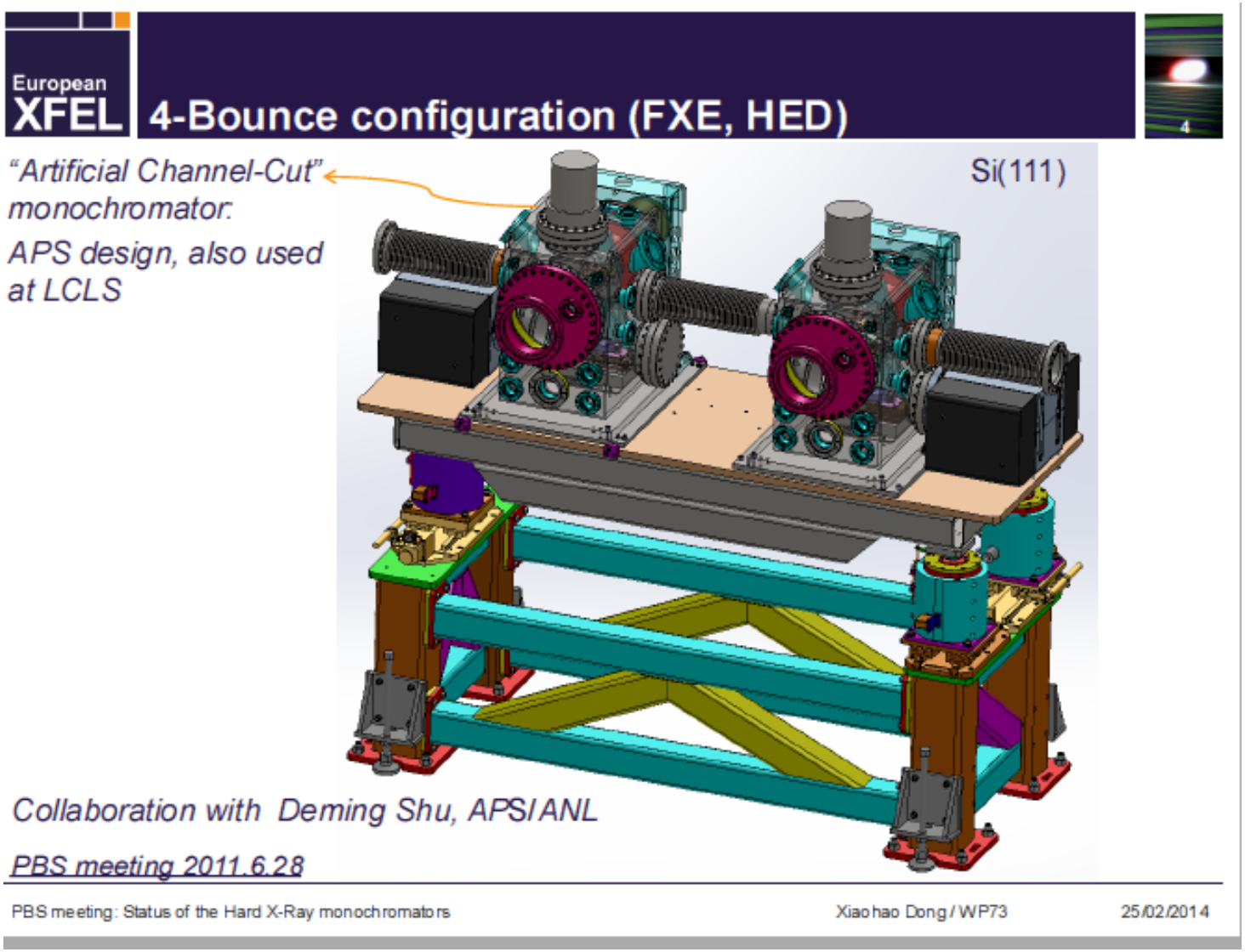

UHV ACCM for x-ray double crystal monochromators at EXFEL

Argonne Work For Others (WFO) project 857Y2 with EXFEL
for Cryo-cooling UHV ACCM design collaboration

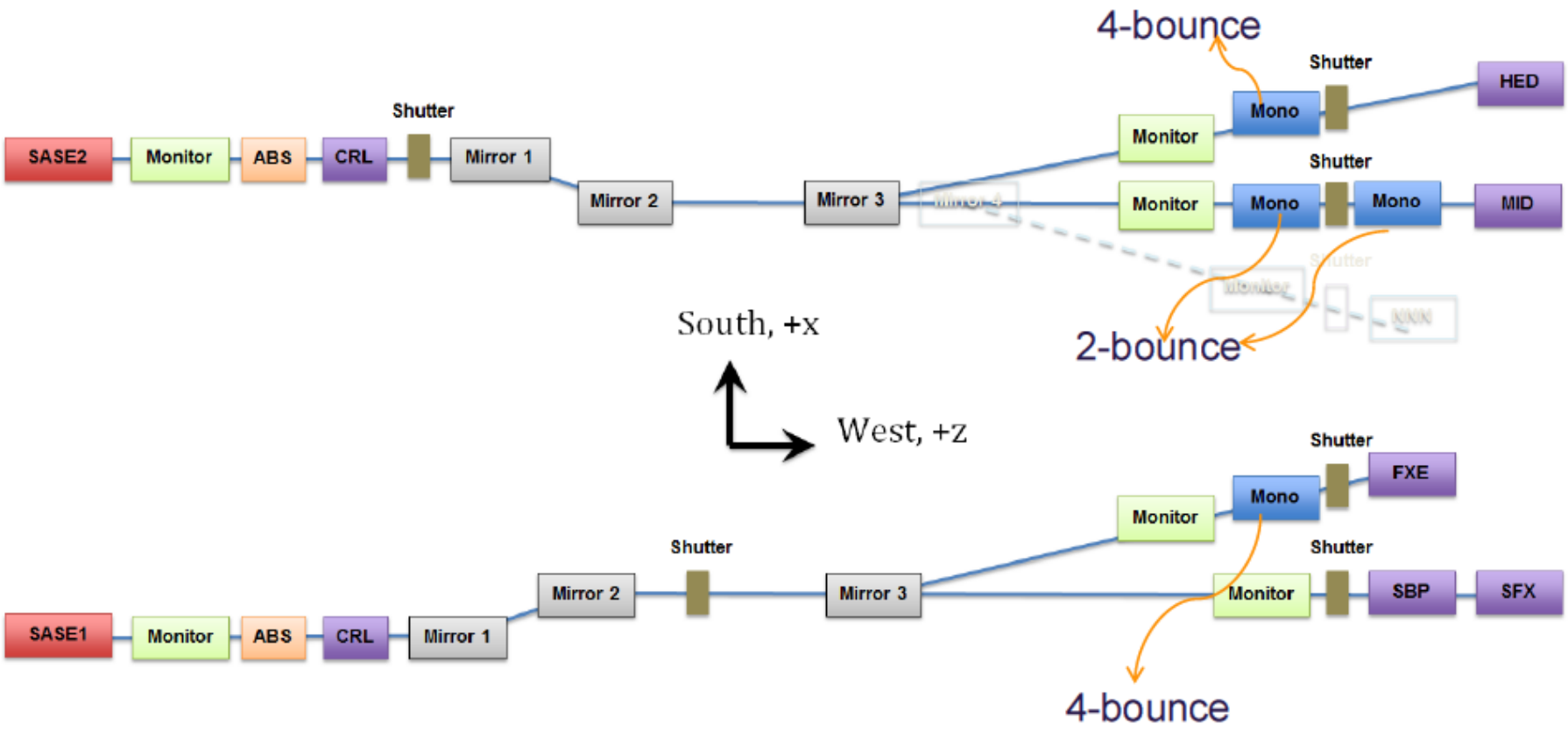

TDR WP73 update

UHV ACCM for x-ray double crystal monochromators at EXFEL

Option for Si(111) Energy range: 5 – 25 KeV Bragg angle: 23.3 – 4.72 deg.

Mechanical design for angle range available (+32) – (-3) deg.

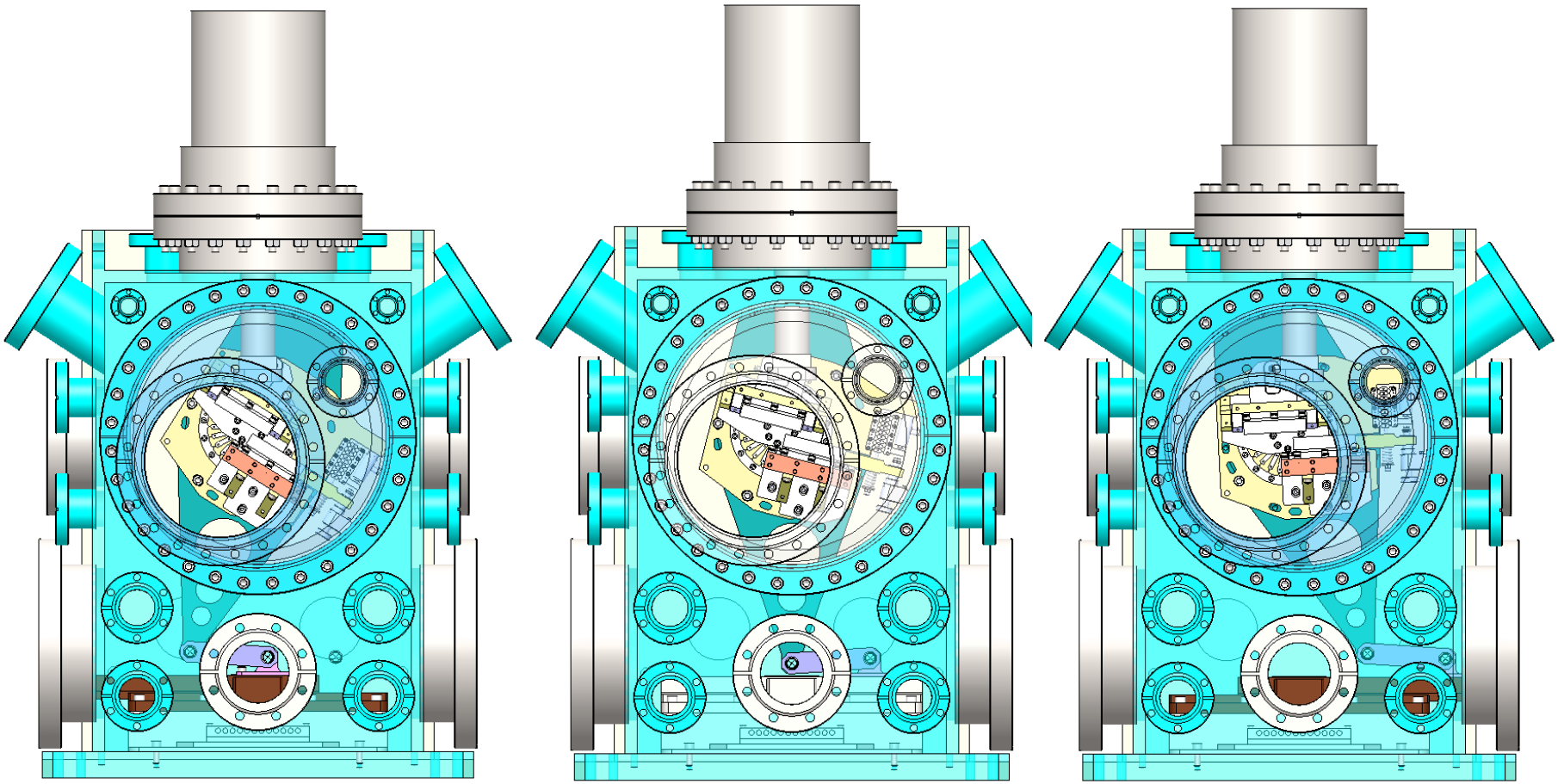

UHV ACCM for x-ray double crystal monochromators at EXFEL

Option for Si(220) Energy range: 5 – 25 KeV Bragg angle: 40.5 – 7.5 deg.

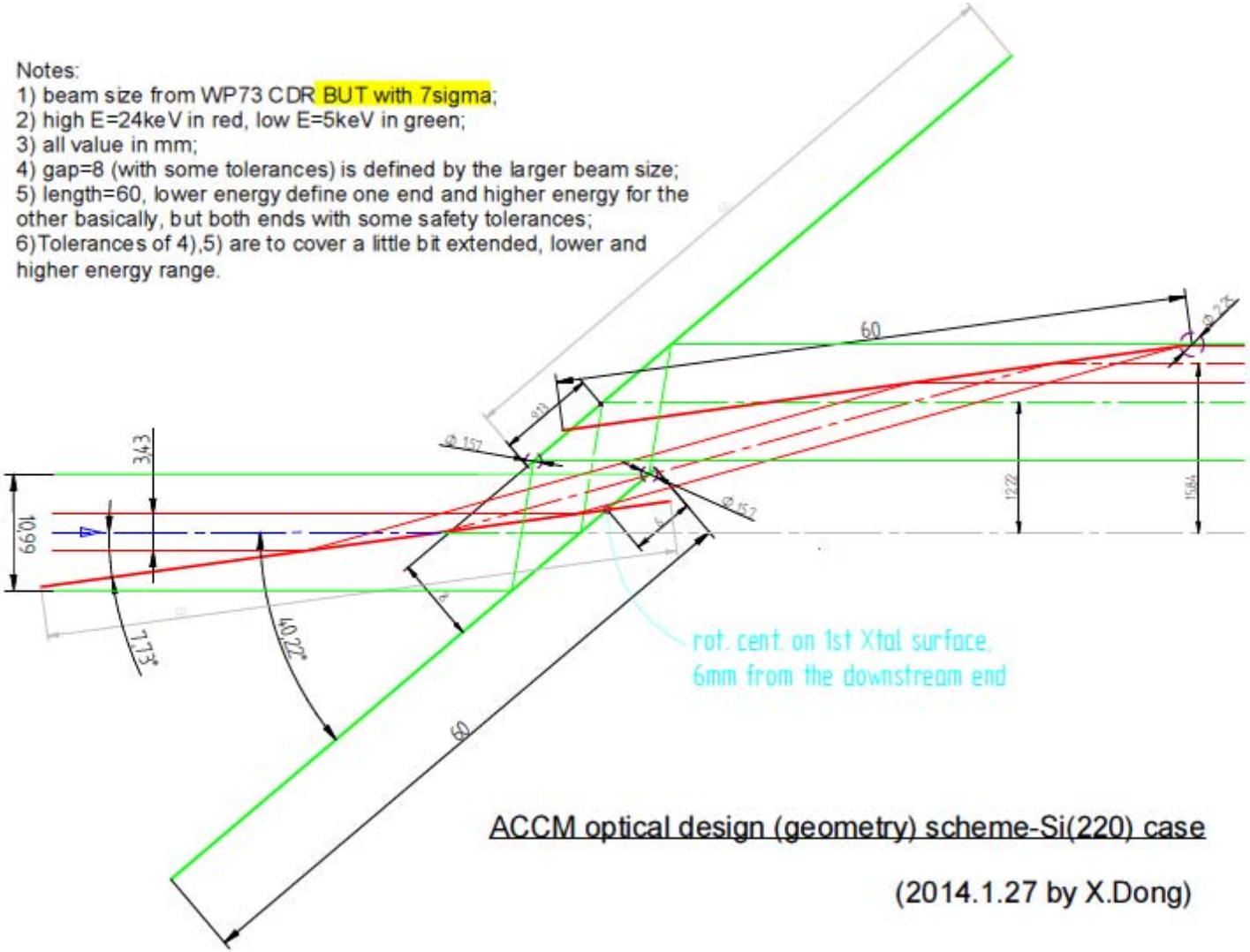

UHV ACCM for x-ray double crystal monochromators at EXFEL

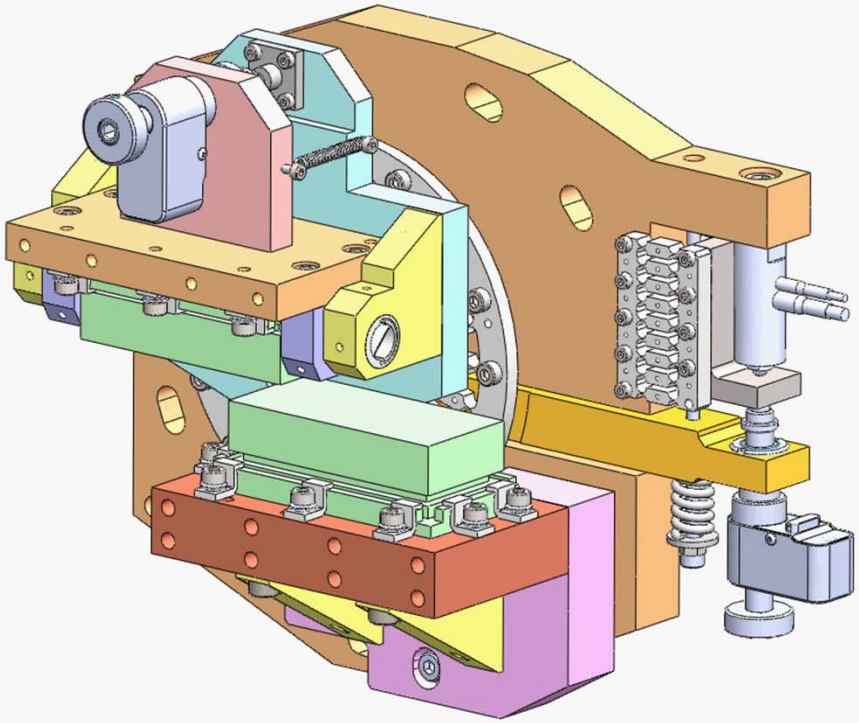

UHV ACCM for x-ray double crystal monochromators at EXFEL

EXFEL received first UHV ACCM manufactured by A.J.R. Industrials, Inc. USA

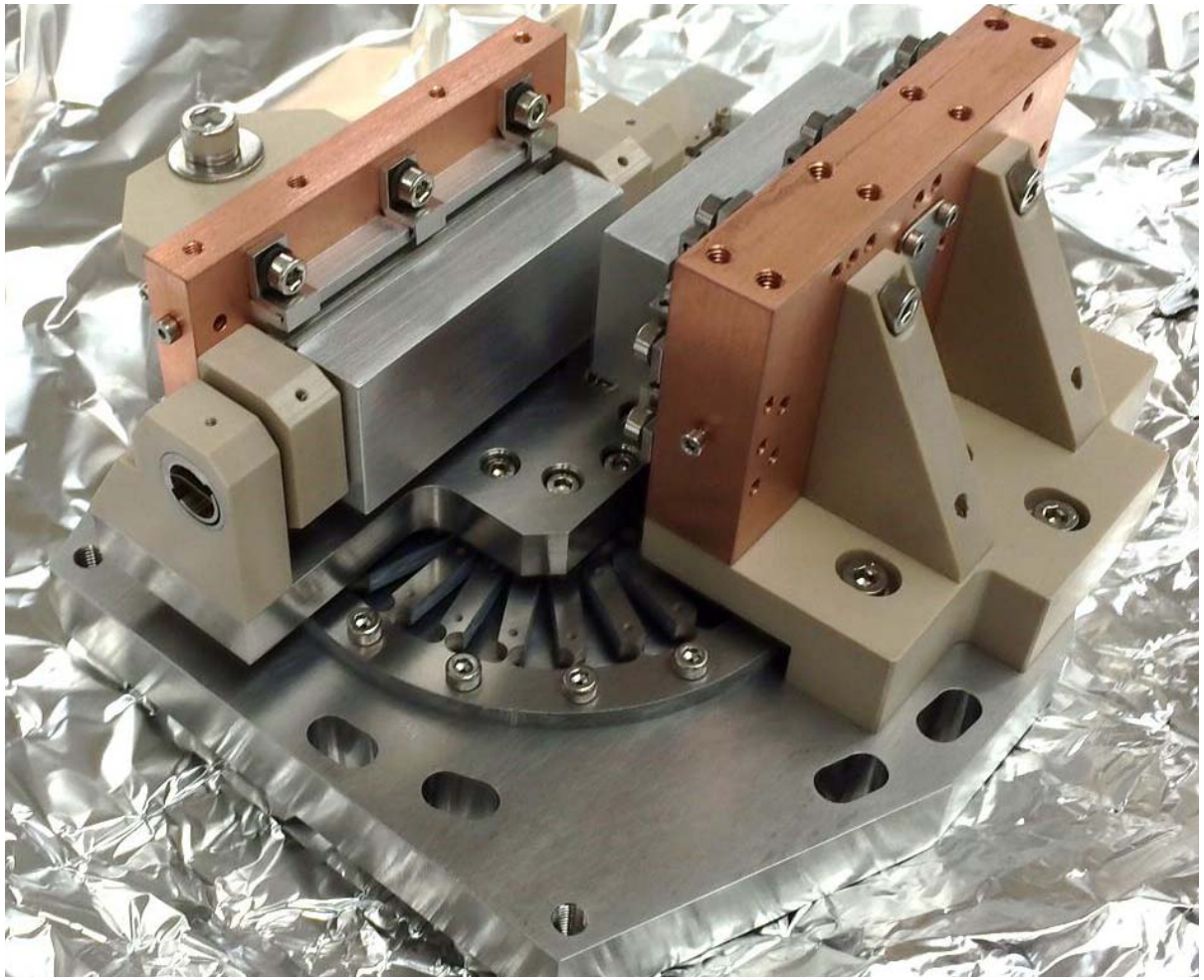

Summary

Applications of the weak-link-based high precision mechanisms

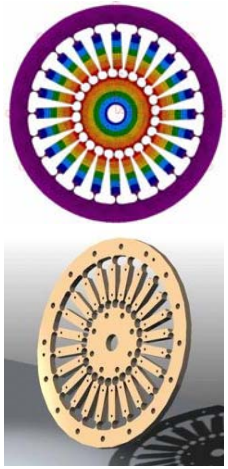

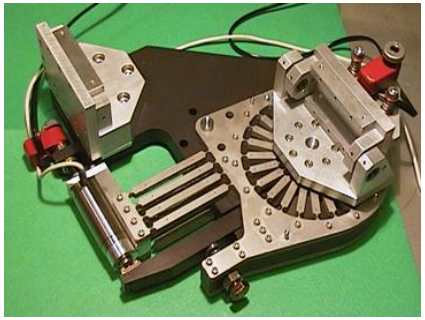

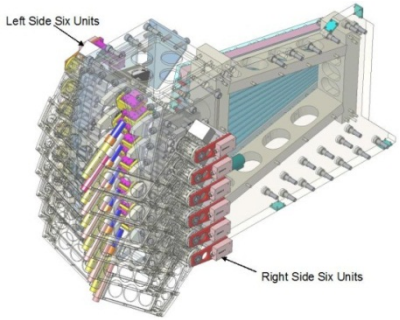

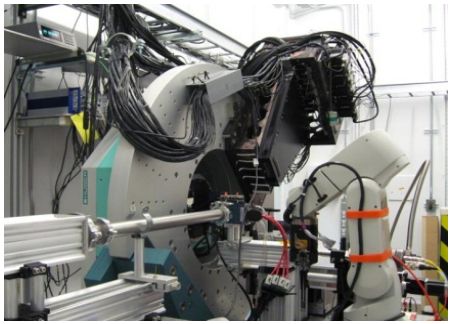

Twelve-analyzer detector system for high-resolution powder diffraction (11-BM)

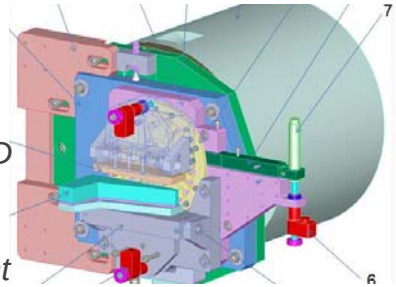

A 3D model of the 15-ID artificial channel-cut crystal stage for the APS USAXS instrument crystal analyzer system :

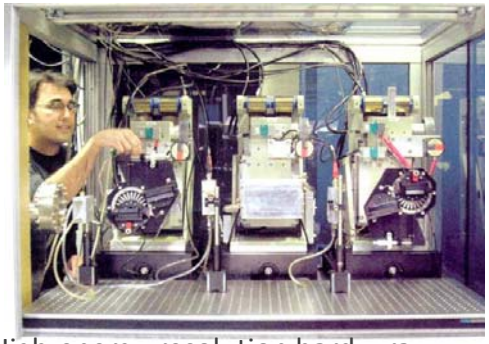

High-energy-resolution hard x-ray monochromators (3-ID)

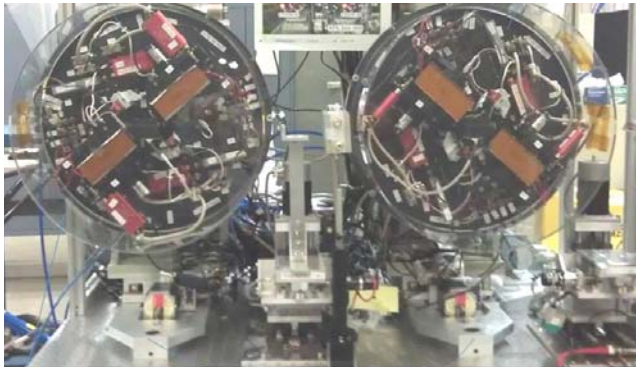

CDFDW prototype (30-ID)

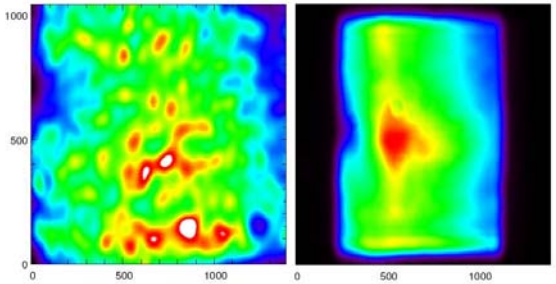

UHV-compatible artificial channel-cut crystal monochromator for XPCS (8-ID) Figure b (right) shows the Ge(111)-monochromatized beam (7.35 keV) produced by the new monochromator. Evidently, its transverse intensity profile is considerably more uniform than that produced by the traditional channel-cut monochromator previously installed in Beamline 8-ID-I (Fig. a).

Summary

Applications of the flexural-stage-based high precision mechanisms

- ***Scanning stage system for x-ray nanoprobes***
  - *ANL CNM hard x-ray nanoprobe at APS (26-ID)*
  - *Australian soft x-ray nanoprobe at APS (2-ID)*
  - *Multi-axis alignment apparatus for ANL CNM/APS/NSLS-II MLL-based x-ray nanoprobe test bed at APS (26-ID) and Diamond Light Source (I13L), UK*

- ***High precision x-ray crystal monochromators, analyzers, and etc.***
  - *High-energy-resolution hard x-ray monochromators (3-ID)*
  - *HERIX and MERIX monochromators (30-ID)*
  - *Four-crystal high-energy high-resolution x-ray monochromator (1-ID)*
  - *Twelve-analyzer detector system for high-resolution powder diffraction (11-BM)*
  - *Artificial channel-cut crystal stage for a Bonse-Hart USAXS Instrument (15-ID)*
  - *Twelve-analyzer detector system for high-resolution powder diffraction (11-BM)*
  - *Multi-axis precision flexure stage system for x-ray stereo imaging instrument for particle tracking velocimetry (PTV) (32-ID)*
  - *UHV-compatible artificial channel-cut crystal monochromator for XPCS (8-ID)*
  - *UHV-compatible artificial channel-cut crystal monochromator for HP studies (16-BM)*
  - *UHV-compatible artificial channel-cut crystal monochromator for XPCS (LCLS/SLAC)*
  - *UHV-compatible diamond monochromator for XFEL self-seeding (LCLS/SLAC)*
  - *UHV-compatible cryo-cooling crystal monochromators for XFEL beamlines (European-XFEL)*

* *A.J.R. Industrials, Inc. had a license from Argonne to commercialize the weak-link nanopositioning stages worldwide. (http://www.ajrindustries.com)*

References

[1] http://www.aps.anl.gov/Upgrade/ APS Upgrade project.
[2] Kirkpartrick, P. and Baez, A. V. Formation of Optical Images by X-Rays. JOSA. 1948; 38(9): 766-773.
[3] Liu, W., Ice, G. E., Assoufid, L., Liu, C., Shi, B., Khachatryan, R., Qian, J., Zschack, P., Tischler, J. Z. and Choi, J.-Y. J. Synchrotron Rad. 2011; 18: 575-579.
[4] J. Maser, B. Lai, T. Buonassisi, Z. Cai, C. Si, L. A. Finney, C. Gleber, C. Jacobsen, C. A. Preissner, C. Roehrig, V. Rose, D. Shu, D. Vine, S. Vogt, Metallurgical and Materials Transactions A, Volume 45, Issue 1, pp 85-97, 2014.
[5] D. Shu, T. S. Toellner, and E. E. Alp, Nucl. Instrum. and Methods A 467-468, 771-774 (2001)
[6] D. Shu, Y. Han, T. S. Toellner, and E. E. Alp, Proc. SPIE, Vol. 4771 (2002) 78-90
[7] U.S. Patent granted No. 6,607,840, D. Shu, T. S. Toellner, and E. E. Alp, 2003
[8] T. S. Toellner, APS Science 2004, ANL-05/04, p. 130
[9] U.S. Patent granted No. 6,984,335, D. Shu, T. S. Toellner, and E. E. Alp, 2006
[10] Y. Zhang, A. P. Wilkinson, P. L. Lee, S. D. Shastri, D. Shu, D. –Y. Chung, M. G. Kanatzidis, J. Appl. Cryst. 38, 433-441 (2005).
[11] J. Ilavsky et al., SRI-2006 Conf. Proc. 879, AIP (2007) 1833-1836.
[12] S. Narayanan et al., J. Sychrotron Rad. (2008) 15, 12-18
[13] U.S. Patent granted No. 7,331,714, D. Shu, J. Maser, B. Lai, S. Vogt, M. Holt, C. Preissner, R. Winarski, G. Stephenson, 2008
[14] D. Shu et al., SRI-2006 Conf. Proc. 879, AIP (2007) 1073-1076
[15] D. Shu et al., SRI-2006 Conf. Proc. 879, AIP (2007) 1321-1324
[16] P. L. Lee et al., J. Sychrotron Rad. (2008) 15, 427-432
[17] B. Jakobsen et al., Science 312, 889-892 (2006)
[18] H. Yan, V. Rose, D. Shu, E. Lima, H. C. Kang, R. Conley, C. Liu, N. Jahedi, A. Macrander, G. B. Stephenson, M. Holt, Y. S. Chu, M. Liu, and J. Maser, Optics Express 15069 Vol.19, No.16 (2011)
[19] Y. Shvyd'ko et al., Physical Review A, 84 053823(2011)
[20] Yuri Shvyd'ko, Stanislav Stoupin, Deming Shu, Stephen P. Collins, Kiran Mundboth, John Sutter, and Martin Tolkiehn, "High-contrast sub-millivolt inelastic X-ray scattering for nano- and mesoscale science," Nature Communications, (2014). DOI:10.1038/ncomms5219
[21] D. Shu, MEDSI 2004, ESRF, Grenoble, France, 2004
[22] D. Shu et al., Proc. SPIE, Vol. 5877 (2005) 58770E, DOI: 10.1117/12.617723
[23] D. Shu et al., proceedings of SPIE Vol. 6665, 66650O1-8 (2007)
[24] W. Yang et al., proceedings of SRI-2008, Saskatoon, Canada, June 10-13 2008
[25] D. Shu et al., APS Science 2010, p134, ANL-10/35, ISSN 1931-5007 (2011)
[26] J. Amann, W. Berg, V. Blank, F.-J. Decker, Y. Ding, P. Emma*, Y. Feng, J. Frisch, D. Fritz, J. Hastings, Z. Huang, J. Krzywinski, R. Lindberg, H. Loos, A. Lutman, H.-D. Nuhn, D. Ratner, J. Rzepiela, D. Shu, Yu. Shvyd'ko, S. Spampinati, S. Stoupin, S. Terentyev, E. Trakhtenberg, D. Walz, J. Welch, J. Wu, A. Zholents and D. Zhu, „Demonstration of self-seeding in a hard-X-ray free-electron laser", Nature Photonics, DOI: 10.1038/NPHOTON.2012.180.
[27] Alexander A. Zholents, "What's Next? The FEL Manifesto," Synch. Rad. News 25(6), 27 (2012)
[28] H. Sinn et al., TDR X-ray Optics and Beam Transport, XFEL.EU TR-2012-006 (2012)

Thanks for Your Attention